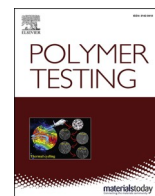


12. ZAŁĄCZNIKI

12.1. KOPIE ARTYKUŁÓW NAUKOWYCH STANOWIĄCYCH CYKL PUBLIKACJI ROZPRAWY

Publikacja [P1]

Structure and properties of poly(vinyl chloride)/graphene nanocomposites



Material Behaviour

Structure and properties of poly(vinyl chloride)/graphene nanocomposites

Sławomir Wilczewski^{*}, Katarzyna Skórczewska, Jolanta Tomaszewska, Krzysztof Lewandowski

Faculty of Chemical Technology and Engineering, UTP University of Science and Technology in Bydgoszcz, Seminaryjna 3, PL-85326, Bydgoszcz, Poland



ARTICLE INFO

Keywords:

Nanocomposites
Structure
Electrical properties
Swelling behavior

ABSTRACT

The goal of the paper was to investigate the influence of graphene (GN) on properties and structure of suspensive poly(vinyl chloride) (PVC). PVC/GN nanocomposites were obtained by the solvent evaporation method, and their structures were evaluated using optical microscopy, SEM, FT-IR, XRD and Raman spectroscopy methods. Thermal properties of the obtained materials were studied by TGA. Electrical properties and swelling behaviour were also determined.

The microscopic observations confirm a uniform distribution of graphene in the PVC matrix. The investigations carried out indicated an effect of graphene on a decrease in resistivity to a value which enabled to include the PVC/GN nanocomposites into anti-static materials group. On the basis of swelling studies, it has been found that the PVC/GN nanocomposites have a higher chemical resistance against acetone while compared to pure poly(vinyl chloride). The properties of the obtained materials depend significantly on content and dispersion level of graphene in the PVC matrix. An impact of GN on the acceleration of the PVC degradation process was found.

1. Introduction

Obtaining of graphene more than a decade ago by graphite exfoliation by Andre Geim and Konstantin Novoselov, initiated a series of studies on properties and production methods of this material, as well as its potential applications [1]. Graphene is a flat carbon structure shaped in a hexagonal network with a thickness of 0.334 nm. In one-layer graphene, three valence electrons undergo an sp^2 hybridisation, forming a σ bond. The fourth valence electron, occupying the $2p_z$ orbital, perpendicular to the graphene plane, forms π bonds [2–6]. This unusual structure of graphene affects its properties. Graphene is characterised by a very good thermal and electrical conductivities, as well as excellent barrier and mechanical properties (Young modulus of 1 TPa and tensile strength of 130 GPa) [7–12]. Therefore, extensive studies on utilisation of these unique properties in various fields are carried out, including modification of polymer materials [4,5,7].

At present, poly(vinyl chloride) (PVC) is one of the most frequently used thermoplastics. It sets apart because of its good chemical resistance and resistance to atmospheric agents, favourable mechanical and utility properties, including fire resistance and low productions cost [13]. One of the disadvantages of PVC consists in its low thermal resistance, and that is why use of thermal stabilisers is necessary while processing this polymer [13–16].

Modification of PVC using fillers of natural origin [17,18] and nanofillers [19,20], including also carbon nanoparticles such as carbon nanotubes (CNT) [21–24], graphene oxide (GO) and graphene (GN) [25–36] leads to an improvement in thermal resistance in many cases, but its main goal remains to create new engineering materials having favourable properties, particularly electrostatic and barrier properties, as well as improved chemical resistance.

Both a higher thermal stability of nanocomposites with carbon fillers [26,28,35], and their mechanical properties are strictly connected with interfacial interactions occurring between the filler and the matrix [31, 34].

The impact of graphene fillers on mechanical properties of PVC described in the literature depends also on the structure of nanomodifiers and their concentration, as well as the method of their introduction into the polymeric matrix. The PVC/graphene nanocomposites are characterised by a high modulus of elasticity while compared to the unmodified polymer; the value of the modulus is the higher, the larger the graphene content in the matrix. On the other hand, their tensile strength increases only to a specific filler concentration. After exceeding this concentration, the tensile strength value does not change or even decreases [26,30,31,33–35]. Another effect of the modification of poly(vinyl chloride) with graphene fillers consists in a change of glass transition temperature (T_g) [16,27,28,31,34,35]. The T_g values depend

^{*} Corresponding author.

E-mail address: slawomir.wilczewski@utp.edu.pl (S. Wilczewski).

significantly on the properties of the materials used in production of nanocomposites, concentration of fillers, and interfacial interactions between the fillers and the polymeric matrix [33,36].

The basic method for synthesis of nanocomposites of poly(vinyl chloride) with graphene fillers (graphene, graphene oxide) is the solvent evaporation method. Most frequently used PVC solvent is tetrahydrofuran (THF), and the obtained nanocomposites have a form of thin polymer films (foils) or fibres [25–32]. Advantage of this method consists in the possibility to use ultrasound to increase dispergation of nanoparticles in the solution. However, working with solvents and small amount of produced materials are problematic. Additionally, solvent evaporation may lead to secondary aggregation of the nanofiller. This method is of a small practical significance only in specific applications. It is used mainly at a laboratory scale. The materials obtained thanks to it allow for studying the interactions between the nanofiller and the matrix using small amounts of materials.

Other literature methods for obtaining nanocomposites of poly(vinyl chloride) with graphene (PVC/GN) or graphene oxide (PVC/GO) are the mixing with melted polymer and the *in situ* polymerisation method [33–36]. The materials prepared by various methods are characterised by a good dispergation of the fillers in the PVC matrix, while the fillers exhibit a tendency to form aggregates at higher concentrations [25–36].

An interesting direction for modification of PVC with graphene consists in a change of electrical properties with the increase of the filler content in the matrix [31,34].

Summarising, the properties of poly(vinyl chloride)/graphene nanocomposites depend on many factors, including the structure of the applied nanofillers, the composition of the polymeric mixture and its processing method, level of dispersion in the whole matrix volume, and interactions between the carbon filler and the matrix. In spite of the increasingly higher number of literature reports on nanocomposites of poly(vinyl chloride) with graphene and graphene oxide, these materials are still poorly known [25,26,29,33–36]. These papers do not present the impact of graphene on the swelling behaviour of PVC nanocomposites. Moreover, literature contains only scarce information on the change of electrical properties of PVC nanocomposites resulting from the introduction of unmodified graphene into the matrix. The goal of the paper was to obtain nanocomposites of unmodified PVC with unmodified graphene by solvent evaporation, and characterisation of their structure and selected properties. Lack of introduction of additives

used commonly in PVC processing (thermal stabilisers, flow modifiers, lubricants, etc.) enabled a broad characterisation of the interactions between the PVC macromolecules with graphene.

2. Experimental

2.1. Materials

As a matrix of the PVC/GN nanocomposites, unmodified suspensive poly(vinyl chloride) S-61 Neralit-601 (Czech Republic, Spolana s.r.o. Anwil S.A. Group) was used. According to the manufacturer's information, k-value is in the range of 59–61, corresponding numerically to the average molecular mass at the level of ca. 50000 g mol⁻¹. Graphene in a nanopowder form (USA Graphene Laboratories Inc.) was used as a filler. According to the manufacturer's information, graphene flakes have the following characteristics: flake thickness 1.6 nm (max. 3 atomic monolayers), flake length 10 μm, specific surface area 400 ÷ 800 m²g⁻¹. For preparation of PVC solutions, tetrahydrofuran (THF) (Chempur, Poland) was used.

2.2. Preparation of the PVC/GN nanocomposites

The nanocomposites were prepared by the solution casting and solvent evaporation method. In the first stage, PVC was being dissolved in THF at 25 °C for ca. 48 h, yielding a solution with a concentration of 6%. Graphene was dispersed in 10 cm³ of THF using ultrasound with a frequency of 20 kHz and amplitude of 40% (Sonopuls 3200, sonotrode type WS 70T, Bandelin) for 30 min at 20 °C, yielding a homogeneous dispersion. In the next stage, during mixing by a homogenizer (T25, dispersing element 25 NK - 19 G, IKA) with a rotational speed of 8000 rpm, 30 cm³ of PVC solution were added to the prepared dispersion, and the obtained mixture was subjected to further sonication for 60 min under the same conditions. The PVC/GN dispersion was cast onto a Petri dish with a diameter of 10 cm and the solvent was evaporated (60 °C, 24 h), ultimately yielding nanocomposites in the form of a film with a thickness of ca. 0.07 mm. Average thickness of obtained polymeric films was 0.07 mm ± 0.003 mm. The thickness measurement was carried out using an electronic micrometer screw with an accuracy of 0.001 mm. To remove the THF residue, the film were dried in a vacuum drier under a reduced pressure (max 20 mbar absolute) at 65 °C for 6 weeks. The

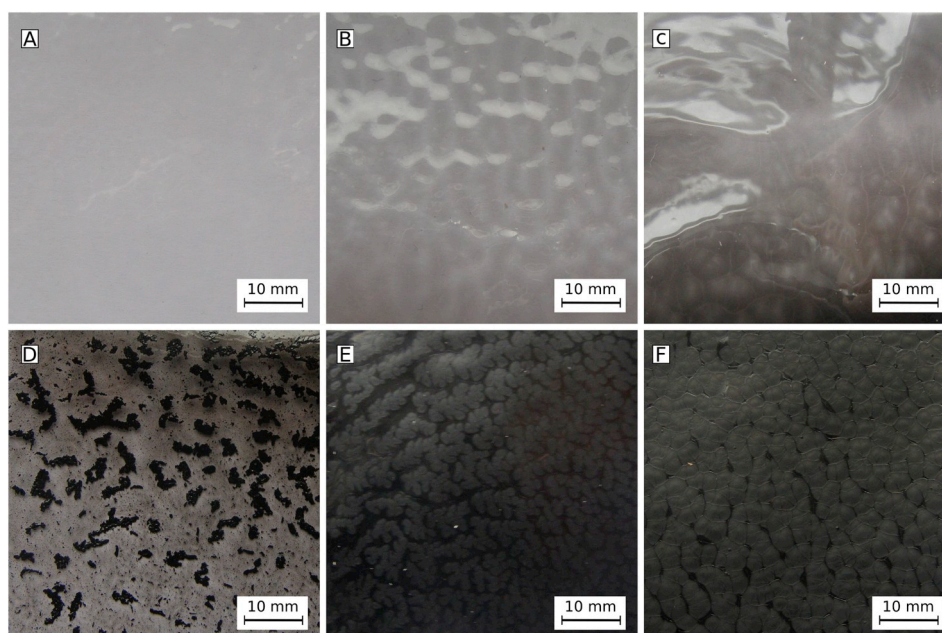


Fig. 1. Digital photographs (A) PVC, (B) PVC/0.01% GN, (C) PVC/0.1% GN, (D) PVC/0.5% GN, (E) PVC/1% GN, (F) PVC/5% GN.

Table 1
Sampling time in swelling behaviour test.

Swelling time, s	Sampling time, s
0–120	10
120–390	30
390–920	60
920–1640	120
1640–3500	300
3500–5300	600
5300–8900	1800

obtained PVC/GN nanocomposites contained 0.01, 0.1, 0.5, 1.0 and 5.0 wt% of graphene. Films of unmodified PVC were obtained under the same conditions. Digital photographs of PVC films and PVC/GN nanocomposites are shown in Fig. 1.

2.3. Characterization

A Nikon ECLIPSE E400 POL optical microscope in transmitted light and a SEM ZEISS AVO 40 scanning electron microscope were used for microstructure evaluation. The samples for SEM observations were constituted by cryogenic fractures of the film with a sputtered gold layer.

Intermolecular interactions between the polymeric matrix and graphene were investigated by Fourier-transform infrared spectroscopy (FT-IR). The study was carried out using an Alpha apparatus from Bruker, using the ATR (reflective) technique, in the range of 4400–200 cm^{-1} , 32 scans at a resolution of 4 cm^{-1} were applied. The structures of graphene and PVC nanocomposites with graphene were characterised also using an X-Ray URD 6 diffractometer from Rich Seifert & Co GmbH, Monochromatic X-ray diffraction with wavelength of $\lambda = 1,5406 \text{ \AA}$ ($\text{CuK}\alpha$) in the 2θ angle range from 7 to 60° with step 0.05 was used.

Thermal stability of the nanocomposites was evaluated by thermogravimetric analysis (TGA) using a TG 209 F3 Tarsus apparatus (Netzsch). The samples (c.a. 3 mg) were heated with a rate of 10 $^{\circ}\text{C min}^{-1}$ in an open ceramic crucible under nitrogen atmosphere, in the temperature range of 30–900 $^{\circ}\text{C}$. Change in sample mass vs. temperature was determined.

Electrical properties of PVC and PVC/GN nanocomposites were characterised by studying surface resistivity and volume resistivity at room temperature. The measurement was carried out using a measuring system consisting of a 6517A electrometer and an 8009 measurement chamber (Keithley Instrument Inc.). The volume resistivity and surface resistivity measurements were carried out using film samples with a diameter of 70 mm in air, at a temperature of 23 $^{\circ}\text{C}$, and 50% humidity. Considering the large differences in resistivity of the obtained

nanocomposites, the measurements were carried out using a voltage of 1 V at 5% graphene fraction to 100 V for the PVC. The determined resistivity value is an average of 10 measurements. The obtained results are characterised by a small coefficient of variation (below 1%), so it is not taken into account in the graph.

Because of the form of the sample (thin polymer film), measurements of the swelling degree based on the change of mass of the sample are difficult [37,38]. Solvent molecules penetrating the polymer cause not only a change in mass, but also in dimensions of the material. Therefore, a method based on determination of changes in sample dimensions was proposed, in this case – changes in its diameter. Evaluation of the swelling dynamics was carried out by a comparative analysis of the swelling rate of samples with the same geometry and various filler fractions. Changes in dynamics of swelling are connected only with the sample composition. Resistance to swelling agent was determined by the swelling in acetone method. The measurement consisted in determination of a change in the swelling degree (S_d), defined by Equation (1), depending on the time of immersion in the swelling agent. Sample diameters were determined based on photographs, using NIS Elements 4.0 software. The frequency with which the photographs were taken depended on the time of exposure to the swelling agent, which was presented in Table 1. The measurement temperature was 20 $^{\circ}\text{C}$, and the initial dimensions of the sample were $h_0 = 10 \text{ mm}$.

Resistance to swelling agent was determined by the swelling in acetone method. The measurement consisted in determination of a change in the swelling degree (S_d), defined by Equation (1), depending on the time of immersion in the swelling agent. Sample diameters were determined using the NIS-Elements 4.0 software. The measurement temperature was 20 $^{\circ}\text{C}$, and the initial dimensions of the sample were $h_0 = 10 \text{ mm}$.

$$S_d = \frac{h - h_0}{h_0} \cdot 100\% \quad (1)$$

where:

- h – sample diameter after time t (mm),
- h_0 – initial sample diameter (mm).

Analysis of the results of the resistance to swelling agent was carried out using the Origin 8.6PRO software.

The Raman spectrum was recorded in the range of 100–3200 cm^{-1} using a Renishaw InVia Raman microscope, equipped with an Argon-ion laser emitting the wavelength of 514.5 nm. The power of the laser beam focused on the sample, with a $\times 50$ objective lens, was maintained below 0.5 mW. Spatial resolution of the optical system achieved using an

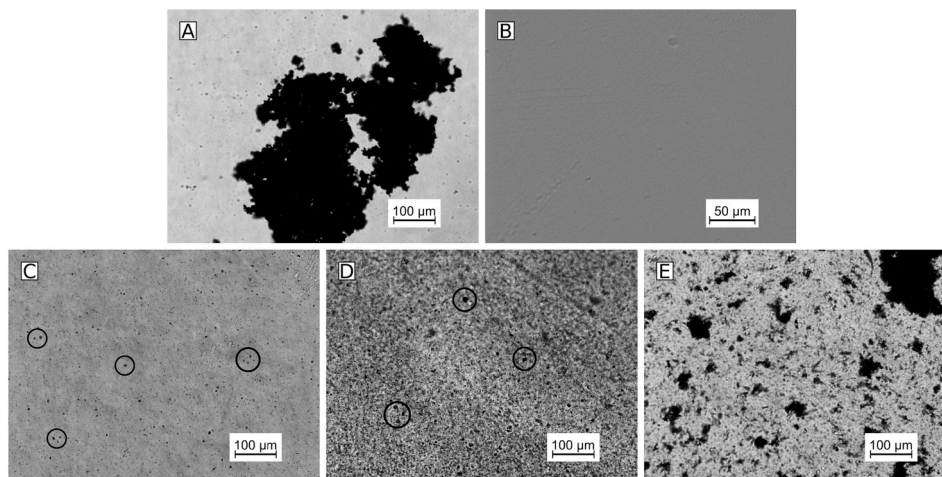


Fig. 2. Photomicrographs (A) GN, (B) PVC, (C) PVC/0,01% GN, (D) PVC/0,1% GN, (E) PVC/0,5% GN

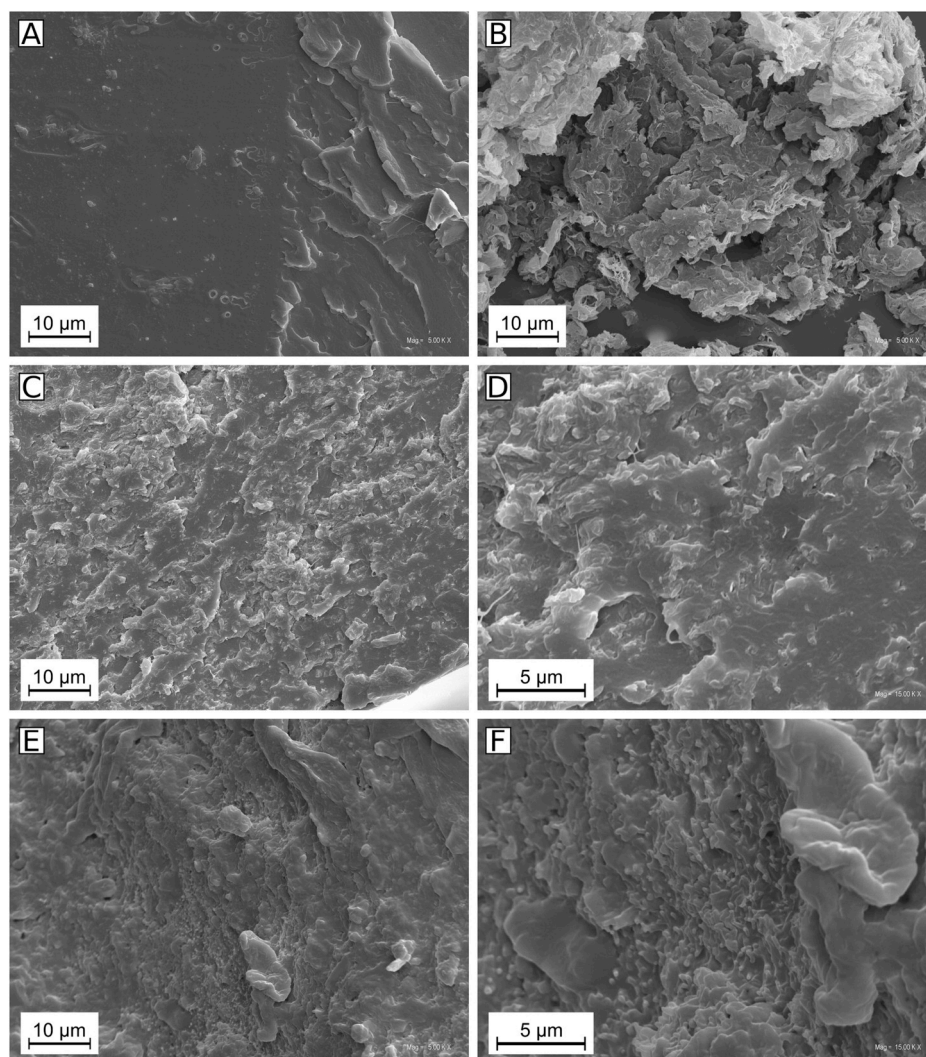


Fig. 3. SEM images (A) PVC, (B) GN, (C), (D) PVC/1% GN, (E), (F) PVC/5% GN.

objective lens with a long working distance was better than 2 μm . Positions of the peaks were calibrated before data collection using a crystalline Si sample as an internal standard.

3. Result and discussion

3.1. Graphene dispersion level test

The most important features affecting the properties of polymer nanocomposites include the homogeneity of dispersion of the filler in the matrix. In Fig. 2, photomicrographs of graphene, PVC and nanocomposites containing from 0.01 to 0.5 wt% of the filler are shown. The unmodified polymer in the form of a film (Fig. 2b) is a homogeneous material without evident structural defects and pores.

In the photomicrographs of the PVC/GN nanocomposites, defects or pores haven't been observed either (Fig. 2c–e). The filler is dispersed uniformly in the nanocomposite volume. Occurrence of sparse graphene aggregates has been observed, their number increasing with an increase in the filler fraction in the nanocomposite to 0.5%. The tendency of graphene fillers to form aggregates in PVC nanocomposites is a known phenomenon described in the literature [25,39]. Light is not transmitted through nanocomposites containing 1% and 5% of graphene, so their homogeneity cannot be determined by optical microscopy in the transmitted light.

3.2. Scanning electron microscopy

In Fig. 3, SEM images of graphene as well as cryogenic fractures of PVC and nanocomposites containing 1% and 5% of GN are shown. In the SEM image of graphene (Fig. 3b), flake structures characteristic for materials of such a type are evident, occurring in the form of layered aggregates with crumpled morphology. This type of morphology may

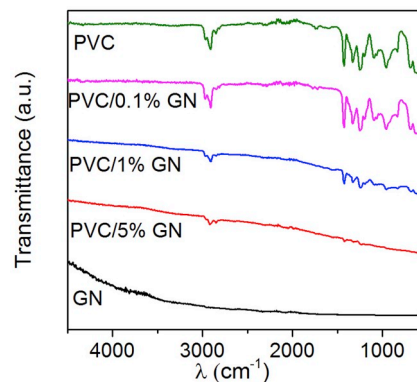


Fig. 4. FT-IR spectra of PVC, GN and PVC/0,1% GN, PVC/1% GN, PVC/5% GN nanocomposites.

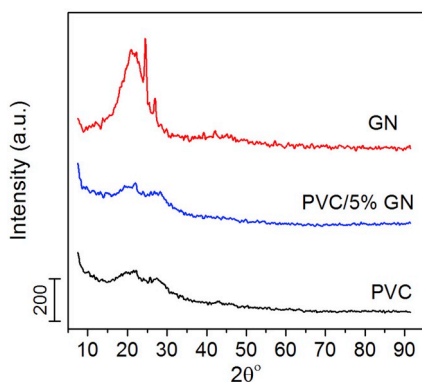


Fig. 5. XRD of PVC, GN and PVC/5% GN nanocomposite.

result from a high shape factor (thickness 1.6 nm, average flake length 10 μm) [40] and a high elasticity of the material used. The surface of the cryogenic fracture of unmodified PVC (Fig. 3b) is characteristic for brittle fracture of thermoplastics. On the other hand, the surface structure of fractures of the nanocomposites is uneven and rugged, indicating a ductile character of cracking and an increased resistance to brittle failure of the produced materials. Most probably, it results from the high elasticity of graphene and increased interfacial interactions between the nanofiller and the matrix [32–36]. Moreover, in the SEM images of PVC/5% GN nanocomposites (Fig. 3e and f), a high number of spherical tips may be noticed, confirming ductile fracture of the obtained materials. Good interfacial interactions between the matrix and the filler may be also proved by a lack of a visible interface.

3.3. FT-IR analysis

In the case of chemical interactions between the filler and the matrix, one may expect that FT-IR spectra of nanocomposites with graphene fillers will exhibit differences as for the range and intensity of the absorption bands [25,26].

The FT-IR spectrum of the unmodified PVC is typical for this material. No bands which could indicate undesirable degradation processes caused by a long time of sample drying at 65 °C are observed. In the spectra of the PVC and PVC/GN nanocomposite samples with various graphene concentrations, shown in Fig. 4, bands at the wave numbers of 2912 cm^{-1} and 1425 cm^{-1} were observed, attributed to the presence of C–H bonds in the PVC macromolecule [25,27,39]. The peak at 1252 cm^{-1} corresponds to bending vibrations of the C–H originating from CHCl [39]. The bands at 1099 cm^{-1} and 680 cm^{-1} are results of C–C and C–Cl tensile stress, respectively [25,39]. The increase in the graphene concentration in the PVC matrix is accompanied by a decrease in the intensity of peaks characteristic for the polymeric matrix.

The FT-IR spectrum of the PVC/5% GN nanocomposite is close to

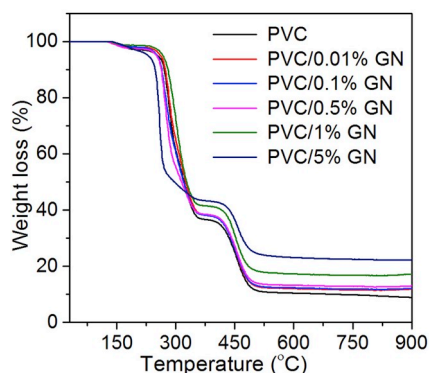


Fig. 6. TGA thermograms of PVC and PVC/GN nanocomposites.

Table 2

TGA results analysis.

Material	$T_{5\%}^{\circ}$ C	$T_{50\%}^{\circ}$ C	cont. of THF, %	max DTG, °C	Residual mass, %
PVC	255.0	320.9	2.2	284.1	8.9
PVC/0.01% GN	260.1	324.7	1.9	282.2	11.9
PVC/0.1% GN	252.3	319.9	1.9	284.0	12.1
PVC/0.5% GN	250.0	315.0	2.3	282.2	13.0
PVC/1% GN	262.4	324.9	1.3	299.2	17.2
PVC/5% GN	230.9	296.9	2.1	258.5	22.3

that of graphene. It is connected with the IR absorption by the graphene filler. The recorded spectra are flat and difficult to interpret. However, basing on the literature reports [27,39], it may be supposed that no chemical bonds form between graphene and PVC. The character of the interactions between graphene and PVC cannot be defined unambiguously based on the analysis of the spectra.

3.4. X-ray diffraction (XRD)

In Fig. 5, XRD spectra of unmodified PVC, graphene, and the nanocomposite containing 5 wt% of the filler are compared. The spectral image of the PVC film, lacking sharp diffraction peaks, confirms amorphous structure of the polymer; presence of a broad diffraction maximum corresponds to spacing of groups of atoms at average distances of 0.36 and 0.50 nm (van der Waals spacing between groups of atoms observed in most amorphous polymers) (Fig. 5) [41,42]. The broad diffraction peak with a maximum at 2θ ca. 21°, occurring in the XRD spectrum, is characteristic for graphene and reduced graphene oxide [43–45]. Narrow peaks at $2\theta = 26.5^{\circ}$ and 23.8° indicate the form of graphite C crystal structure (002). The presented spectrum confirms that graphene used as the filler is not a monolayer material. In the XRD spectrum of the PVC/5% GN nanocomposite, decay of the peaks characteristic for the graphite crystal structure has been observed, which may indicate exfoliation of graphene planes of the filler [28]. The effect results from the applied method of nanocomposite preparation, particularly from the impact of ultrasound treatment.

3.5. Thermogravimetric analysis (TGA)

In the TGA thermograms of PVC/GN nanocomposites (Fig. 6), one may observe occurrence of a slight mass loss at a temperature up to 170 °C, connected with the evaporation of the THF residue [27,28]. Further two-stage course of degradation of the nanocomposites is typical for poly(vinyl chloride), regardless of the graphene content. The first degradation stage (from 200 °C to 375 °C) is connected with dehydrochlorination, whereas the second stage (from 375 °C to 600 °C) – with

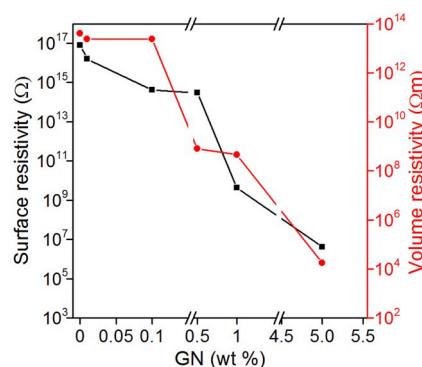


Fig. 7. Surface and volume resistivity of PVC and PVC/GN nanocomposites.

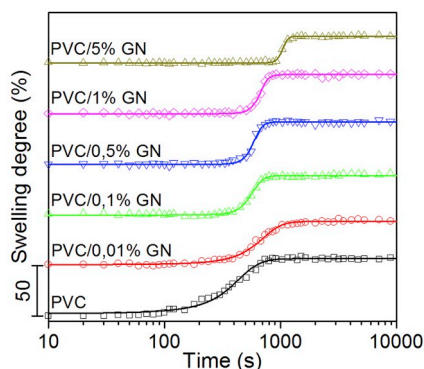


Fig. 8. Swelling degree of PVC and PVC/GN nanocomposites vs. time.

further degradation of the polymeric matrix [26–28,34]. The value of temperature of a 5% mass loss ($T_{5\%}$), treated as thermal stability, is similar for PVC and for the nanocomposites containing up to 1% GN, and the observed differences are no larger than $\pm 5\%$ (Table 2.). However, the PVC/5% GN nanocomposites are characterised by a distinctly lower thermal stability while compared to the other materials, which is proved by the value of temperature of a 5% mass loss lower by ca. 24 °C. The deterioration of thermal stability may result from the interfacial interactions of PVC and GN. They cause a weakening of the C–Cl bond in the polymer chain, leading to formation of chlorine radicals at a lower temperature, and as a consequence, acceleration of the thermal degradation process, which has been proved in publications [16,31]. In the paper [34], a good compatibility of multilayer graphene with the plasticiser and polymer, resulting in a weakening of the C–Cl bond was pointed out as a cause of the decrease in thermal stability of plasticised nanocomposites of poly(vinyl chloride) with graphene in relation to the unmodified matrix material. The THF residue found in the samples during TGA studies may effect a weakening of bonds in the poly(vinyl chloride) polymer chain in the presence of graphene, what consequently cause deterioration of thermal stability of highly filled PVC/GN nanocomposites [46].

3.6. Electrical properties

In papers [31,34,47,48], it was shown that a modification of electrical properties of poly(vinyl chloride) using graphene is possible, the impact of GN on resistivity or conductivity of the PVC/GN nanocomposites being strongly connected with proper dispersion of the filler in the polymer matrix. An increase in electrical conductivity is observed for materials, in which the number of well-distributed nanoparticles is high enough for them to be able to contact, which allows for forming conductive paths.

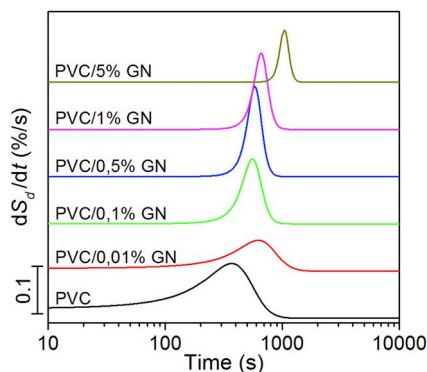


Fig. 9. The first derivative of swelling degree of PVC and PVC/GN nanocomposites vs. time.

Table 3

Parameters of the model describing the swelling process.

Material	S_{E_s} %	t_M , s	p , s^{-1}	R^2
PVC	56.9 (0.47)	370 (7.0)	0.0035 (0.00016)	0.992
PVC/0,01% GN	43.6 (0.34)	627 (8.2)	0.0026 (0.00009)	0.995
PVC/0,1% GN	39.0 (0.26)	556 (4.7)	0.0061 (0.00034)	0.996
PVC/0,5% GN	41.8 (0.30)	583 (4.6)	0.0079 (0.00058)	0.995
PVC/1% GN	38.7 (0.39)	661 (4.9)	0.0073 (0.00051)	0.995
PVC/5% GN	26.5 (0.19)	1041 (5.9)	0.0072 (0.00060)	0.996

In Fig. 7, resistivity of PVC and PVC-based composites as function of mass concentration of graphene is shown. It has been found that surface resistivity of poly(vinyl chloride) amounts to $8.08 \times 10^{16} \Omega$, and it decreases together with an increase in the graphene content in nanocomposites. A significant change in resistivity occurs in materials containing 1% and 5% of the filler, and its value in the case of PVC/5% GN samples is $4.3 \times 10^6 \Omega$. Assuming that surface resistance of anti-static materials amount to less than $3 \times 10^8 \Omega$ [34,47], one may include PVC films containing 1% and 5% of graphene in this group of materials. Similar effects of reduction of surface resistivity below $10^8 \Omega$ have been obtained for a PVC composite containing 3.5 wt% of reduced graphene oxide [32]. Thus, the method for preparation of nanocomposites proposed in our work allows for obtaining anti-static materials with a comparable carbon nanofiller fraction in the polymeric matrix.

Volume resistivity of the studied materials decreases with an increase in graphene concentration in the PVC matrix, and its rapid change occurs already at the filler content of 0.5 wt%. Volume resistivity determined for the PVC/5% GN amounts to $1.75 \times 10^4 \Omega m$, which is a 9-order change in comparison to the resistivity of unmodified poly(vinyl chloride) ($4.04 \times 10^{13} \Omega m$).

Such a significant change in volume and surface resistivities of the studied materials indicates the fact that in spite of a high aggregation tendency of the filler, its dispersion in the PVC matrix has been sufficient to form conductive paths.

3.7. Swelling behaviour

Poly(vinyl chloride) is commonly used for production of various types of pipes, tubes, films and gloves because of, among others, its resistance to various chemicals [26,49,50]. However, while exposed to ketones, ethers, esters and aromatic or chlorinated hydrocarbons, PVC undergoes swelling, and in some cases, even dissolution [37]. Poly(vinyl chloride) dissolves completely in THF and cyclohexanone, while in contact with acetone, it undergoes only limited swelling.

The impact of graphene on chemical against acetone of PVC-based

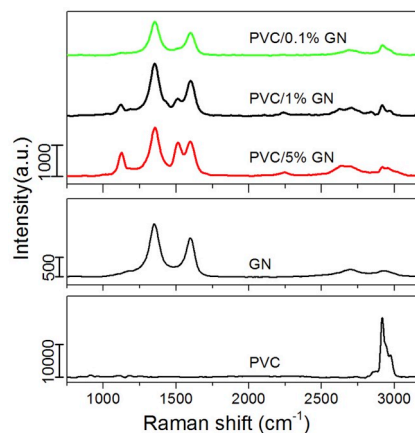


Fig. 10. Raman spectra of PVC, GN and PVC/0,1% GN, PVC/1% GN, PVC/5% GN nanocomposites.

nanocomposites was investigated by analysis of the swelling process in acetone. Swelling degree curves as function of time, are shown in Fig. 8. To illustrate the swelling kinetics of the studied materials better, also the first derivative was determined for the obtained dependences and shown in Fig. 9.

On the basis of the results of the sorption tests, it has been ascertained that all studied materials undergo limited swelling, and the dependence of the swelling degree on time of exposure to the swelling agent has a sigmoidal course. Therefore, Equation (2) has been proposed, which has been used as a basis for an approximation of the swelling curves.

$$S_d = \frac{S_E}{1 + 10^{(t_M - t)^p}} \quad (2)$$

where:

- S_d – swelling degree, %,
- S_E – equilibrium swelling, upper asymptote, %,
- t_M – time in which the swelling occurs with a maximum rate, s,
- t – time of exposure to the swelling agent, s,
- p – comparison parameter, 1/s.

Parameters of the equation and coefficient of determination R^2 describing the fitting degree of the experimental results the assumed model are gathered in Table 3. Standard error of the parameter estimation is reported in parentheses.

The proposed model describes the experimental results with a high accuracy, which is proved by high values of the coefficient of determination (close to one).

It has been found that the time, after which the PVC swelling process starts (10 s), increases with an increase in the nanofiller fraction in the matrix. For instance, this time amounts to 50 s for PVC/0.01% GN and 170 s for PVC/0.5% GN. The swelling process of nanocomposites with 5% of graphene starts no sooner than after 670 s. Simultaneously, it has been observed that the time of swelling with maximum rate (t_M) also increases. PVC/GN composites, even having the lowest used filler fraction, are characterised by a significantly lower value of the equilibrium swelling degree (S_E) while compared to PVC. The values of S_E for poly(vinyl chloride) amounts to 56.9%, whereas in the case of nanocomposites containing from 0.01% to 1.0% GN, it is similar and amounts to ca. 40%. The equilibrium swelling degree of PVC/5% GN is lower by 53% than that of the unmodified matrix material.

The presented results of experiments indicate that addition of graphene may effect an increase in chemical resistance of PVC against swelling agents. A similar effect was found using other carbon nanofillers [37,49] or in the case of chemical modification of PVC by additional chlorination of the polymer chain [51]. Most probably, the cause of the improvement of poly(vinyl chloride) chemical resistance resulting from modification with graphene consists in an increase of rigidity. Additionally some barrier effects can be observed, of PVC macromolecules and reduction of empty volumes, leading to a reduced access of solvent to the polymer chain [37,38].

3.8. Raman spectroscopy

Raman spectroscopy is a useful technique for examination of crystal structure of carbon materials, including graphene. Based on the

examination results, information on the degree of order or lattice defects of graphene may be obtained. Also, obtaining information on the number of layers and their exfoliation is possible [52]. In the case of graphene materials, peaks at the wavelengths of 1330–1360 cm^{-1} and in the range of 1580–1605 cm^{-1} , as well as at ca. 2700 cm^{-1} may be observed in the Raman spectrum. The peaks correspond to the D, G, and 2D bands, respectively. Moreover, some spectra contain bands at ca. 2900 cm^{-1} connected with secondary interactions, being a combination of the D-G peaks [53,54]. The G peak is connected with the sp^2 carbon crystal structure, while the D band provides information on defecting and impurities in the graphene structure. The 2D is connected with the number of graphene layers [47,52]. In the case of polyvinyl chloride and its composites, the bands occurring at ca. 2900 cm^{-1} correspond to CH_2 groups [55]. Raman spectra of graphene used as the filler, and those of the obtained nanocomposites are shown in Fig. 10. They were characterised by a high intensity of the D band, proving a high number of structural defects of the applied filler. Moreover, the intensity ratio of the D and G peaks (I_D/I_G) (Table 4) is higher in the case of nanocomposites, so the number of defects in the graphene structure increased during formation of the nanocomposites [16,27]. A broad diffraction peak 2D observed in the GN spectrum proves multilayer structure of the applied graphene [47]. Based on the dependence of the intensity ratio of the 2D and G bands (I_{2D}/I_G), the number of graphene layers may be calculated. For mono-, bi-, tri-, and multilayer graphene, this value amounts to >1.6, ~0.8, ~0.30, and ~0.07, respectively [52,56]. The values of I_{2D}/I_G indicate that the applied parameters of nanocomposite formation caused exfoliation of graphene. This is consistent with the results obtained by XRD. Moreover, distinct bands occurring at ca. 1110 and 1500 cm^{-1} were observed in the Raman spectra of PVC/1% GN and PVC/5% GN nanocomposites. It proves dehydrochlorination of the matrix material and formation of C=C double bonds [55]. Thus, graphene affects an accelerated degradation of polyvinyl chloride. The fact was not ascertained based in the FT-IR analysis, however a significant decrease in thermal stability of PVC nanocomposites/5%GN was observed in the TGA. Perhaps this is the effect of the catalytic action of graphene on dehydrochlorination of PVC macromolecules. Similar observations were found in PVC nanocomposites with carbon nanotubes [57].

4. Conclusions

The method applied for synthesis caused a exfoliation of graphene layers, and its satisfactory dispergation in the PVC matrix, which was proven based on the XRD analysis and Raman spectroscopy. However, in spite of the applied disintegration methods, graphene exhibits a tendency to agglomerate, which is evident in the form of aggregates in the PVC/0,5% GN nanocomposites. At a higher concentration of the nanofiller, these aggregates are not noticeable.

Graphene introduced into the PVC matrix exhibits barrier and swelling-inhibiting properties. PVC/GN nanocomposites are characterised by a lower value of equilibrium swelling. Moreover, the PVC/GN nanocomposites exhibit antistatic properties at high GN content.

An impact of GN on the acceleration of the PVC degradation process was found. In PVC/1% GN nanocomposites, the first symptoms of degradation were observed by Raman spectroscopy. In the case of PVC/5% GN nanocomposites, this effect is evident both in Raman spectroscopy spectra, and in the TGA.

Table 4
Raman spectroscopy analysis.

Material	$\lambda_D, \text{cm}^{-1}$	$\lambda_G, \text{cm}^{-1}$	$\lambda_{2D}, \text{cm}^{-1}$	I_D	I_G	I_{2D}	I_D/I_G	I_{2D}/I_G
GN	1348.5	1598.7	2696.3	1348.5	990.7	193.2	1.36	0.19
PVC/0,1% GN	1353.1	1598.7	2689.8	1085	735.4	181.1	1.39	0.25
PVC/1% GN	1353.1	1598.7	2708	1678	1126.8	272.5	1.49	0.24
PVC/5% GN	1354.6	1595.7	2695	1550.4	1109.1	319.3	1.47	0.29

Author statement

Sławomir Wilczewski, Conceptualization, Methodology, Validation, Investigation, Writing - Original Draft, Writing - Review & Editing, Visualization, Supervision. Katarzyna Skórczewska, Methodology, Investigation, Writing - Original Draft, Writing - Review & Editing. Jolanta Tomaszewska, Conceptualization, Writing - Original Draft, Writing - Review & Editing. Krzysztof Lewandowski, Methodology, Validation, Investigation, Writing - Original Draft, Writing - Review & Editing, Visualization.

Declaration of competing interest

The authors declare that they have no known competing financial interests or personal relationships that could have appeared to influence the work reported in this paper.

Acknowledgements

The results presented in this paper were funded with grants for education allocated by the Ministry of Science and Higher Education in Poland.

Appendix A. Supplementary data

Supplementary data to this article can be found online at <https://doi.org/10.1016/j.polymertesting.2019.106282>.

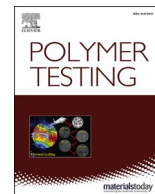
References

- J. Phiri, J. Gane, T.C. Maloney, General overview of graphene: production, properties and application in polymer composites, *Mater. Sci. Eng. B* 215 (2017) 9–28.
- S. Ren, P. Rong, Q. Yu, Preparations, properties and applications of graphene in functional devices: a concise review, *Ceram. Int.* 44 (2018) 11940–11955.
- J. Jonik, M. Purchała, H. Grajek, Methods of synthesis and testing properties of graphene, *Aparatura Badawcza i Dydaktyczna* 2 (2016) 110–117.
- V.D. Mohan, K. Lau, D. Hui, D. Bhattacharyya, Graphene-based materials and their composites: a review on production, applications and product limitations, *Composites Part B* 142 (2018) 200–220.
- M.C. Lemme, L. Li, T. Palacios, F. Schwierz, Two-dimensional materials for electronic applications, *MRS Bull.* 39 (2014) 711–718.
- J. Hass, W.A. de Heer, E.H. Conrad, The growth and morphology of epitaxial multilayer graphene, *J. Phys. Condens. Matter* 20 (2008) 1–27.
- N.A. Abdel Ghany, S.A. Elsherif, H.T. Handal, Revolution of graphene for different applications: state-of-the-art, *Surfaces and Interfaces* 9 (2017) 93–106.
- A.A. Balandin, S. Ghosh, W. Bao, I. Calizo, D. Teweldebrhan, F. Miao, C.N. Lau, Superior thermal conductivity of single-layer graphene, *Nano Lett.* 8 (2008) 902–907.
- T. Schwamb, B.R. Burg, N.C. Schirmer, D. Poulikakos, An electrical method for the measurement of the thermal and electrical conductivity of reduced graphene oxide nanostructures, *Nanotechnology* 20 (2009) 1–5.
- L.A. Jauregui, Y. Yue, A.N. Sidorov, J. Hua, Q. Yue, G. Lopez, R. Jalilian, D. K. Benjamin, et al., Thermal transport in graphene nanostructures: experiments and simulations, *ECS Transaction* 28 (2010) 73–83.
- M. Hebda, A. Lopata, Graphene – material of the future, *Tech. Trans. Mech.* 22 (2012) 45–53.
- C. Lee, X. Wei, J.W. Kysar, J. Hone, Measurement of the elastic properties and intrinsic strength of monolayer graphene, *Science* 321 (2008) 385–388.
- K. Piszczek, Żelowanie Suspensyjnego, Nieplastyfikowanego Poli(chloroku Winylu), *Rozprawa Habilitacyjna*, UTP University Publishing., 2009. ISSN 0209-0597.
- P. Karmal, T. Hjertberg, A. Jansson, R. Dahl, Thermal stability of poly(vinyl chloride) with epoxidised soybean oil as primary plasticizer, *Polym. Degrad. Stab.* 94 (2009) 2275–2281.
- L. Yunhua, K. Santosh, A. Saad, X. Shiai, Mechanical and thermal properties of poly(vinyl chloride) composites filled with carbon microspheres chemically modified by a biopolymer coupling agent, *Compos. Sci. Technol.* 172 (2019) 29–35.
- J. Hu, X. Jia, C. Li, Z. Ma, G. Zhang, W. Sheng, X. Zhang, Z. Wei, Effect of interfacial interaction between graphene oxide derivatives and poly(vinyl chloride) upon the mechanical properties of their nanocomposites, *J. Mater. Sci.* 49 (2014) 2943–2951.
- S. Zajchowski, Polymer-wood composites, *Chemik* 57 (2004) 15–18.
- K. Kłapiszewski, J. Tomaszewska, K. Skórczewska, T. Jesionowski, Preparation and characterization of eco-friendly Mg(OH)₂/Lignin hybrid material and its use as a functional filler for poly(vinyl chloride), *Polymers* 9 (2017) 1–19.
- T.A. Taha, A.A. Azab, Thermal, optical, and dielectric investigations of PVC/La_{0.95}Bi_{0.05}FeO₃ nanocomposites, *J. Mol. Struct.* 1178 (2019) 39–44.
- A. Al Naim, N. Alnaim, S.S. Ibrahim, S.M. Metwally, Effect of gamma irradiation on the mechanical properties of PVC/ZnO polymer nanocomposite, *J. Radiat. Res. Appl. Sci.* 10 (2017) 165–171.
- T. Sterzyński, J. Tomaszewska, K. Piszczek, K. Skórczewska, The influence of carbon nanotubes on the PVC glass transition, *Compos. Sci. Technol.* 70 (2010) 966–969.
- K. Skórczewska, J. Tomaszewska, K. Piszczek, K. Lewandowski, Production and properties of rigid poly(vinyl chloride) nanocomposites with carbon nanotubes and graphite, *Przetwórstwo Tworzyw* 165 (2015) 290–293.
- S. Maiti, R. Bera, S. Kumar Karan, S. Paria, A. De, B.B. Kahtua, PVC bead assisted selective dispersion of MWCNT for designing efficient electromagnetic interference shielding PVC/MWCNT nanocomposite with very low percolation threshold, *Compos. B Eng.* 167 (2019) 377–386.
- A.A. Aljaafari, S.S. Ibrahim, T.A. El-Brolosy, Thermophysical and electrical characterization of PVC-SWNT nanocomposites, *Compos. Appl. Sci. Manuf.* 42 (2011) 394–399.
- K. Deshmukh, S.M. Khatake, G.M. Joshi, Surface properties of graphene oxide reinforced poly(vinyl chloride) nanocomposites, *J. Polym. Res.* 20 (2013) 1–11.
- K. Deshmukh, G.M. Joshi, Thermo-mechanical properties of poly(vinyl chloride)/graphene oxide as high performance nanocomposites, *Polym. Test.* 34 (2014) 211–219.
- H. Mudassir, L. Moonyong, Enhancement of the thermo-mechanical properties and efficacy of mixing technique in the preparation of graphene/PVC nanocomposites compared to carbon nanotubes/PVC, *Prog. Nat. Sci.: Mater. Int.* 24 (2014) 579–587.
- H. Mudassir, N.B. Arghya, L. Moonyong, Enhanced thermo-optical performance and high BET surface area of graphene@PVC nanocomposite fibers prepared by simple facile deposition technique: N₂ adsorption study, *J. Ind. Eng. Chem.* 21 (2015) 828–834.
- G.M. Joshi, K. Deshmukh, Optimized quality factor of graphene oxide-reinforced PVC nanocomposite, *J. Electron. Mater.* 43 (2014) 1161–1165.
- K. Nawaz, M. Ayub, N. Ul-Haq, M.B. Khan, M.B.K. Niaz, A. Hussain, The effect of graphene nanosheets on the mechanical properties of poly(vinyl chloride), *Polym. Compos.* 37 (2016) 1572–1576.
- S. Vadukumpully, J. Paul, N. Mahanta, S. Valiyaveetil, Flexible conductive graphene/poly(vinyl chloride) composite thin films with high mechanical strength and thermal stability, *Carbon* 49 (2011) 198–205.
- H. Wang, G. Xie, Z. Zhu, Z. Ying, Y. Zeng, Enhanced tribological performance of the multi-layer graphene filled poly(vinyl chloride) composites, *Composites Part A* 67 (2014) 268–273.
- H. Wang, G. Xie, Z. Zhu, Z. Ying, Y. Tong, Y. Zeng, Enhanced mechanical properties of multi-layer graphene filled poly(vinyl chloride) composite films, *J. Mater. Sci. Technol.* 31 (2015) 340–344.
- H. Wang, G. Xie, M. Fang, Z. Ying, Y. Tong, Y. Zeng, Electrical and mechanical properties of antistatic PVC films containing multi-layer graphene, *Composites Part B* 79 (2015) 444–450.
- H. Wang, G. Xie, M. Fang, Z. Ying, Y. Tong, Y. Zeng, Mechanical reinforcement of graphene/poly(vinyl chloride) composites prepared by combining the in-situ suspension polymerization and melt-mixing methods, *Composites Part B* 113 (2017) 278–284.
- H. Wang, G. Xie, C. Yang, Y. Zheng, Z. Ying, W. Ren, Y. Zeng, Enhanced toughness of multilayer graphene-filled poly(vinyl chloride) composites prepared using melt-mixing method, *Polym. Compos.* 38 (2017) 138–146.
- M. Khaleghia, K. Didehbana, M. Shabaniab, Simple and fast preparation of graphene oxide@ melamine terephthaldehyde and its PVC nanocomposite via ultrasonic irradiation: chemical and thermal resistance study, *Ultrason. Sonochem.* 43 (2018) 275–284.
- Z. Asgarzadeh, G. Naderi, Morphology and properties of unvulcanized and dynamically vulcanized PVC/NBR blend reinforced by graphene nanoplatelets, *Int. Polym. Process.* 33 (2018) 497–505.
- Y. Xiao, B. Xin, Z. Chen, L. Lin, Y. Liu, Z. Hu, Enhanced thermal properties of graphene-based poly(vinyl chloride) composites, *J. Ind. Text.* 48 (2019) 1348–1363.
- J. Kim, L.J. Cote, J. Huang, Two dimensional soft material: new faces of graphene oxide, *Acc. Chem. Res.* 45 (2012) 1356–1364.
- F. Ammari, M. Dardouri, M. Kahlaoui, F. Meganem, Structure and electrical study of new chemically modified poly(vinyl chloride), *Int. J. Polym. Sci.* (2015) 1–5.
- M. Gilbert, Crystallinity in poly(vinyl chloride), *J. Macromol. Sci. C Polym. Rev.* 34 (1994) 77–135.
- R. Siburian, H. Sihotang, S. Lumban Raja, M. Supeno, C. Simanjuntak, New route to synthesize of graphene nano sheets, *Orient. J. Chem.* 34 (2018) 182–187.
- S. Hareema, H. Mobein, Y.A. Hina, Synthesis route of reduced graphene oxide via thermal reduction of chemically exfoliated graphene oxide, *Mater. Chem. Phys.* 204 (2018) 1–7.
- Ch Fu, G. Zhao, H. Zhang, S. Li, Evaluation and characterization of reduced graphene oxide nanosheets as anode materials for lithium-ion batteries, *Int. J. Electrochem. Sci.* 8 (2013) 6269–6280.
- K. Piszczek, J. Tomaszewska, K. Skórczewska, K. Lewandowski, The resistance of commercial plasticized PVC materials to the swelling factors, *Przetwórstwo Tworzyw* 163 (2015) 33–37.
- Z. Wei, Y. Zhao, Ch Wang, S. Kuga, Y. Huang, M. Wu, Antistatic PVC-graphene composite through plasticizer-mediated exfoliation of graphite, *Chin. J. Polym. Sci.* 36 (2018) 1361–1367.
- F. Ma, N. Yuan, J. Ding, The conductive network made up by the reduced graphene nanosheet/polyaniline/poly(vinyl chloride), *J. Appl. Polym. Sci.* 128 (2013) 3870–3875.

- [49] G. Broza, K. Piszczek, K. Schulte, T. Sterzyński, Nanocomposites of poly(vinyl chloride) with carbon nanotubes (CNT) composites, *Sci. Technol.* 67 (2007) 890–894.
- [50] W. Brostow, H.E. Hagg Lobland, *MATERIALS Introductions and Applications*, Wiley, 2017.
- [51] C. Xu, S. Wang, L. Shao, J. Zhao, Y. Feng, Structure and properties of chlorinated polyvinyl chloride graft copolymer with higher property, *Polym. Adv. Technol.* 23 (2012) 470–477.
- [52] S. Hatamie, O. Akhavan, S. Sadrnezhad, M. Ahadian, M. Shirolkar, H. Wang, Curcumin-reduced graphene oxide sheets and their effects on human breast cancer cells, *Mater. Sci. Eng. C* 55 (2015) 482–489.
- [53] N. Ferralis, Probing mechanical properties of graphene with Raman spectroscopy, *J. Mater. Sci.* 45 (2010) 5135–5149.
- [54] F. Johra, J. Lee, W. Jung, Facile and safe graphene preparation on solution based platform, *J. Ind. Eng. Chem.* 20 (2014) 2883–2887.
- [55] V. Solodovnichenko, V. Polyboyarov, A. Zhdanok, A. Arbuzov, E. Zapevalova, Y. Kryazhev, V. Likhobobov, Synthesis of carbon materials by the short-term mechanochemical activation of polyvinyl chloride, *Procedia Engineering* 152 (2016) 747–752.
- [56] Q. Wang, T. Chen, B. Zhang, M. Li, Y. Lu, K. Chen, All-fiber passively mode-locked thulium-doped fiber ring laser using optically deposited graphene saturable absorbers, *Appl. Phys. Lett.* 102 (2013) 131117.
- [57] E. Abdel-Fattah, A. Alharthi, T. Fahmy, Spectroscopic, optical and thermal characterization of polyvinyl chloride-based plasma-functionalized MWCNTs composite thin films, *Appl. Phys. A* 125 (2019) 475.

Publikacja [P2]

Manufacturing homogenous PVC/graphene nanocomposites using a novel dispersion agent



Manufacturing homogenous PVC/graphene nanocomposites using a novel dispersion agent

Sławomir Wilczewski^{a,*}, Katarzyna Skórczewska^a, Jolanta Tomaszewska^a,
Krzysztof Lewandowski^a, Joanna Szulc^a, Tomasz Runka^b

^a Faculty of Chemical Technology and Engineering, UTP University of Science and Technology in Bydgoszcz, Seminaryjna 3, 85-326, Bydgoszcz, Poland

^b Institute of Materials Research and Quantum Engineering, Poznan University of Technology, Piotrowo 3, Poznań, 60-965, Poland

ARTICLE INFO

Keywords:

Graphene
Dispersion
Nanocomposites
poly(vinyl chloride)

ABSTRACT

The goal of the study was to prepare a graphene (GN) dispersion in a poly (vinyl chloride) (PVC) solution with enhanced stability of the nanofiller thanks to the application of curcuma extract (CE). The stable dispersion was used to obtain PVC/GN nanocomposites with more homogeneous graphene by the solvent evaporation method. The CE effectiveness was compared with two commercially available dispersants in the form of oleic acid (OA) and polysorbate 80 (P80).

The chemical composition of the CE was examined by Fourier-transform infrared spectroscopy. The dispersion stability was tested by the multiple light scattering method (Turbiscan Lab) and evaluated visually over a period of 40 days. The homogeneity of the filler's dispersion in the PVC matrix was evaluated by scanning electron microscopy and Raman spectroscopy.

The application of the dispersing agents led to improved stability of the graphene dispersion in PVC solution. CE was the agent that most effectively improved the homogeneity of graphene dispersion, both in dispersions in a PVC solution and in PVC/GN nanocomposite films.

1. Introduction

Despite the fact that the vast majority of publications concerning poly (vinyl chloride)/graphene (PVC/GN) nanocomposites relate to materials prepared with GN dispersions in a PVC solution or a plasticizer as an intermediate product [1–9], no articles have been found on the impact of this stage on the filler's dispersion in a polymeric matrix. Therefore, the goal of this paper was to investigate the impact of the stability of a GN dispersion in a PVC solution produced with an extract of *Curcuma longa* L. rhizome, and two commercial surfactants in the form of oleic acid and polysorbate 80 on the quality of the filler's dispersion in nanocomposites obtained by the solvent evaporation method.

GN is a two-dimensional nanostructure consisting of carbon atoms with sp^2 hybridization. It may be considered a basic structural unit forming such carbon allotropes as carbon nanotubes, fullerenes, and graphite [10–12]. The isolation of GN from graphite in 2004 initiated a series of studies on its properties and the preparation methods and potential applications of this material [12].

The research carried out to date indicates that GN has exceptional

mechanical properties and is characterized by high tensile strength and high elasticity. It is an excellent conductor of heat and electricity and has 97.7% transparency [13–17]. Additionally, it has unique catalytic properties, a large specific surface area, and interesting barrier and antibacterial properties [10,18]. All of the above properties make this material potentially applicable in chemistry, medicine, the automotive industry, or electronic engineering. Also, a great deal of research is being carried out on the use of GN as a filler for polymer nanocomposites [2, 10,11,15,16,19–23].

Recently, an increase in the interest in polymeric nanocomposite materials can be observed, particularly when it comes to their application as construction materials. Over the last two decades, widespread research on polymer nanocomposites with GN has revealed that the application of GN as a reinforcement in the polymeric matrix can result in a significant improvement of the properties of such materials, simultaneously increasing their application potential [11,13,19–21,24].

Despite the numerous literature reports on polymer nanocomposites with GN, only relatively few papers relate to the modification of PVC. The impact of fillers with GN flakes on the properties of PVC described in

* Corresponding author.

E-mail address: slawomir.wilczewski@utp.edu.pl (S. Wilczewski).

the literature on the subject indicates that adding such fillers to a polymeric matrix leads to increased thermal stability and chemical resistance, among other things [2,3,5,7,9,25]. Also, PVC/GN nanocomposites are characterized by higher values of modulus of elasticity and tensile strength than the unmodified polymer [6,7,9,26–28].

The properties of PVC nanocomposites with carbon fillers depend on the preparation method, the materials used in the production of the nanocomposites, and particularly on the homogeneity of the filler's dispersion in the polymeric matrix [29–32]. As with other nanomaterials, GN exhibits a tendency to form agglomerates or aggregates, degrading their properties [6,9,28,33]; this is particularly evident in the case of nanocomposites with a high GN content [2,6,8].

The tendency of GN to form agglomerates results from strong π - π interactions and van der Waals forces [34–37]. The basic methods for preventing aggregation are divided into non-covalent including particle adsorption on the surface and covalent, including chemical reactions with GN carbon atoms [34,36,38].

The non-covalent methods for preventing the aggregation of GN are divided into four main groups, according to the functionalization mechanism. The first group includes methods connected with π - π interactions [35,39–42]. The second mechanism is based on cation- π interactions [43,44]. Another method for increasing the dispersibility of GN is based on use of hydrophilic/hydrophobic effects [34,36,38,45], while the last non-covalent method is modifying the GN surface with nanoparticles, limiting secondary agglomeration [38,46,47].

Non-covalent modification of GN, leading to better dispersibility, has more advantages over covalent functionalization. Most of all, it does not require the use of dangerous chemicals, and it causes no changes to the structure of the modified GN, which is necessary in order to maintain its many favorable properties. One interesting method for the functionalization of non-covalent GN is to modify its surface with curcumin. Some studies [39,48] used curcumin in the process of reducing graphene oxide. Meanwhile, the authors of another publication [42] used curcumin in the preparation of GN by ultrasonic exfoliation of graphite. It has been reported in the above-cited studies that the deposition of curcumin on the surface of GN effectively prevents its agglomeration. Curcumin is highly chemically stable in its natural form, making it ideal for numerous applications in engineering, medical science, and pharmaceuticals [49,50]. Another paper [42] demonstrated that curcumin is thermally stable up to approximately 180 °C, and in connection with GN, even up to approx. 220 °C. These properties of curcumin make it an interesting compound for use in modifications of polymeric materials, including. This has been confirmed by publications in which curcumin-based modifiers were used for plasticization, coloring, and increasing the antimicrobial properties of PVC [51–53].

However, no studies were found where curcumin was used to obtain PVC/GN nanocomposites. Because curcumin is a relatively expensive chemical reagent, the present study uses an extract obtained from the pulverized rhizome of *Curcuma longa* L. According to the literature, curcumin is the main active ingredient in such extracts [54–56]. The use of the curcuma extract (CE) offers lower costs and less consumption of harmful chemical reagents, thus increasing the applicability of the method described herein.

2. Experimental

2.1. Materials

Dispersions of GN in the PVC solution and the solution of PVC/GN nanocomposites were obtained using unmodified suspensive PVC Neralit-601, (Czech Republic, Spolana S.R.O. Anwil S.A. group) with a K-number of 59–61, a bulk density of 0.56–0.63 g cm⁻³, a specific density of 1.39 g cm⁻³, and a purity of about 97% (manufacturer's data). Nanopowder GN (USA GN Laboratories, Inc.) was used as a filler. According to the manufacturer, the GN flakes have the following characteristics: a flake thickness of 1.6 nm (max. 3 atomic monolayers), a flake

length of 10 μ m, and a specific surface area of 400–800 m² g⁻¹. Tetrahydrofuran (THF) was used as a solvent for the PVC (Chempur, Poland). The GN dispersion was stabilized in the PVC solution using oleic acid (Sigma-Aldrich Sp. z o. o.), polysorbate 80 (Sigma-Aldrich Sp. z o. o.), and *Curcuma longa* L. rhizome extract.

2.2. Preparation of *Curcuma longa* L. rhizome extract

The CE was obtained by extraction in a B-811 Büchi Soxhlet extractor (Switzerland). Twenty grams of *Curcuma longa* L. rhizome powder (Heuschen & Schrouff, Netherlands) was placed in a glass thimble and extracted with methanol (Chempur, Poland) at a temperature of 80 °C for 3 h. The solvent was then evaporated from the extract at 60 °C over 24 h, yielding a *Curcuma longa* L. rhizome extract.

2.3. Preparation of GN dispersion in the PVC solution and the PVC/GN nanocomposites

In the first stage of preparing the dispersion, PVC was dissolved in THF at 25 °C for approx. 48 h, yielding a solution with a concentration of 3% wt. GN was added to this solution and dispersed for 60 min at a temperature of 20 °C by ultrasound with a frequency of 20 kHz and an amplitude of 40%, using a SONOPULS homogenizer from Bandelin equipped with a rod probe until a visually homogeneous dispersion was obtained. Mixtures containing auxiliary dispersing agents were prepared in the same way, adding 1% wt. of a dispersing agent in relation to the weight of the PVC. The amount of GN in the prepared dispersions was 0.01%, 0.1%, and 1% wt. of the polymer weight.

PVC/GN nanocomposites in the form of a thin polymer film were obtained by the solvent evaporation method. The dispersion was poured onto Petri dishes with a diameter of 7 cm and the solvent was evaporated at a temperature of 50 °C for 24 h.

2.4. Methods

2.4.1. Fourier-transform infrared spectroscopy analysis

Identification of the chemical moieties present in the *Curcuma longa* L. rhizome extract, characterization of the intermolecular interactions between the GN filler and the matrix, and evaluation of the impact of the auxiliary dispersing agents on the structure of the PVC were carried out by Fourier-transform infrared spectroscopy (FT-IR) using the ATR technique. The study was performed with an Alpha apparatus from Bruker, in the range of 4000–400 cm⁻¹. A total of 32 scans at a resolution of 4 cm⁻¹ were performed. PVC films containing 0.1% GN were used for spectroscopic analysis.

2.4.2. Dispersion stability analysis

The evaluation of the stability of the obtained dispersions was carried out using the multiple light scattering method. To this end, 30 cm³ of PVC dispersions, containing 0.01%, 0.1%, and 1% GN, obtained without and with dispersing agents, were placed in glass cylindrical measurement test tubes with a working height of 53 mm, immediately after obtaining the dispersions. Then, the samples were placed in a Turbiscan Lab apparatus (Formulation SA, France) and subjected to scanning with light at a wavelength of 880 nm. The scans were carried out every hour for 24 h (sufficient time for THF to evaporate from the PVC solutions at room temperature and, as a result, to obtain a polymer film) at constant temperature of 23 °C.

The measuring system of this apparatus consists of two synchronized optical sensors. The first sensor receives light backscattered by the sample being examined (45° from the light source), while the second one receives light transmitted through the sample at an angle of 180° from the light source. During scanning, the head moves from the bottom to the top of the measurement cell. The result of the measurement using the Turbiscan Lab apparatus is represented by a percentage of transmitted light (*LT*) and backscattered light (*BS*) vs. the sample over a defined

time, automatically plotted by the Turbisoft 2.0.0.33 program. The physical principle of the Turbiscan Lab operation is based on the Lambert–Beer law (Formulas (1–2)). In the case of one sample, the proportion of LT depends only on the value of λ (Formula (1)), affected by particle size (d) and the volume concentration of the dispersive phase (\emptyset). If the initial \emptyset value is known, the main factor affecting the value of LT is d .

$$LT(\lambda, r_i) = LT_0 e^{-\frac{2r_i}{\lambda}} \quad (1)$$

$$\lambda(d, \emptyset) = \frac{2d}{3\emptyset Q_s} \quad (2)$$

where,

LT is the transmittance value
 λ is the mean free-path of photon
 r_i is the vial inner radius
 d is the average particle size
 \emptyset is the volume concentration of dispersion phase
 Q_s is the optical parameter according to Mie theory

As shown in Formula (3), light backscattering also depends on the particle size and volume concentration of the sample in suspension.

$$BS = \sqrt{\frac{3\emptyset(1-g)Q_s}{2d}} \quad (3)$$

where,

BS is the backscattering value
 \emptyset is the volume concentration of dispersion phase
 g is the optical parameter based on Mie theory
 d is the average particle size
 Q_s is the optical parameter according to Mie theory

Basically, the value of the transmitted light signal is used to analyze transparent liquids, while the value of the backscattered light signal is used to analyze non-transparent systems or samples with high concentrations [57–59]. Using the Turbisoft 2.0.0.33 software, the average values of transmitted light (LT_{Avg}) and backscattered light (BS_{Avg}) can be plotted for the whole height of the measurement cell, which are used for comparisons of dispersion systems. However, the most effective method of quantitative comparison of several systems (usually two-phase systems) consists in determining the Turbiscan Stability Index (TSI). For non-transparent systems, the TSI is determined from Formula (4); the higher the TSI value, the less stable the system [35,60,61].

$$TSI = \sqrt{\frac{\sum_{i=1}^n (X_i - X_{BS})^2}{n-1}} \quad (4)$$

where,

TSI is the Turbiscan Stability Index value
 X_i is the average backscattering for each time of measurement
 X_{BS} is the average value of x_i
 n is the number of scans

The stability of GN dispersions in a PVC solution was also determined by visual evaluation of the re-agglomeration and particle sedimentation processes. To this end, 1% dispersion of GN in PVC solution was placed in a tightly sealed test tube and observed for 40 days.

2.4.3. UV–vis spectroscopy

The UV–Vis absorption spectra of dispersions containing 0.01% GN and CE in a solution of PVC in THF were measured at 23 °C using a UV–Vis spectrophotometer (Hewlett-Packard Gmb, G1103A) in the

range of 200–800 nm with a 1-nm resolution.

2.4.4. GN dispersion level test in nanocomposites

Evaluation of the structure of prepared PVC/GN films on a macroscopic scale was carried out based on digital photographs taken with an OLYMPUS SP-510 UZ camera mounted on a tripod. A ZEISS AVO 40 scanning electron microscope (SEM) was used for microstructure evaluation. The samples for SEM observations were constituted by cryogenic fractures of the film with a sputtered gold layer.

2.4.5. Raman spectroscopy

Dispersion of the filler in the PVC matrix was also examined by Raman spectroscopy. The Raman spectrum of PVC nanocomposites containing 1% GN was recorded in the range of 100–3200 cm^{-1} using a Renishaw InVia microscope, equipped with a semiconductor laser emitting a wavelength of 785 nm. The power of the laser beam focused on the sample, with a 50 × objective lens, was maintained below 0.1 mW. The spatial resolution of the optical system achieved using an objective lens with a long working distance was better than 2 μm . The positions of the peaks were calibrated before data collection using a crystalline Si sample as an internal standard.

The UV–vis and Raman spectra analyses and other mathematical calculations were carried out using Origin 8.6 PRO software.

3. Results and discussion

3.1. FT-IR analysis of *Curcuma longa* L. rhizome extract

The main compounds contributing to the chemical activity of CE are curcuminoids, including curcumin (curcumin I), demethoxycurcumin (curcumin II), bisdemethoxycurcumin (curcumin III), and cyclocurcumin. Depending on the plant's origin and the soil conditions in which it is cultivated, curcuma contains from 2% to 9% curcuminoids, wherein curcumin I constitutes approx. 77% [50,54,62]. The phenolic compounds (mainly curcumin) listed above are also the main active components of extracts obtained by alcohol extraction of *Curcuma longa* L. rhizome [54–56].

In the FT-IR spectrum of the obtained CR shown in Fig. 1 bands originating from functional groups of curcuminoids are prevalent [54–56], which confirms that the extraction was carried out properly. The characteristic absorption bands of curcuma are presented in Table 1.

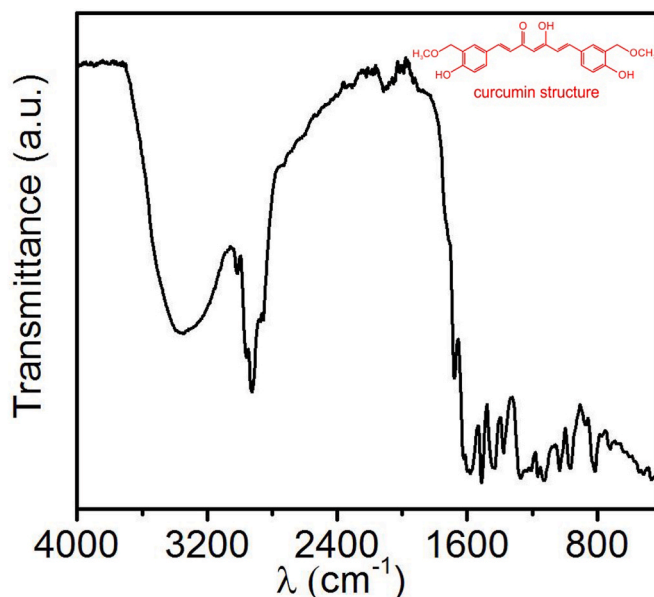


Fig. 1. FT-IR spectra of *Curcuma longa* L. rhizome extract.

Table 1Assignment of FTIR spectral bands of the extract obtained from the rhizome of *Curcuma longa* L.

Wave numbers, cm^{-1}	Functional groups
3347	-O-H stretching vibration
3015	C-H aromatic stretching vibration
2924	-CH ₂ asymmetric stretching
1678	C=O stretching
1581	C=C aromatic stretching
1511	Benzene ring bending vibration
1442	CH ₂ bending
1376	CH ₃ bending
1271	enol C-O peak
1124	C-O stretching
1029	C-O-C peak
964	benzoate trans-CH vibration
815	aromatic CH bending

3.2. Dispersion stability analysis

3.2.1. Turbiscan analysis

The multiple light scattering method (utilized in the Turbiscan Lab instrument) is more and more frequently used for examination of dispersion stability; it also indicates the cause of any instability (flocculation, aggregation, or migration). For this reason, it is applicable in studies on various types of suspensions, including systems containing GN materials [35,60,61,63–65].

The plots presented in Fig. 2 show percentages of *LT* and *BS* vs. the sample height for a 0.1% GN dissipation in a PVC solution over the whole measurement time. Based on the results, it was found that all prepared suspensions were stable ($T = 0\%$) at the moment of starting the

observation (completion of ultrasound sonication process). In the case of the dispersion sample prepared with no auxiliary dispersing agents, an increase in transparency and backscattered light intensity over time was observed, indicating that the suspension was stratified as a result of the formation of secondary GN aggregates [59,61]. Moreover, the study indicated that the GN agglomerates which formed underwent sedimentation, leading to a densification of the lower dispersion layer, which was manifested by the fact that the sample transparency did not increase between 1 and 3 mm of the cell height, while there was a simultaneous increase in *BS* intensity. Flocculation and agglomeration processes [66] are particularly evident in the top layer of the PVC/0.1% GN suspension. The PVC/0.1%GN dispersions prepared using additional dispersing agents did not undergo stratification, which is proven by the lack of increased transparency [64]. The *LT* value recorded in the plots at *H* close to 0 mm, amounting to approx. 2%, is connected with the design of the measuring cell, and not with changes occurring in the dispersion. The observations of backscattered light indicate a slight increase in *BS* intensity over time in the bottom layer of suspensions prepared with the addition of OA and CE. This fact may indicate sedimentation of particles which have not undergone disaggregation during the sonication process, or a secondary process of GN agglomeration and sedimentation [35]. However, this process is less intense than in the case of a dispersion with no additional auxiliary agents. In the *BS* plot for the suspension prepared with the addition of P80, spots of a higher backscattered light intensity (between 23 mm and 53 mm) may be observed, constant over 24 h. Most likely, they are connected with the presence of GN agglomerates which have not undergone disaggregation in the sonication process. These agglomerates do not undergo sedimentation.

The stability of dispersions containing various concentrations of GN in a PVC solution were compared on the basis of the average value of

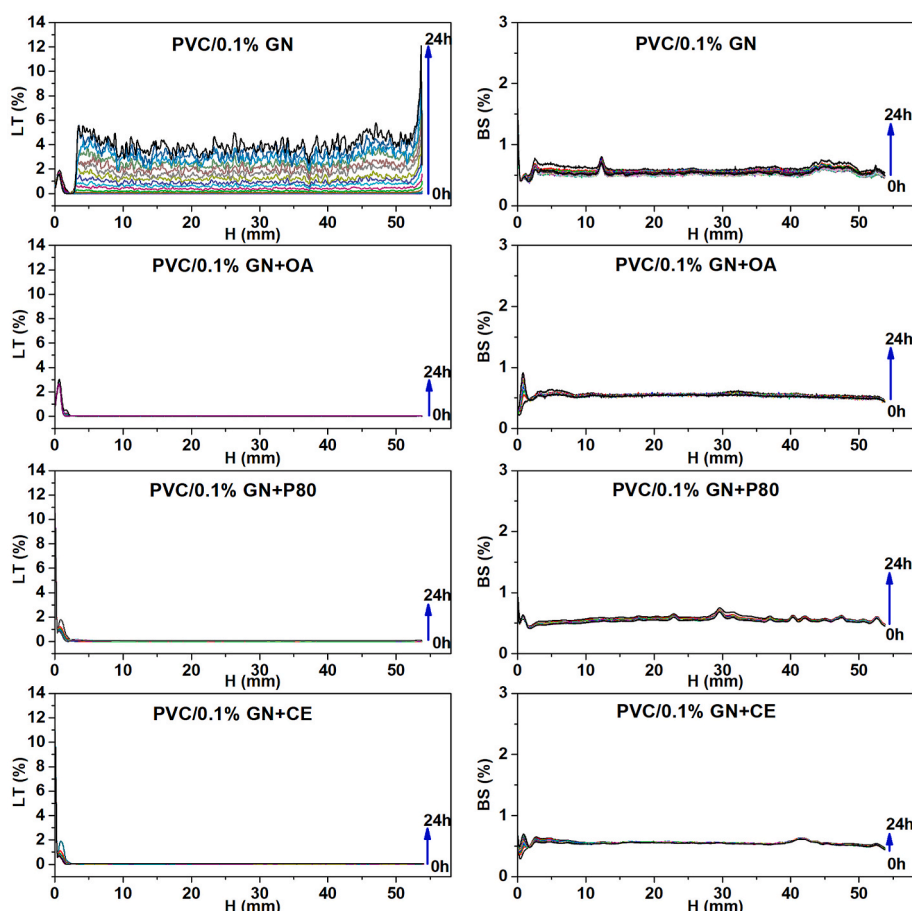


Fig. 2. *LT* and *BS* of GN dispersions containing 0.1% GN in a PVC solution.

transmitted light LT_{Avg} (Fig. 3). The lower average LT_{Avg} values of dispersions containing 0.01% GN and dispersing agents in comparison to dispersions obtained without these agents and the LT_{Avg} values close to 0% in the case of systems containing dispersing agents and GN, over the whole measurement range, indicate an increase in the stability of GN dispersions in PVC solution [64,66] connected with the application of dispersing agents. The low LT_{Avg} value for systems containing 0.01% GN and auxiliary agents indicates that applying dispersing agents not only increases the stability time of GN dispersions, but also ensures better disaggregation in the ultrasound sonication process. It was also observed that the dispersion containing 0.1% GN was stable for 12 h, while the system containing 1% GN was only stable for 3 h. In the system containing 0.01% GN, only a slight change in the amount of transmitted light occurred during the measurement, i.e., over 24 h. This indicates that an increase in GN concentration in the systems obtained without dispersing agents causes a reduction of the dispersion stability time. Thus, it may be concluded that the results confirm the previously-mentioned observations which indicate a better ultrasonic disaggregation of GN in a PVC solution when dispersing agents are used. It should be emphasized that an improvement in GN distribution in the dispersions was found irrespective of its concentration.

The destabilization kinetics of the prepared dispersions may also be determined based on the *BS* results (according to Formula (4)). Based on the generated TSI curves (Fig. 4), it was ascertained that a suspension with 0.01% GN prepared without dispersing agents destabilizes gradually from the beginning, a finding that is indicated by the constant increase in the TSI value over time [61,63]. The PVC/0.01%GN + P80 dispersion was characterized by the highest TSI value in the first hour of the measurement, which could indicate instability. However, in next hours of measurement, the TSI value of this dispersion was constant, contradicting the above supposition. The systems containing 0.01% GN, as well as OA and CE, exhibited the highest stability, confirmed by the TSI value being close to zero and the slight change during measurement [35,61,63]. An analysis of the destabilization kinetics of dispersions containing 0.1% GN confirmed the higher stability of systems containing dispersing agents that was observed earlier. Also, in this case, the suspensions containing oleic acid and CE yielded the lowest TSI values and were constant during the whole measurement time. On the other hand,

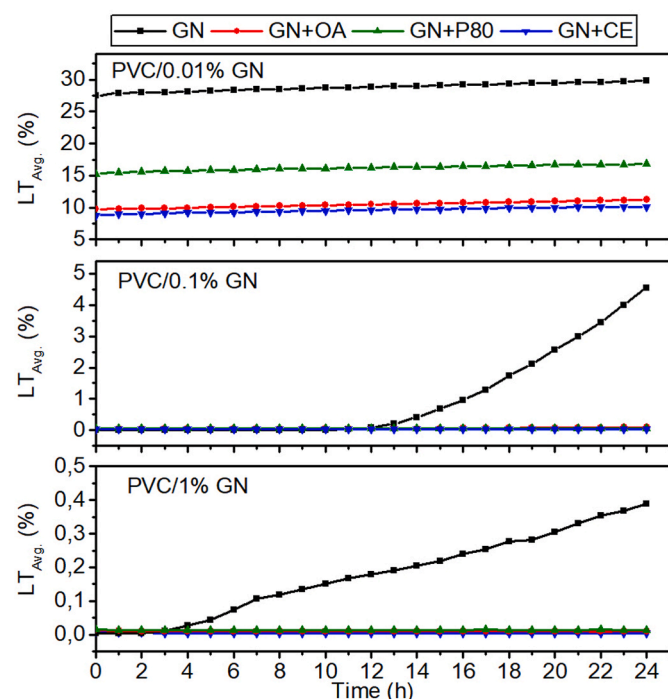


Fig. 3. LT_{Avg} value of GN dispersions in a PVC solution.

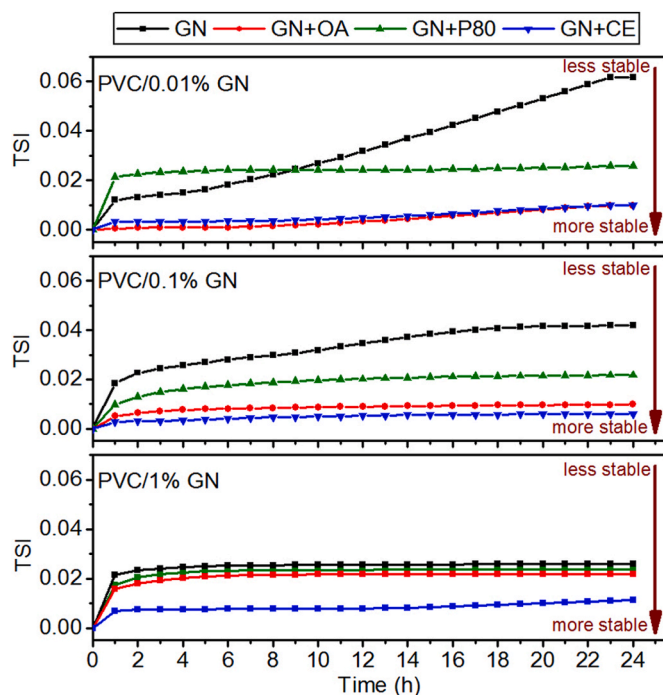


Fig. 4. Turbiscan stability index of GN dispersion in a PVC solution.

in the case of dispersions containing 1% GN, systems without auxiliary agents and systems with OA and P80 were characterized by similar TSI values. Only for the PVC/1%GN + CE dispersion was the TSI value distinctly lower and demonstrated slight changes in time, indicating that this system was the most stable [35,60,61].

The turbidimetric analysis of stability of the GN dispersions in a PVC solution proved that the application of auxiliary dispersing agents improved the stability of these systems. Additionally, dispersing agents in the form of polysorbate 80, oleic acid, and CE turned out to be effective in the ultrasound sonication process, causing an increase in GN dispersion in the PVC solution. However, based on the results confirming the effectiveness of using P80, OA, and CE as agents for improving the dispersion of GN in a PVC solution and the stability of the resulting dispersions, one cannot conclude unambiguously about their usefulness in the preparation of homogeneous PVC/GN nanocomposites. This is particularly important in the case of materials with relatively high nanofiller content, wherein as indicated in various studies [2,6,30] GN exhibits the highest tendency to form agglomerates. Therefore, a visual assessment of the re-agglomeration and sedimentation of GN containing 1% nanoparticles was carried out.

3.2.2. Visual assessment of GN dispersion in a PVC solution

Visual assessment of re-agglomeration and sedimentation is a relatively simple, but effective method for evaluating the dispersion of carbon nanoparticles [29]. The test that was done consisted in observing the suspensions until the first noticeable signs of instability occurred. The moment such signs occurred was considered to be the dispersion destabilization time. The results of these observations, shown in Fig. 5, confirmed that the destabilization of GN dispersions in a PVC solution proceeds in two stages. In the first stage, the carbon material undergoes a secondary agglomeration, while in the second stage, the GN agglomerates undergo sedimentation. A GN dispersion prepared without auxiliary agents destabilizes after approx. 15 h. Suspensions prepared with the addition of oleic acid and polysorbate 80 exhibited inhomogeneity after approx. 7 and 12 days, respectively. Dispersions prepared with the addition of CE did not show any noticeable signs of instability during the whole study, i.e., for 40 days.

These observations are consistent with the results of the

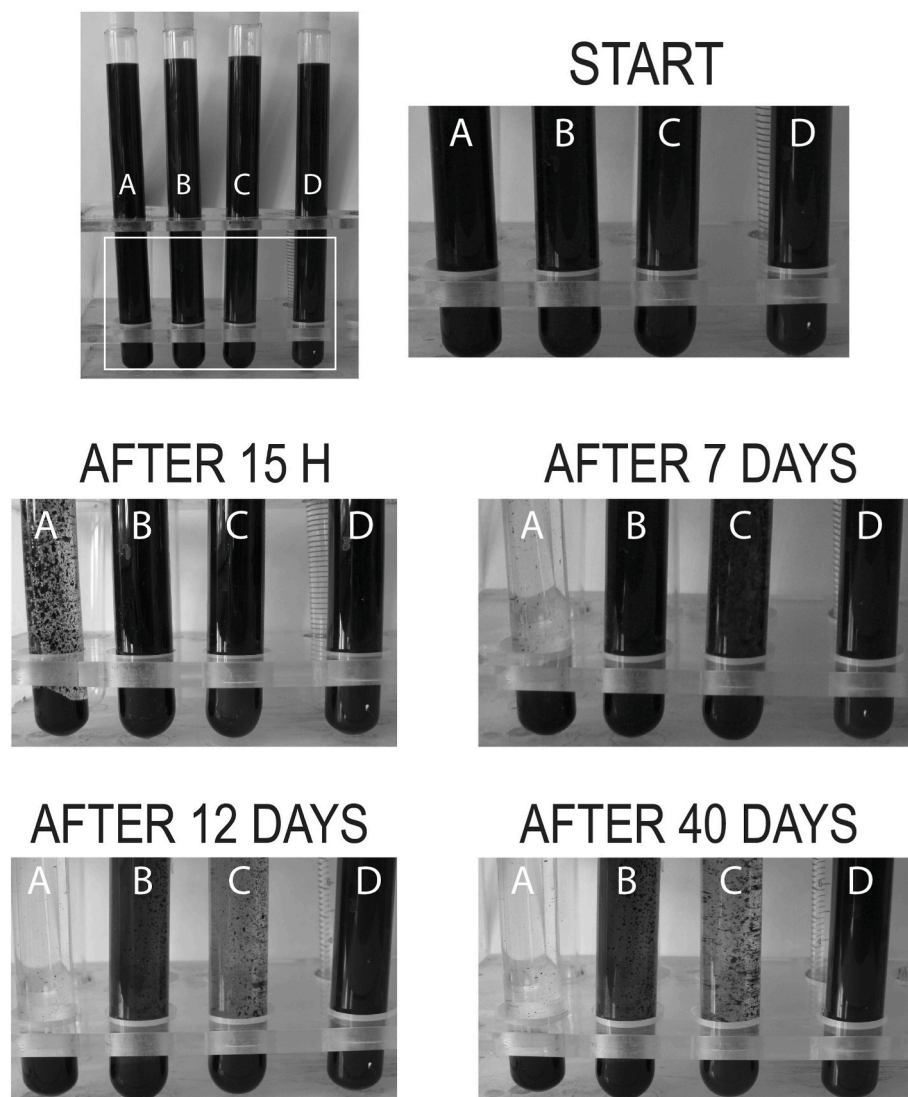


Fig. 5. Digital photographs of PVC/1%GN dispersions (A) GN, (B) GN + P80, (C) GN + OA, and (D) GN + CE.

turbidimetric analysis and confirm the effectiveness of all dispersing agents used in the study in terms of improving the stability of a GN dispersion in a PVC solution, particularly in the case of CE. Observations of changes of the dispersion over a longer period, i.e., 40 days, also led to the determination that the dispersion of a PVC solution with 1% GN and polysorbate 80 was stable for longer than the dispersion with oleic acid, which was not found during the turbidimetric tests.

3.3. UV-vis spectroscopy and stabilization mechanism

Based on the results reported in other papers [36–38], it was ascertained that the stabilization of GN nanoparticle dispersions using non-ionic surface active agents, including oleic acid and polysorbate 80, occurs due to hydrophilic/hydrophobic effects. Meanwhile, some authors have shown that the increase in the dispersibility of GN by curcumin occurs thanks to π - π complexation [39,42]. On the basis of these literature reports and the results obtained in the current study, it may be stated that the stabilization of a GN suspension by the complexation mechanism is an effective method for preventing GN secondary agglomeration in PVC solutions.

UV-visible spectroscopy studies were performed on dispersions containing 0.01% GN and CE in a solution of PVC in THF to investigate the π - π interactions. Fig. 6 presents the UV-Vis spectra of the GN, CE,

and GN + CE dispersions. As for the GN sample, one absorption peak at 264 nm can be seen, which was assigned to the π - π transition of C-C bonds [12,67]. The CE spectrum exhibits two absorption bands: the first with a maximum at 247 nm, which was assigned to the π - π transition of C-C bonds, and the second with a maximum at 425 nm, which corresponded to the n - π^* transition of C=O bonds [39,67]. The sample of GN + CE showed two absorption peaks at 240 and 410 nm. Changes in the width and shift of the maximum absorption of the dispersion peaks in relation to the UV-Vis spectrum of the extract confirm the π - π interactions GN and curcumin from CE [39,67,68]. Based on the literature presented above and the results of UV-Vis spectroscopy, the GN stabilization mechanism in a PVC solution shown in Fig. 7 was proposed.

3.4. GN dispersion level test in nanocomposites

The results of stability tests of GN dispersions in a PVC solution that are described above indicate a higher stability in systems prepared with auxiliary dispersing agents. To assess the impact of the dispersion stability on the homogeneity of GN distribution in PVC/GN nanocomposites formed after evaporation of THF, macro- and microscopic observations of the films were carried out. The homogeneity of a filler's dispersion in a polymer matrix is one of the most important features that affects the properties of nanocomposites [29–32].

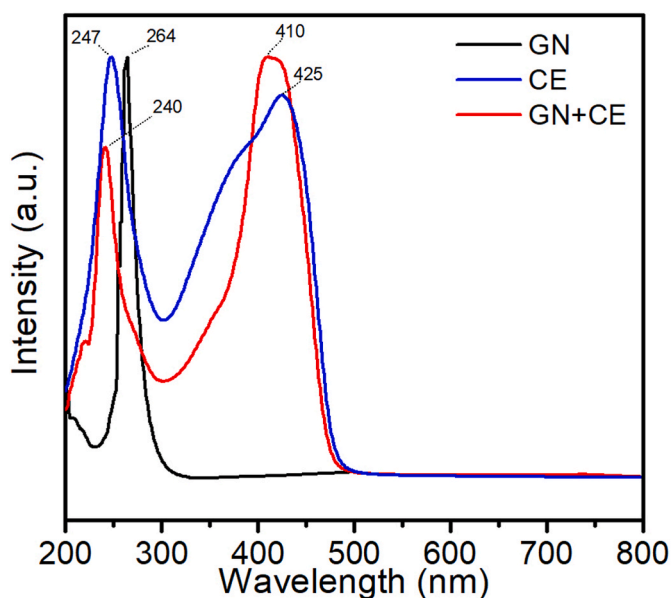


Fig. 6. UV-Vis spectra of the GN, CE, and GN + CE dispersion in a solution of PVC in THF.

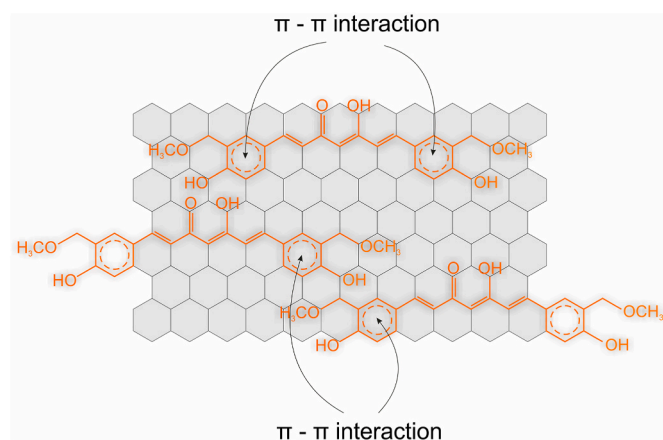


Fig. 7. GN stabilization mechanism.

The microscopic observations described in our earlier paper [30] proved that the amount of poorly dispersed (agglomerated) GN in PVC-based nanocomposites increases significantly in materials containing 0.5% or more of the filler. Therefore, only the nanocomposite films formed after solvent evaporation from dispersions containing 1% of the filler, prepared with or without dispersing agents, were tested in this study.

3.4.1. Macroscopic observations

The film obtained from the unmodified polymer (Fig. 8A) was a homogeneous material with no visible structural defects or pores. In the photographs of the nanocomposites (Fig. 8B–E) pores or other signs of structural discontinuity were not observed either. The observations have proven that GN is not dispersed uniformly in the whole volume of the nanocomposite. The largest aggregates of filler were observed in the photographs of films obtained without auxiliary dispersing agents and the PVC/1%GN + P80 film (Fig. 8B and D). Application of oleic acid improved the dispersion of nanoparticles in the nanocomposite significantly (Fig. 8C), which is proven by the smaller number and size of the agglomerates. The best dispersion of GN in the polymer matrix was observed in the photographs of the materials with CE (Fig. 8E).

3.4.2. Scanning electron microscopy

In Fig. 9, the SEM images of GN and the cryogenic fractures of the PVC and nanocomposites obtained from dispersions containing 1% GN are shown. In the SEM image of GN (Fig. 9A1, 9A2), flake structures characteristic of such materials are evident, occurring in the form of layered aggregates with crumpled morphology. Such morphology may result from the large GN flakes [25] and high elasticity of the material used. The surface of the cryogenic fracture of the unmodified PVC (Fig. 9B1, 9B2) is characteristic of the brittle fracture of the thermoplastics. On the other hand, the surface structure of fractures of nanocomposites is uneven and jagged (Fig. 9C2–9F2), indicating a ductile fracture of the prepared materials. Most likely, this results from the high elasticity of GN and the increased interfacial interactions between the nanofiller and the matrix [26–28,33,69]. On the basis of SEM images of the whole fracture surface of the nanocomposites (Fig. 9C1–9F1) the dispersion of GN in the materials can be assessed. These images (Fig. 9C1–9E1) confirm the tendency of GN to form agglomerates in a PVC matrix, as ascertained from the macroscopic observations. The most homogeneous distribution of GN on the fracture surface was observed in the case of the PVC/1%GN + CE composite (Fig. 9F1), confirming that using CE as a dispersing agent effectively improved the dispersion of GN in the matrix.

The analyses of nanocomposite photographs and SEM images carried out confirmed our suppositions that adding auxiliary dispersing agents is necessary in the preparation of PVC/GN nanocomposites by the solvent evaporation method with a homogeneous structure. These agents should simultaneously improve the disaggregation of the filler during the ultrasonic disintegration process and the stability (longevity) of the dispersion.

3.5. FT-IR analysis of nanocomposites

To assess the impact of the auxiliary dispersing agents on the chemical structure of polyvinyl chloride, the FT-IR spectra of unmodified matrix material and nanocomposites containing 0.1% GN were recorded (Fig. 10). In the spectrum of the PVC sample, bands at wavenumbers of 2909 cm^{-1} and 1430 cm^{-1} were observed, attributed to the presence of C–H bonds in the PVC macromolecule [3,8,70]. The peak at 1256 cm^{-1} corresponds to bending vibrations of the C–H group originating from CHCl [3]. The bands at 1093 cm^{-1} and 683 cm^{-1} result from C–C and C–Cl tensile stress, respectively [3,8]. Additionally, bands at wavenumbers of 3372 cm^{-1} and 1770 cm^{-1} and 1723 cm^{-1} may be observed in the PVC spectrum, connected with the presence of hydroxyl and carbonyl groups, respectively. Usually, bands originating from the above-mentioned chemical groups is not observed in PVC spectra. Most likely, their presence results from partial oxidation of PVC during the production process or from the presence of suspension stabilizers used in its polymerization [71,72]. The bands described above are also present in the spectra of samples of PVC/0.1%GN, PVC/0.1%GN + P80, and PVC/0.1%GN + CE nanocomposites. The lack of changes in infrared absorption bands in the spectra of these materials indicates that neither GN nor the auxiliary agents (polysorbate 80 and CE) change the chemical structure of PVC. On the other hand, in the PVC/0.1%GN + OA spectrum, a band from the carbonyl group at 1710 cm^{-1} may be observed, typical of oleic acid [73,74]. The relatively intense C=O group band in comparison to the content of oleic acid in the nanocomposite (1%) may indicate the fact that OA, as with some plasticizers used for PVC modification, migrates to the polymer surface [75,76]. However, as in the case of the dispersing agent mentioned above, its impact on the chemical structure of PVC was not found in the FT-IR analysis.

3.6. Raman spectroscopy

Raman spectroscopy provides important information on the structure of polymers [77] and carbon-containing materials. In Fig. 11, the Raman spectra of PVC, GN, and nanocomposites containing 1% GN and

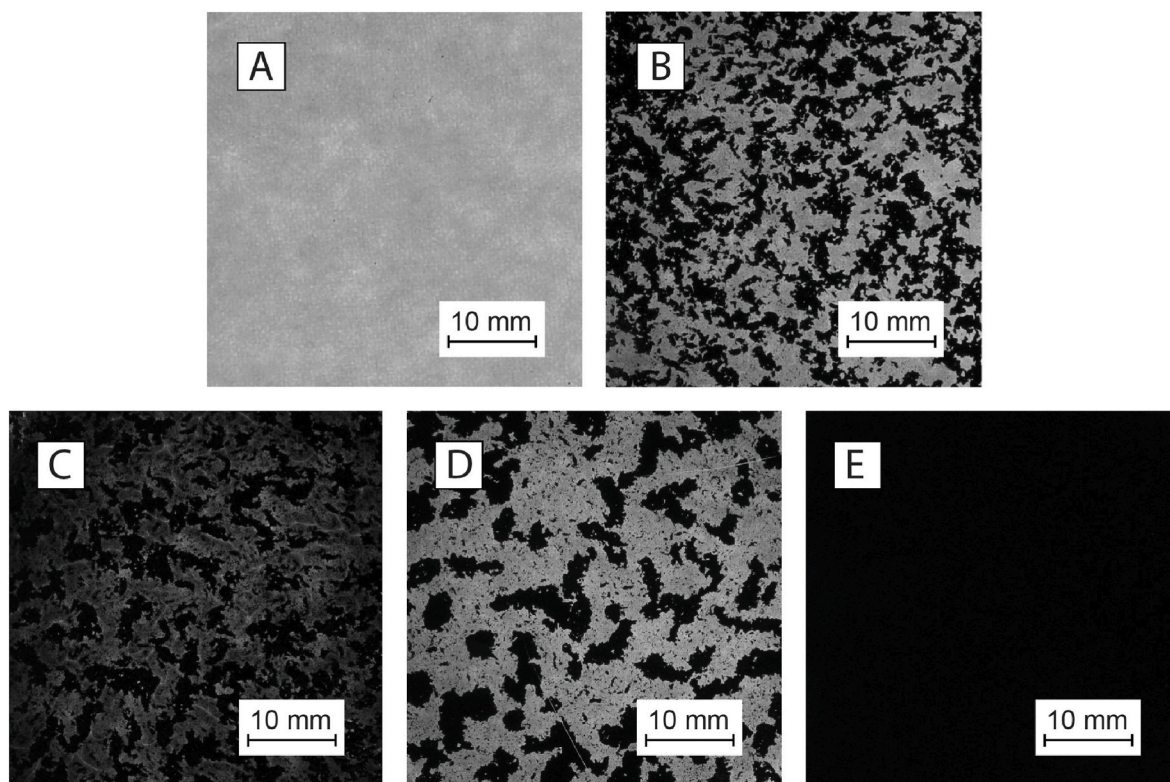


Fig. 8. Digital photographs of (A) PVC, (B) PVC/1%GN, (C) PVC/1%GN + OA, (D) PVC/1%GN + P80, and (E) PVC/1%GN + CE nanocomposites.

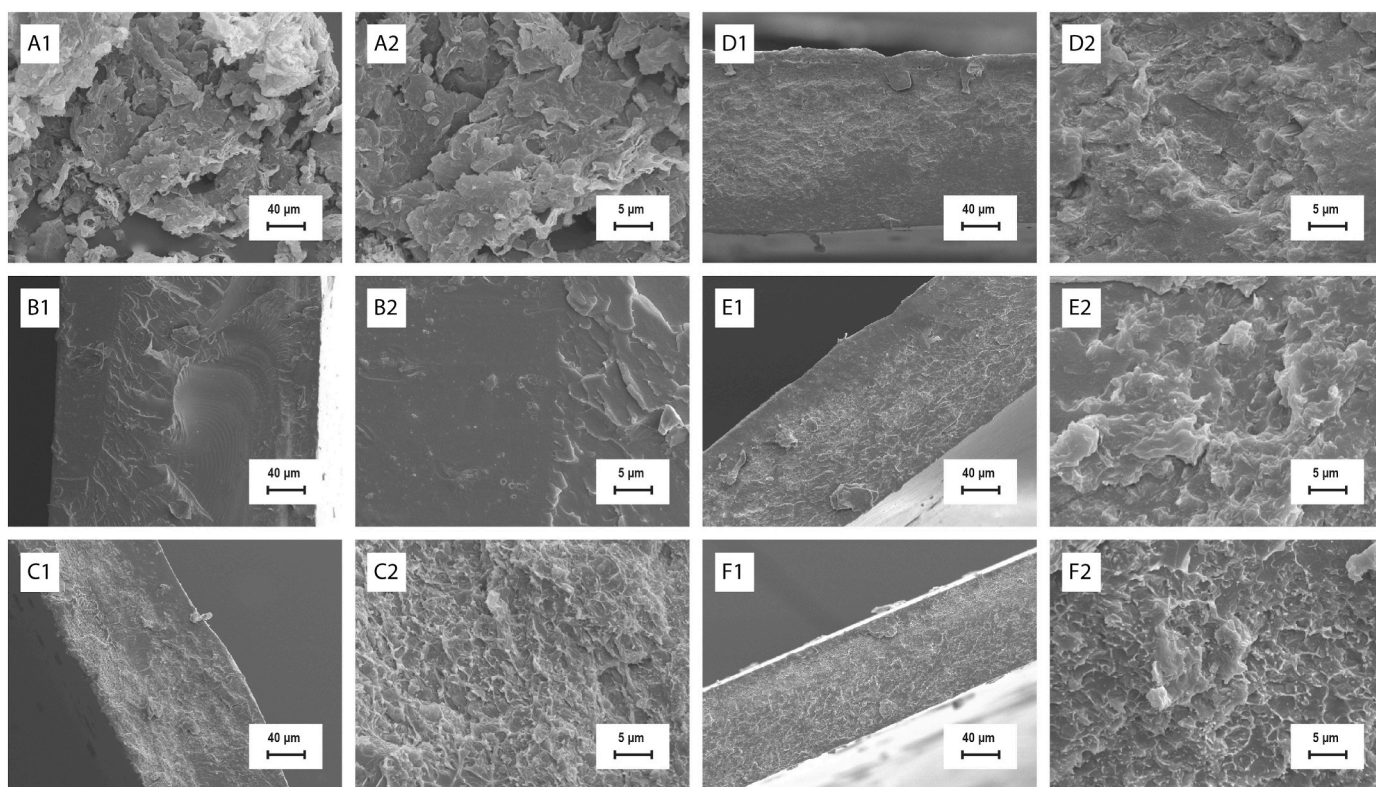


Fig. 9. SEM images (A) GN, (B) PVC, (C) PVC/1%GN, (D) PVC/1%GN + P80, (E) PVC/1%GN + OA, and (F) PVC/1%GN + CE.

auxiliary dispersing agents are shown. The spectrum of the unmodified matrix material is typical of PVC [78,79]. Simultaneously, a band characteristic of tetrahydrofuran was observed at 915 cm^{-1} in the

spectral image of the polymeric film formed after the solvent evaporation [80], indicating the fact that THF residue is present in the resulting materials, despite using the solvent evaporation method.

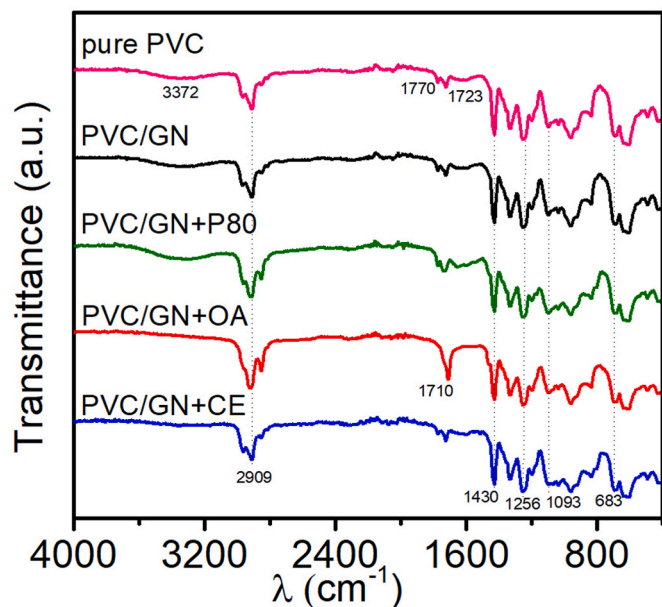


Fig. 10. FT-IR spectra of PVC and PVC/0.1%GN nanocomposites.

D and G bands characteristic of GN may be observed in the spectra of the filler and nanocomposites. The D band is connected with a disordered, diffuse carbonic structure, while the G band forms as a result of C–C bond stretching in graphite materials. In the case of GN, it may be connected to the formation of the filler's agglomerates [61,81]. The band intensity ratio, I_D/I_G , is commonly used for estimating GN domain size and the relative degree of graphitization of the material. This value

is inversely proportional to the crystallite size [34,61,82–84]. An analysis of the intensities of the D and G bands (Table 2) did not reveal any significant difference in GN dispersion between the nanocomposites obtained with the addition of OA and CE and the materials without auxiliary dispersing agents; the I_D/I_G values in these materials amounted to 1.8. The value of the band intensity ratio for the D and G bands in PVC/1%GN + P80 nanocomposites amounted to 1.7, which was lower than that of PVC/1%GN, indicating a worse dispersion of the filler in the materials with polysorbate 80. However, the analysis of the I_D/I_G ratio has some limitations; the distribution of domains with various sizes causes smaller domains to have a greater weight, which leads to an underestimation of the distribution of medium sizes. Using full width at half maximum of the D band (increasing significantly while the FWHM of the G peak is relatively stable) for the analysis seems to be a more precise method for estimating GN particle size, taking into account materials containing several layers [84]. The FWHM analysis of the D and G peaks revealed a significant increase in the $FWHM_D/FWHM_G$ ratio (Table 2) in the materials prepared with CE in relation to PVC/1%GN. This indicates a better dispersion of GN (which occurs in the form of sheets consisting of several layers) in these nanocomposites in relation

Table 2
Raman spectroscopy analysis.

Materials	I_D	FWHM _D	I_G	FWHM _G	I_D/I_G	$FWHM_D/FWHM_G$
PVC/1% GN	1957	103	1087	68	1.8	1.5
PVC/1% GN + P80	1491	110	866	68	1.7	1.6
PVC/1% GN + OA	2283	114	1270	68	1.8	1.7
PVC/1% GN + CE	1635	140	916	68	1.8	2.1

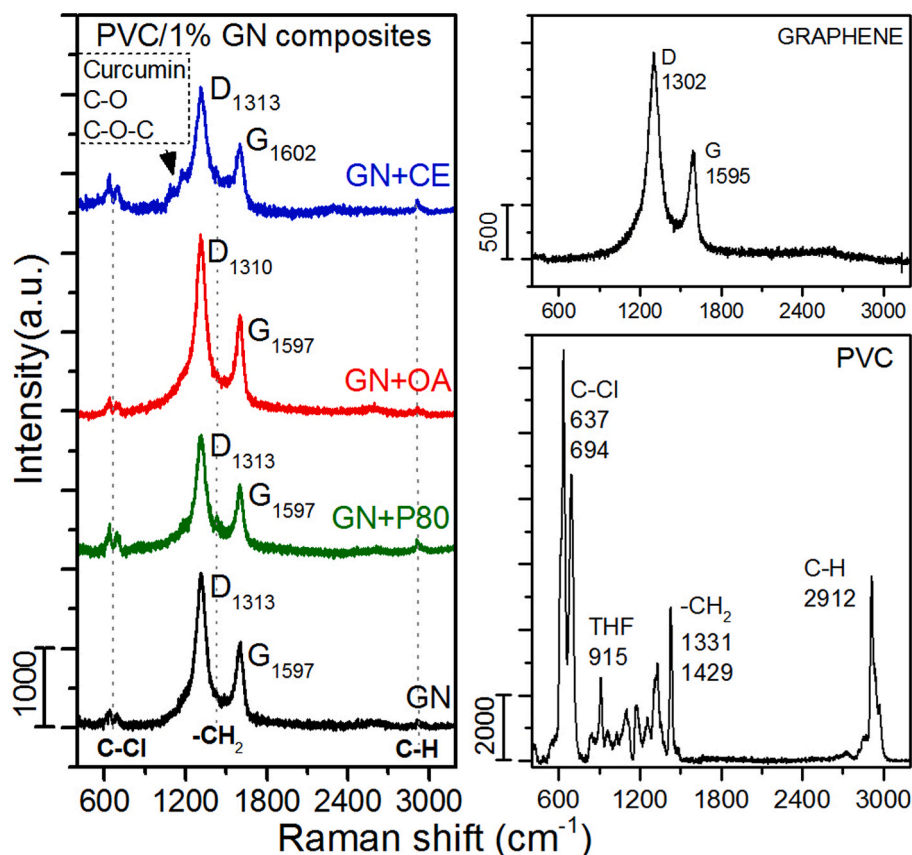


Fig. 11. Raman spectra of PVC, GN, and PVC/1%GN, PVC/1%GN + P80, PVC/1%GN + OA, and PVC/1%GN + CE nanocomposites.

to the other materials, a finding which is confirmed by the earlier SEM observations. One paper [39] points out the fact that the position of the G band peak shifts towards lower wavenumbers after laying a larger number of GN layers. In the case of PVC/1%GN and materials with P80 and OA, the position of the G band is shifted by 2 cm^{-1} towards higher wavenumbers in comparison to GN. In PVC/1%GN + CE nanocomposites, the position of the G peak is shifted towards higher frequencies by 7 cm^{-1} in relation to GN and by 5 cm^{-1} in relation to PVC/1%GN. This indicates an effective dispersion (disaggregation) of the filler in the PVC matrix by ultrasound and confirms that its distribution is best when CE is used.

The Raman spectra of the nanocomposites (Fig. 11) contain bands connected with the presence of C–Cl, $-\text{CH}_2$, and C–H groups characteristic of the PVC structure. This confirms earlier results of the FT-IR analysis, based on which it was ascertained that neither GN nor the dispersing agents have an impact on the chemical structure of PVC. In the spectral image of the PVC/1%GN + CE sample, one may also observe bands from C–O and C–O–C bands characteristic of curcuma [85].

4. Conclusions

The application of dispersing agents oleic acid, polysorbate 80, and curcuma extract improved the disaggregation of graphene or prolonged the stable period of its dispersion in a PVC solution. However, to obtain nanocomposites with a filler that is homogeneously distributed in a PVC matrix by the solvent evaporation method, it is necessary to use a dispersing agent that affects both of these parameters simultaneously.

Curcuma longa L. rhizome extract meets both criteria of effective disaggregation of the filler in the dispersion and improvement of dispersion stability, which has been confirmed by turbidimetric and visual analyses of the stability of GN dispersion in the PVC solution.

The better exfoliation of GN in nanocomposites with PVC prepared using curcuma extract has been confirmed by SEM analysis and Raman spectroscopy. PVC/GN nanocomposites with CE are characterized by a much better dispersion of GN in the polymer matrix in comparison to materials obtained without any auxiliary agents or those prepared using oleic acid and polysorbate 80.

CRediT authorship contribution statement

Slawomir Wilczewski: Conceptualization, Methodology, Validation, Investigation, Writing - original draft, Writing - review & editing, Visualization, Supervision. **Katarzyna Skórczewska:** Conceptualization, Methodology, Investigation, Writing - original draft, Writing - review & editing. **Jolanta Tomaszewska:** Conceptualization, Writing - original draft, Writing - review & editing. **Krzysztof Lewandowski:** Validation, Writing - original draft, Writing - review & editing, Visualization. **Joanna Szulc:** Conceptualization, Methodology, Investigation, Writing - original draft. **Tomasz Runka:** Investigation, Writing - original draft.

Declaration of competing interest

The authors declare that they have no known competing financial interests or personal relationships that could have appeared to influence the work reported in this paper.

Acknowledgements

The results presented in this paper were funded with grants for education allocated by the Ministry of Science and Higher Education in Poland.

Appendix A. Supplementary data

Supplementary data to this article can be found online at <https://doi.org/10.1016/j.polymertesting.2020.106868>.

[org/10.1016/j.polymertesting.2020.106868](https://doi.org/10.1016/j.polymertesting.2020.106868).

References

- [1] A. Godínez-García, D.D. Vallejo-Arenas, E. Salinas-Rodríguez, S.A. Gómez-Torres, J.C. Ruiz, Spraying synthesis and ion permeation in polyvinyl chloride/graphene oxide membranes, *Appl. Surf. Sci.* 489 (2019) 962–975, <https://doi.org/10.1016/j.apsusc.2019.05.319>.
- [2] Y. Xiao, B. Xin, Z. Chen, L. Lin, Y. Liu, Z. Hu, Enhanced thermal properties of graphene-based poly (vinyl chloride) composites, *J. Ind. Textil.* 48 (2019) 1348–1363, <https://doi.org/10.1177/1528083718760805>.
- [3] M. Khaleghi, K. Didehban, M. Shabaniyan, Simple and fast preparation of graphene oxide@ melamine terephthaldehyde and its PVC nanocomposite via ultrasonic irradiation: chemical and thermal resistance study, *Ultrason. Sonochem.* 43 (2018) 275–284, <https://doi.org/10.1016/j.ultsonch.2017.12.049>.
- [4] Z.B. Wei, Y. Zhao, C. Wang, S. Kuga, Y. Huang, M. Wu, Antistatic PVC-graphene composite through plasticizer-mediated exfoliation of graphite, *Chin. J. Polym. Sci.* 36 (2018) 1361–1367, <https://doi.org/10.1007/s10118-018-2160-5>.
- [5] M. Khaleghi, K. Didehban, M. Shabaniyan, Effect of new melamine-terephthaldehyde resin modified graphene oxide on thermal and mechanical properties of PVC, *Polym. Test.* 63 (2017) 382–391, <https://doi.org/10.1016/j.polymertesting.2017.08.018>.
- [6] K. Nawaz, M. Ayub, N. Ul-Haq, M.B. Khan, M.B.K. Niazi, A. Hussain, The effect of graphene nanosheets on the mechanical properties of polyvinylchloride, *Polym. Compos.* 37 (2016) 1572–1576, <https://doi.org/10.1002/pc>.
- [7] K. Deshmukh, G.M. Joshi, Thermo-mechanical properties of poly (vinyl chloride)/graphene oxide as high performance nanocomposites, *Polym. Test.* 34 (2014) 211–219, <https://doi.org/10.1016/j.polymertesting.2014.01.015>.
- [8] K. Deshmukh, S.M. Khatake, G.M. Joshi, Surface properties of graphene oxide reinforced polyvinyl chloride nanocomposites, *J. Polym. Res.* 20 (2013) 1–11, <https://doi.org/10.1007/s10965-013-0286-2>.
- [9] S. Vadukumpully, J. Paul, N. Mahanta, S. Valiyaveetil, Flexible conductive graphene/poly(vinyl chloride) composite thin films with high mechanical strength and thermal stability, *Carbon N. Y.* 49 (2011) 198–205, <https://doi.org/10.1016/j.carbon.2010.09.004>.
- [10] P. Kumar, P. Huo, R. Zhang, B. Liu, Antibacterial properties of graphene-based nanomaterials parveen, *Nanomaterials* 737 (2019) 1–32.
- [11] B. Sreenivasulu, B.R. Ramji, M. Nagaral, A review on graphene reinforced polymer matrix composites, *Mater. Today Proc.* 5 (2018) 2419–2428, <https://doi.org/10.1016/j.matpr.2017.11.021>.
- [12] H. Saleem, M. Haneef, H.Y. Abbasi, Synthesis route of reduced graphene oxide via thermal reduction of chemically exfoliated graphene oxide, *Mater. Chem. Phys.* 204 (2018) 1–7, <https://doi.org/10.1016/j.matchemphys.2017.10.020>.
- [13] V.B. Mohan, K. Lau, D. Hui, D. Bhattacharyya, Graphene-based materials and their composites: a review on production, applications and product limitations, *Compos. B Eng.* 142 (2018) 200–220, <https://doi.org/10.1016/j.compositesb.2018.01.013>.
- [14] R. Siburian, H. Sihotang, S. Lumban Raja, M. Supeno, C. Simanjuntak, New route to synthesize of graphene nano sheets, *Orient. J. Chem.* 34 (2018) 182–187, <https://doi.org/10.13005/ojc/340120>.
- [15] N.A. Abdel Ghany, S.A. Elsherif, H.T. Handal, Revolution of graphene for different applications: State-of-the-art, *Surfaces and Interfaces* 9 (2017) 93–106, <https://doi.org/10.1016/j.surfin.2017.08.004>.
- [16] R. Świercz, Graphene - directions of development, application, *Mechanika* 12 (2015) 67–70, <https://doi.org/10.17814/mechanik.2015.12.541>.
- [17] B. Stańczyk, L. Dobrzański, A. Jagoda, M. Możdżonek, S. Natarajan, Graphene obtained by electrolytic method on silicon carbide substrates, *Electron. Mater.* 42 (2014) 20–25.
- [18] J. Jonik, M. Purchała, H. Grajek, Metody syntezy i badania właściwości grafenu, *Apar. Badaw. i Dydak.* 2 (2016) 110–117.
- [19] S. Ren, P. Rong, Q. Yu, Preparations, properties and applications of graphene in functional devices: a concise review, *Ceram. Int.* 44 (2018) 11940–11955, <https://doi.org/10.1016/j.ceramint.2018.04.089>.
- [20] J. Phiri, P. Gane, T.C. Maloney, General overview of graphene: production, properties and application in polymer composites, *Mater. Sci. Eng. B Solid-State Mater. Adv. Technol.* 215 (2017) 9–28, <https://doi.org/10.1016/j.mseb.2016.10.004>.
- [21] Z. Trzaska, M. Trzaska, Nanokompozyty z grafenem: wytwarzanie, właściwości i znaczenie w budownictwie, *Maz. Stud. Reg. Anal. Stud.* (2016) 223–245, <https://doi.org/10.21858/msr.19.15>.
- [22] B. Szczęśniak, J. Choma, M. Jaroniec, Synthesis and adsorption properties of graphene - based materials, *Wiadomości Chem.* 70 (2016) 189–217.
- [23] C. Fu, G. Zhao, H. Zhang, S. Li, Evaluation and characterization of reduced graphene oxide nanosheets as anode materials for lithium-ion batteries, *Int. J. Electrochem. Sci.* 8 (2013) 6269–6280.
- [24] W. Brostow, H.E. Hagg Lobland, *Materials: Introduction and Applications*, John Wiley & Sons, 2017.
- [25] Z. Asgarzadeh, G. Naderi, Morphology and properties of unvulcanized and dynamically vulcanized PVC/NBR blend reinforced by graphene nanoplatelets, *Int. Polym. Process.* 33 (2018) 497–505, <https://doi.org/10.3139/217.3515>.
- [26] H. Wang, G. Xie, M. Fang, Z. Ying, Y. Tong, Y. Zeng, Mechanical reinforcement of graphene/poly(vinyl chloride) composites prepared by combining the in-situ suspension polymerization and melt-mixing methods, *Compos. B Eng.* 113 (2017) 278–284, <https://doi.org/10.1016/j.compositesb.2017.01.053>.

- [27] H. Wang, G. Xie, Z. Ying, Y. Tong, Y. Zeng, Enhanced mechanical properties of multi-layer graphene filled poly(vinyl chloride) composite films, *J. Mater. Sci. Technol.* 31 (2015) 340–344, <https://doi.org/10.1016/j.jmst.2014.09.009>.
- [28] H. Wang, G. Xie, M. Fang, Z. Ying, Y. Tong, Y. Zeng, Electrical and mechanical properties of antistatic PVC films containing multi-layer graphene, *Compos. B Eng.* 79 (2015) 444–450, <https://doi.org/10.1016/j.compositesb.2015.05.011>.
- [29] K. Skórczewska, D. Chmielewska, K. Piszczek, J. Tomaszewska, T. Sterzyński, Wytwarzanie nanokompozytów PVC/CNT z zastosowaniem czynników dyspergujących, *Chemik* 65 (2011) 337–339.
- [30] S. Wilczewski, K. Skórczewska, J. Tomaszewska, K. Lewandowski, Structure and properties of poly (vinyl chloride)/graphene nanocomposites, *Polym. Test.* 81 (2020), 106282, <https://doi.org/10.1016/j.polymertesting.2019.106282>.
- [31] K. Skórczewska, J. Tomaszewska, K. Piszczek, K. Lewandowski, Production and properties of modified poly(vinyl chloride) PVC nanocomposites with carbon nanotubes, *Przetwórstwo Tworzyw.* 20 (2014) 567–571.
- [32] K. Skórczewska, J. Tomaszewska, K. Piszczek, K. Lewandowski, Production and properties of rigid poly(vinyl chloride) nanocomposites with carbon nanotubes and graphite, *Przetwórstwo Tworzyw.* 3 (2015) 290–293.
- [33] H. Wang, G. Xie, C. Yang, Y. Zheng, Z. Ying, W. Ren, Y. Zeng, Enhanced toughness of multilayer graphene-filled poly(vinyl chloride) composites prepared using melt-mixing method, *Polym. Compos* 38 (2017) 138–146, <https://doi.org/10.1002/pc.20177>.
- [34] J. Ma, J. Liu, W. Zhu, W. Qin, Solubility study on the surfactants functionalized reduced graphene oxide, *Colloids Surfaces A Physicochem. Eng. Asp.* 538 (2018) 79–85, <https://doi.org/10.1016/j.colsurfa.2017.10.071>.
- [35] J. Dai, G. Wang, L. Ma, C. Wu, Study on the surface energies and dispersibility of graphene oxide and its derivatives, *J. Mater. Sci.* 50 (2015) 3895–3907, <https://doi.org/10.1007/s10853-015-8934-z>.
- [36] E.E. Tkalya, M. Ghislandi, G. De With, C.E. Koning, The use of surfactants for dispersing carbon nanotubes and graphene to make conductive nanocomposites, *Curr. Opin. Colloid Interface Sci.* 17 (2012) 225–232, <https://doi.org/10.1016/j.cocis.2012.03.001>.
- [37] T. Kuila, S. Bose, A.K. Mishra, P. Khanra, N.H. Kim, J.H. Lee, Chemical functionalization of graphene and its applications, *Prog. Mater. Sci.* 57 (2012) 1061–1105, <https://doi.org/10.1016/j.pmatsci.2012.03.002>.
- [38] D.W. Johnson, B.P. Dobson, K.S. Coleman, A manufacturing perspective on graphene dispersions, *Curr. Opin. Colloid Interface Sci.* 20 (2015) 367–382, <https://doi.org/10.1016/j.cocis.2015.11.004>.
- [39] S. Hatamie, O. Akhavan, S.K. Sadrnezhad, M.M. Ahadian, M.M. Shirolkar, H. Q. Wang, Curcumin-reduced graphene oxide sheets and their effects on human breast cancer cells, *Mater. Sci. Eng. C* 55 (2015) 482–489, <https://doi.org/10.1016/j.msec.2015.05.077>.
- [40] S. Grimme, Do special noncovalent π - π stacking interactions really exist? *Angew. Chem. Int. Ed.* 47 (2008) 3430–3434, <https://doi.org/10.1002/anie.200705157>.
- [41] W. Wang, Y. Zhang, Y.B. Wang, Noncovalent π - π interaction between graphene and aromatic molecule: structure, energy, and nature, *J. Chem. Phys.* 140 (2014), <https://doi.org/10.1063/1.4867071>.
- [42] R. Navik, Y. Gai, W. Wang, Y. Zhao, Curcumin-assisted ultrasound exfoliation of graphite to graphene in ethanol, *Ultrason. Sonochem.* 48 (2018) 96–102, <https://doi.org/10.1016/j.ultsonch.2018.05.010>.
- [43] Y.K. Yang, C.E. He, R.G. Peng, A. Baji, X.S. Du, Y.L. Huang, X.L. Xie, Y.W. Mai, Non-covalently modified graphene sheets by imidazolium ionic liquids for multifunctional polymer nanocomposites, *J. Mater. Chem.* 22 (2012) 5666–5675, <https://doi.org/10.1039/c2jm16006d>.
- [44] S.Y. Jeong, S.H. Kim, J.T. Han, H.J. Jeong, S.Y. Jeong, G.W. Lee, Highly concentrated and conductive reduced graphene oxide nanosheets by monovalent cation- π interaction: toward printed electronics, *Adv. Funct. Mater.* 22 (2012) 3307–3314, <https://doi.org/10.1002/adfm.201200242>.
- [45] J. Texter, Graphene dispersions, *Curr. Opin. Colloid Interface Sci.* 19 (2014) 163–174, <https://doi.org/10.1016/j.cocis.2014.04.004>.
- [46] A. Achari, K. Datta, M. De, V. Dravid, M. Eswaramoorthy, Amphiphilic aminoclay-RGO hybrids: a simple strategy to disperse a high concentration of RGO in water, *Nanoscale* 5 (2013) 5316–5320, <https://doi.org/10.1039/c3nr01108a>.
- [47] L. Kou, C. Gao, Making silica nanoparticle-covered graphene oxide nanohybrids as general building blocks for large-area superhydrophilic coatings, *Nanoscale* 3 (2011) 519–528, <https://doi.org/10.1039/c0nr00609b>.
- [48] S. Hatamie, M.M. Ahadian, A. Irajizad, O. Akhavan, E. Jekar, Photoluminescence and electrochemical investigation of curcumin-reduced graphene oxide sheets, *J. Iran. Chem. Soc.* 15 (2018) 351–357, <https://doi.org/10.1007/s13738-017-1236-4>.
- [49] M. Lestari, G. Indrayanto, Curcumin, profiles drug subst, Excipients Relat. Methodol. 39 (2014) 113–204, <https://doi.org/10.1016/B978-0-12-800173-8.00003-9>.
- [50] K.I. Priyadarsini, The chemistry of curcumin: from extraction to therapeutic agent, *Molecules* 19 (2014), <https://doi.org/10.3390/molecules191220091>, 20091–20112.
- [51] J.A. Salto, W. Shi, A. Mancuso, C. Sun, T. Park, N. Averick, K. Punia, J. Fatab, K. Raja, Curcumin-derived green plasticizers for Poly(vinyl) chloride, *RSC Adv.* 4 (2014) 54725–54728.
- [52] E. Larrañeta, M. Imízcoz, J.X. Toh, N.J. Irwin, A. Ripolin, A. Perminova, J. Domínguez-Robles, A. Rodríguez, R.F. Donnelly, Synthesis and characterization of lignin hydrogels for potential applications as drug eluting antimicrobial coatings for medical materials, *ACS Sustain. Chem. Eng.* 6 (2018) 9037–9046, <https://doi.org/10.1021/acssuschemeng.8b01371>.
- [53] S. Velho, L. Brum, C. Petter, J.H. dos Santos, S. Simunić, W.H. Kappa, Development of structured natural dyes for use into plastics, *Dyes Pigments* 136 (2017) 248–254, <https://doi.org/10.1016/j.dyepig.2016.08.021>.
- [54] A. Rohman, D. Sudjadi, D. Ramadhani, A. Nugroho, Analysis of curcumin in curcuma longa and Curcuma xanthorrhiza using FTIR spectroscopy and chemometrics, *Res. J. Med. Plant* 9 (2015) 179–186, <https://doi.org/10.3923/rjmp.2015.179.186>.
- [55] P. Mohan, G. Sreelakshmi, C.V. Muraleedharan, R. Joseph, Water soluble complexes of curcumin with cyclodextrins: characterization by FT-Raman spectroscopy, *Vib. Spectrosc.* 62 (2012) 77–84, <https://doi.org/10.1016/j.vibspec.2012.05.002>.
- [56] N. Sofyan, F.W. Situmorang, A. Ridhova, A.H. Yuwono, A. Udhiarto, Visible light absorption and photosensitizing characteristics of natural yellow 3 extracted from Curcuma Longa L. for Dye-Sensitized solar cell, *IOP Conf. Ser. Earth Environ. Sci.* 105 (2018) 1–6, <https://doi.org/10.1088/1755-1315/105/1/012073>.
- [57] Y. Ren, J. Zheng, Z. Xu, Y. Zhang, J. Zheng, Application of Turbiscan LAB to study the influence of lignite on the static stability of PCLWS, *Fuel* 214 (2018) 446–456, <https://doi.org/10.1016/j.fuel.2017.08.026>.
- [58] M. Luo, X. Qi, T. Ren, Y. Huang, A.A. Keller, H. Wang, B. Wu, H. Jin, F. Li, Heteroaggregation of CeO₂ and TiO₂ engineered nanoparticles in the aqueous phase: application of turbiscan stability index and fluorescence excitation-emission matrix (EEM) spectra, *Colloids Surfaces A Physicochem. Eng. Asp.* 533 (2017) 9–19, <https://doi.org/10.1016/j.colsurfa.2017.08.014>.
- [59] X. Qi, Y. Dong, H. Wang, C. Wang, F. Li, Application of Turbiscan in the homoaggregation and heteroaggregation of copper nanoparticles, *Colloids Surfaces A Physicochem. Eng. Asp.* 535 (2017) 96–104, <https://doi.org/10.1016/j.colsurfa.2017.09.015>.
- [60] Z. Zhong, K. Woo, I. Kim, H. Hwang, S. Kwon, Y.M. Choi, Y. Lee, T.M. Lee, K. Kim, J. Moon, Roll-to-roll-compatible, flexible, transparent electrodes based on self-nanoembedded Cu nanowires using intense pulsed light irradiation, *Nanoscale* 8 (2016) 8995–9003, <https://doi.org/10.1039/c6nr00444j>.
- [61] J.W. Lee, S.W. Kim, Y.L. Cho, H.Y. Jeong, Y. Il Song, S.J. Suh, Characterization and dispersion stabilities of multi-layer graphene-coated copper prepared by electrical wire-explosion method, *J. Nanosci. Nanotechnol.* 16 (2016) 11286–11291, <https://doi.org/10.1166/jnn.2016.13495>.
- [62] A. Bagchi, Extraction of curcumin, *IOSR J. Environ. Sci. Toxicol. Food Technol.* 1 (2012) 1–16, <https://doi.org/10.1079/2402-0130116>.
- [63] I. Polowczyk, Stabilność Zawiesiny Łupka Miedzionośnego, *Łupek Miedzionośny II*, vols. 38–43, 2016. ISBN978-83-942205-1-8.
- [64] J.S. Kim, S. Hong, D.W. Park, S.E. Shim, Water-borne graphene-derived conductive SBR prepared by latex heterocoagulation, *Macromol. Res.* 18 (2010) 558–565, <https://doi.org/10.1007/s13233-010-0603-0>.
- [65] Z. Lili, Z. Hongfei, S. Shoukat, Z. Xiaochen, Z. Bolin, Screening lactic acid bacteria strains with ability to bind di-n-butyl phthalate via Turbiscan technique, *Antonie van Leeuwenhoek, Int. J. Gen. Mol. Microbiol.* 110 (2017) 759–769, <https://doi.org/10.1007/s10482-017-0846-2>.
- [66] Formulation, Stability of Suspensions for Electronic Applications, 2009. <http://www.titanex.com.tw/doc/tecsupport/ANA-TLab-application paper on elect ronic.pdf>.
- [67] Z.M. Marković, D.P. Kepić, D.M. Matijašević, V.B. Pavlović, S.P. Jovanović, N. K. Stanković, D.D. Milivojević, Z. Spitalsky, I.D. Holclajtner-Antunović, D.V. Bajuk-Bogdanović, M.P. Nikšić, B.M. Todorović Marković, Ambient light induced antibacterial action of curcumin/graphene nanomesh hybrids, *RSC Adv.* 7 (2017) 36081–36092, <https://doi.org/10.1039/c7ra05027e>.
- [68] M. Deka, D. Chowdhury, Tuning electrical properties of graphene with different π -stacking organic molecules, *J. Phys. Chem. C* 120 (2016) 4121–4129, <https://doi.org/10.1021/acs.jpcc.5b12403>.
- [69] H. Wang, G. Xie, Z. Zhu, Z. Ying, Y. Zeng, Enhanced tribological performance of the multi-layer graphene filled poly(vinyl chloride) composites, *Compos. Part A Appl. Sci. Manuf.* 67 (2014) 268–273, <https://doi.org/10.1016/j.compositesa.2014.09.011>.
- [70] M. Hasan, M. Lee, Enhancement of the thermo-mechanical properties and efficacy of mixing technique in the preparation of graphene/PVC nanocomposites compared to carbon nanotubes/PVC, *Prog. Nat. Sci. Mater. Int.* 24 (2014) 579–587, <https://doi.org/10.1016/j.pnsc.2014.10.004>.
- [71] K.M. McGinty, W.J. Brittain, Hydrophilic surface modification of poly(vinyl chloride) film and tubing using physisorbed free radical grafting technique, *Polymer* 49 (2008) 4350–4357, <https://doi.org/10.1016/j.polymer.2008.07.063>.
- [72] E. Youusif, A. Ahmed, R. Abood, N. Jaber, R. Noaman, R. Yusop, Poly(vinyl chloride) derivatives as stabilizers against photodegradation, *J. Taibah Univ. Sci.* 9 (2015) 203–212, <https://doi.org/10.1016/j.jtusci.2014.10.003>.
- [73] N.S. Labidi, A. Iddou, Adsorption of oleic acid on quartz/water interface, *J. Saudi Chem. Soc.* 11 (2007) 221–234.
- [74] W. Premaratne, W. Priyadarshana, S. Gunawardena, A. De Alwis, Synthesis of nanosilica from paddy husk ash and their surface functionalization, *J. Sci. Univ. Kelaniya Sri Lanka* 8 (2014), <https://doi.org/10.4038/josuk.v8i0.7238>, 33.
- [75] F. Münch, C. Höllner, A. Klapproth, E. Eckert, A. Ruffer, R. Cesnjevar, T. Göen, Effect of phospholipid coating on the migration of plasticizers from PVC tubes, *Chemosphere* 202 (2018) 742–749, <https://doi.org/10.1016/j.chemosphere.2018.03.136>.
- [76] A. Marcilla, S. García, J.C. García-Quesada, Study of the migration of PVC plasticizers, *J. Anal. Appl. Pyrolysis* 71 (2004) 457–463, [https://doi.org/10.1016/S0165-2370\(03\)00131-1](https://doi.org/10.1016/S0165-2370(03)00131-1).
- [77] U.W. Gedde, *Polymer Physics*, Chapman & Hall, London, Glasgow, Weinheim, New York, Tokyo, Melbourne, Madras, 1995.
- [78] V.S. Solodovichenko, V.A. Polyboyarov, A.A. Zhdanok, A.B. Arbutov, E. S. Zapevalova, Y.G. Kryazhev, V.A. Likhobobov, Synthesis of carbon materials by the short-term mechanochemical activation of polyvinyl chloride, *Procedia Eng* 152 (2016) 747–752, <https://doi.org/10.1016/j.proeng.2016.07.684>.

- [79] Y. Zhang, X. Zhang, L. Yang, Q. Zhang, M.L. Fitzgerald, A. Ueda, Y. Chen, R. Mu, D. Li, L.M. Bellan, Thermal transport in electrospun vinyl polymer nanofibers: effects of molecular weight and side groups, *Soft Matter* 14 (2018) 9534–9541, <https://doi.org/10.1039/c8sm01696h>.
- [80] R.K. Arya, Calibration curves to measure concentrations in multicomponent polymeric coatings using confocal Raman spectroscopy, *Int. J. Chem. Eng. Appl.* 2 (2011) 421–424, <https://doi.org/10.7763/ijcea.2011.v2.145>.
- [81] S. Mikhailov, *Physics and Applications of Graphene- Experiments*, InTech, 2011, <https://doi.org/10.5772/1938>.
- [82] H. Akhina, M.R. Gopinathan Nair, N. Kalarikkal, K.P. Pramoda, T. Hui Ru, L. Kailas, S. Thomas, Plasticized PVC graphene nanocomposites: morphology, mechanical, and dynamic mechanical properties, *Polym. Eng. Sci.* 58 (2018), <https://doi.org/10.1002/pen.24711>. E104–E113.
- [83] Q. Wang, T. Chen, B. Zhang, M. Li, Y. Lu, K.P. Chen, All-fiber passively mode-locked thulium-doped fiber ring laser using optically deposited graphene saturable absorbers, *Appl. Phys. Lett.* 102 (2013), <https://doi.org/10.1063/1.4800036>.
- [84] N. Ferralis, Probing mechanical properties of graphene with Raman spectroscopy, *J. Mater. Sci.* 45 (2010) 5135–5149, <https://doi.org/10.1007/s10853-010-4673-3>.
- [85] S. Dhakal, K. Chao, W. Schmidt, J. Qin, M. Kim, D. Chan, Evaluation of turmeric powder adulterated with metanil yellow using FT-Raman and FT-IR spectroscopy, *Foods* 5 (2016), <https://doi.org/10.3390/foods5020036>, 36.

Publikacja [P3]

Curcuma longa L. rhizome extract as a poly(vinyl chloride)/graphene nanocomposite green modifier

Article

Curcuma longa L. Rhizome Extract as a Poly(vinyl chloride)/Graphene Nanocomposite Green Modifier

Sławomir Wilczewski ^{1,*}, Katarzyna Skórczewska ¹, Jolanta Tomaszewska ¹, Krzysztof Lewandowski ¹, Waldemar Studziński ¹, Magdalena Osiał ^{2,*}, Piotr Jencyk ², Hubert Grzywacz ² and Agata Domańska ³

¹ Faculty of Chemical Technology and Engineering, Bydgoszcz University of Science and Technology, Seminaryjna 3 Street, 85-326 Bydgoszcz, Poland

² Institute of Fundamental Technological Research, Polish Academy of Sciences, Pawinskiego 5B Street, 02-106 Warsaw, Poland

³ Łukasiewicz Research Network—Institute for Engineering of Polymer Materials and Dyes, Marii Skłodowskiej-Curie 55 Street, 87-100 Toruń, Poland

* Correspondence: slawomir.wilczewski@pbs.edu.pl (S.W.); mosial@ippt.pan.pl (M.O.)

Abstract: In this work, a method to increase the dispersion of graphene (GN) in the matrix of rigid poly(vinyl chloride) (PVC) by using a natural plant extract from *Curcuma longa* L. (CE) is proposed. Currently, despite the increasing number of reports on the improvement of GN dispersion in PVC blends, still there is a need to find environmentally friendly and economical dispersion stabilizers. We proposed a stabilizer that can be easily obtained from a plant offering thermal stability and high effectiveness. PVC/GN nanocomposites stabilized with the proposed extract were investigated by SEM, AFM (structure), TGA, and Congo red test (thermal properties). Additionally, static and dynamic mechanical properties and electrical resistivity were measured. The use of CE as a graphene dispersant improved its dispersion in the PVC matrix, influenced tensile properties, increased the storage modulus and glass transition temperature, and extended the thermal stability time of nanocomposites. In this work, a CE extract is proposed as an efficient eco-friendly additive for the production of nanocomposites with an improved homogeneity of a nanofiller in the matrix and promising characteristics.

Keywords: nanocomposites; graphene; poly(vinyl chloride); curcuma extract



Citation: Wilczewski, S.; Skórczewska, K.; Tomaszewska, J.; Lewandowski, K.; Studziński, W.; Osiał, M.; Jencyk, P.; Grzywacz, H.; Domańska, A. *Curcuma longa* L. Rhizome Extract as a Poly(vinyl chloride)/Graphene Nanocomposite Green Modifier. *Molecules* **2022**, *27*, 8081. <https://doi.org/10.3390/molecules27228081>

Academic Editor: Ibrahim M. Alarifi

Received: 28 October 2022

Accepted: 18 November 2022

Published: 21 November 2022

Publisher's Note: MDPI stays neutral with regard to jurisdictional claims in published maps and institutional affiliations.



Copyright: © 2022 by the authors. Licensee MDPI, Basel, Switzerland. This article is an open access article distributed under the terms and conditions of the Creative Commons Attribution (CC BY) license (<https://creativecommons.org/licenses/by/4.0/>).

1. Introduction

Research concerning graphene application is carried out in many areas, such as medicine, chemistry, materials engineering, energetics, and electronics [1–5]. A large area of graphene-related research is its use as a filler for polymer nanocomposites; however, its use is limited by the lack of large-scale methods for obtaining a high-quality filler and its poor dispersion in the polymer matrix [6–10]. Despite numerous studies on polymer nanocomposites containing graphene, a relatively small number of them concern the modification of poly(vinyl chloride). This polymer is distinguished by high chemical resistance and favorable mechanical and performance characteristics [11–13]; however, it has low thermal stability under molten state processing conditions [14,15]. Therefore, it is widely modified with additives that improve its functionality [16–21]. Literature data on poly(vinyl chloride) nanocomposites with graphene fillers (PVC/GN) prove that a good dispersion of graphene in the matrix results in an increase in tensile strength, longitudinal modulus of elasticity [22–27], and impact resistance [27,28]. Such a composite is also characterized by higher thermal stability and glass transition temperature (T_g) [24–27,29,30] as well as lower volume and surface resistivity in comparison with the matrix material [25,31,32].

The key problems to be solved in the case of PVC/GN nanocomposites, regardless of the method of their production, include obtaining a good dispersion of the filler in the

matrix and increasing the filler–polymer interfacial interactions. Thus, a poor dispersion of the filler in the polymer matrix affects its physicochemical properties [23–28,30,31]. However, it should be emphasized that obtaining a good dispersion of the graphene filler in PVC is related to its low agglomeration and favorable interfacial interactions of the filler and polymer [22,24,26,28,31].

The tendency of graphene to form agglomerates results from strong π – π interactions and van der Waals forces [33–36]. The basic methods for increasing the dispersibility of GN are divided into noncovalent and covalent ones [2,33,35]. The covalent modification of graphene materials used in PVC composites is based on the use of chemical reagents that usually are harmful to health and the environment [37–41]. In addition, these methods change the structure of graphene, affecting its characteristics. Noncovalent methods are based on increasing the dispersion of graphene in the PVC matrix by its dispersion in a plasticizer [25] and mechanical exfoliation of graphite in the plasticizer environment [32]. Generally, they are based on the use of a modifier that significantly affects the properties of PVC [15].

An interesting method for noncovalent functionalization of graphene in order to limit its agglomeration is surface modification with curcumin (CU). The π – π interactions between CU aromatic rings and the graphene surface were used in its synthesis to reduce graphene oxide [42,43]. Curcumin was also used during the graphite exfoliation by sonication [44].

Curcumin is a natural, biologically active chemical compound belonging to the group of curcuminoids that are extracted from turmeric, particularly *Curcuma longa* L. The content of the curcuminoids in the plant depends on the environmental and soil conditions and ranges from 2% to 9% of curcuminoid content in the plant [45–47]. These compounds show high chemical stability in their natural form, which makes them ideal for many applications in engineering, medicine, and pharmacy [47,48]. In [44], the authors demonstrated that curcumin is thermally stable up to approximately 180 °C and in combination with graphene even up to approximately 220 °C. Some studies show that CU can be used as a polymer additive for its chemical stability [47]. It was used for plasticization, coloring, and increasing the antibacterial resistance of PVC [49–51].

The aim of the presented study was to investigate the impact of the curcuminoid-based extract obtained from the rhizome of *Curcuma longa* L. on the structure and properties of PVC nanocomposites with graphene. The use of this extract as a component of the composite is a new, economical solution that is safe for health and the environment. Additionally, the use of CE improved the dispersion of graphene in PVC.

2. Results and Discussion

2.1. Analysis of *Curcuma longa* L. Rhizome Extract

Curcuminoids are the main active compounds contributing to the chemical activity of *Curcuma longa* L. Turmeric usually contains 2% to 9% of curcuminoids, mainly curcumin, approximately 77% [45–47]. The phenolic compounds are also the main active ingredients of turmeric alcoholic extracts. To confirm the presence of these compounds in the as-prepared extract, Fourier Transformed Infrared spectroscopy (FT-IR) was performed. Figure 1a shows the following bands, where the band at 3347 cm^{-1} can be attributed to the -O-H stretching vibration. The subsequent bands can be described as follows: 3015 cm^{-1} C-H aromatic stretching vibration, 2924 cm^{-1} -CH₂ to asymmetric stretching, 1678 cm^{-1} C=O stretching, 1581 cm^{-1} C=C aromatic stretching, 1511 cm^{-1} benzene ring bending vibration, 1442 cm^{-1} CH₂ bending, 1376 CH₃ bending, 1271 cm^{-1} enol C-O peak, 1124 cm^{-1} C-O stretching, 1029 cm^{-1} C-O-C peak, 964 cm^{-1} benzoate trans-CH vibration, and 815 cm^{-1} aromatic CH bending. These bands are characteristic of curcumin, demethoxycurcumin, and bisdemethoxycurcumin functional groups [45,52,53].

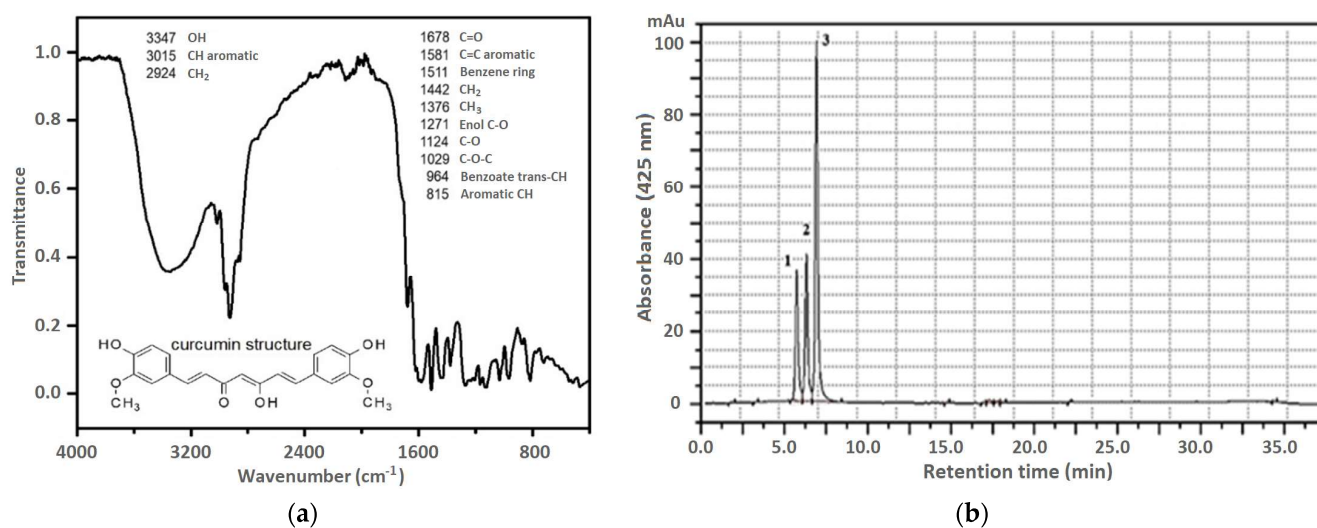


Figure 1. (a) FTIR spectra; (b) HPLC chromatogram of *Curcuma longa* L. rhizome extract.

In addition to curcuminoids, essential oils are the main active ingredients in turmeric. The analysis of the curcuminoids in turmeric is critical to determining the quality of the plant material or its processed products [54]. To determine the individual components of turmeric, HPLC and GC–MS were used in the paper. These methods were most often used and described in the literature [55]. The quantitative HPLC method has been validated. The three analytes showed good linearity ($R^2 \geq 0.999$) in the concentration range of 2–80 $\mu\text{g mL}^{-1}$. The RSD values were 1.48%. The HPLC chromatogram of the fresh turmeric extract is shown in Figure 1b. Peaks 1, 2, and 3 showed similar UV–vis spectra that are characteristic of curcuminoids at wavelength $\lambda = 425$ nm. They were identified as bisdemethoxycurcumin (1), demethoxycurcumin (2), and curcumin (3), respectively, on the basis of the retention times compared with the retention times of the reference compounds.

It was calculated that the sum of the three curcuminoids' content in the extract is 150 mg g^{-1} , of which the curcumin content is 84 mg g^{-1} . Based on the analysis, it can be concluded that curcumin was the most common compound, and the sum of the demethoxycurcumin and bisdemethoxycurcumin contents was lower than that of curcumin. Therefore, the turmeric extract can be classified as type A [56].

Volatile compounds in the turmeric extract were also identified from GC–MS analysis. In total, eight peaks were identified (Figure 2) when compared with the NIST database and literature data [56,57]. The following compounds have been identified: Ar-curcumene (4), (-)-zingiberene (5), β -sesquiphellandrene (6), Ar-turmerone (7), α -turmerone (8), β -turmerone (9), (6R,7R)-bisabolene (10), and (E)-atlantone (11). Mass spectra of the compounds are shown on Figures S1–S8 in Supplementary File.

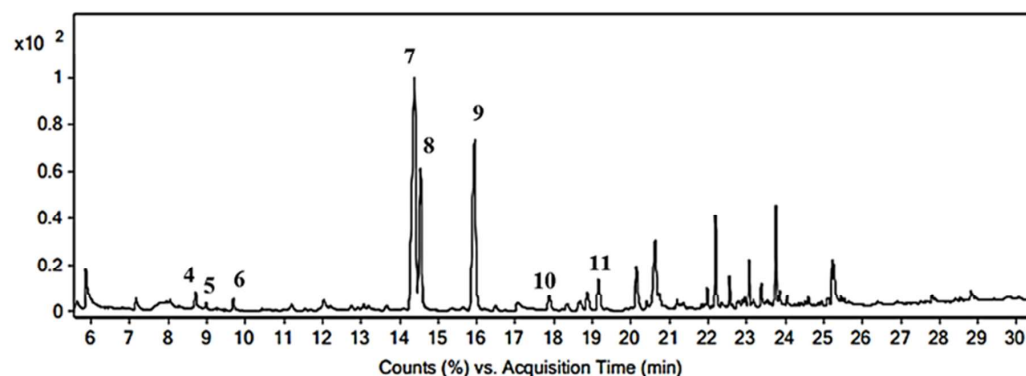


Figure 2. GC–MS chromatogram of *Curcuma longa* L. rhizome extract.

Additionally, the ratio of the heights of individual compounds on the GC–MS chromatogram makes the extract qualify as type A. According to Xu et al. [56], the turmeric extract of type A is characterized by the fact that peak 7 is higher than peak 8, and peak heights are 5 and 6, which are in total less than 33% of the height of peak 4. This is exactly the case here. The analyses of the obtained extract from the rhizome of *Curcuma longa* L. confirm the effectiveness of the extraction. Curcuminoids have been shown to be the main active ingredients of CE used as an auxiliary in poly(vinyl chloride)/graphene nanocomposites.

2.2. Structure of PVC/GN Nanocomposites

The morphology of the nanocomposites' cross section was investigated using scanning electron microscopy (SEM), where fracture was performed under liquid nitrogen conditions. Figure 3 presents unmodified ingredients and a graphene-filled PVC nanocomposite containing 1 wt.% of graphene. As can be seen in Figure 3A, graphene reveals multilayered wrinkle-like flake structures that are characteristic to the elasticity of the material and large size of graphene flakes [58]. The fracture area of poly(vinyl chloride) (Figure 3B) is characteristic of the brittle fracture of thermoplastics. Fractures of nanocomposites reveal a jagged morphology [27,28,31,59,60]. Based on SEM images of the fracture surfaces of nanocomposites (Figure 3C,D), GN dispersion in the materials was assessed. The image of a PVC/1% GN sample (Figure 3C) shows the presence of filler agglomerates in the fracture edge. On the other hand, the fracture area of the PVC/1% GN + CE nanocomposite (Figure 3D) is characterized by a homogeneous dispersion of the filler in the PVC matrix, and no areas of an unmodified polymer structure were observed.

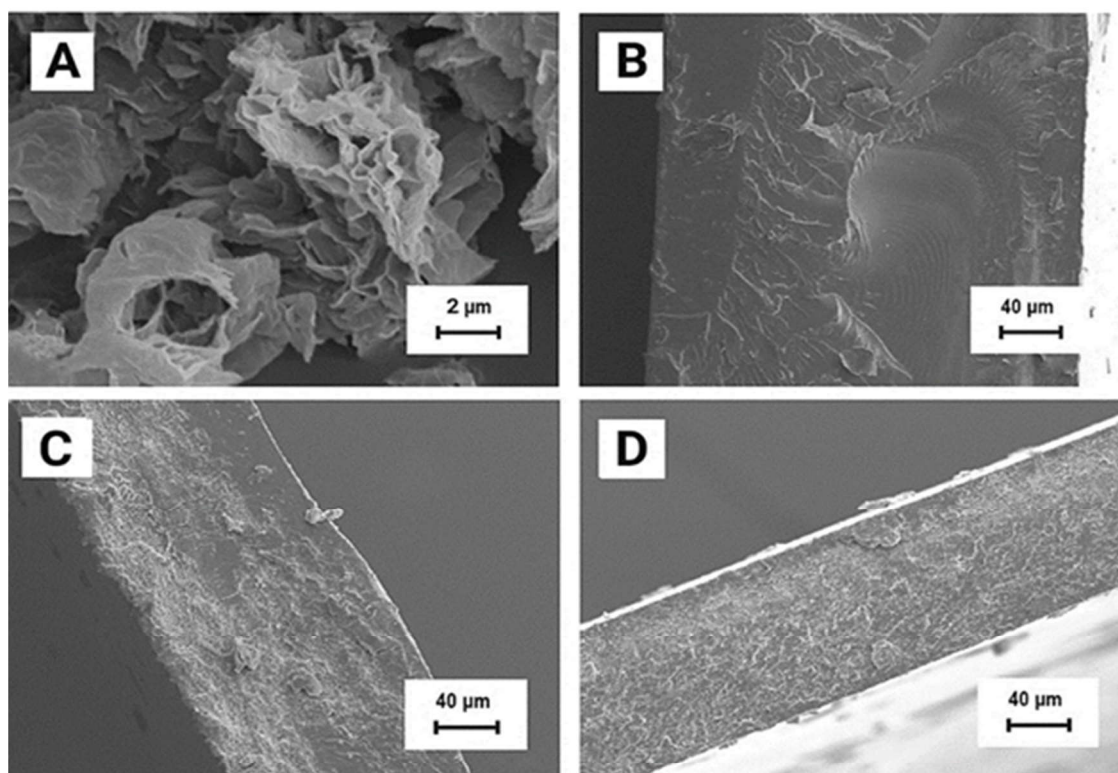


Figure 3. SEM images of (A) GN, (B) PVC, (C) PVC/1% GN, and (D) PVC/1% GN + CE.

In order to assess the surface structure of the obtained composite films, atomic force microscopy was used, enabling the direct assessment of the dispersion of graphene materials in nanocomposites and the determination of their roughness [61,62]. Figure 4 presents 3D images of the surface structure of PVC, PVC + CE, and nanocomposites containing 1 wt.% of graphene. The test was carried out in contact mode on the surface that was not in contact with the Petri dish during the evaporation of the solvent (polymer film formation). Topog-

roughness studies revealed the presence of corrugation and roughness (7.322 ± 0.424 nm) on the surface of unmodified poly(vinyl chloride), which results from solvent evaporation during the formation of the polymer film. The roughness was estimated to be 12.017 ± 0.302 nm for PVC + CE, 52.111 ± 1.257 nm for PVC/1% GN, and 36.216 ± 0.234 nm for PVC/1% GN + CE. A significant increase in the surface roughness of GN-containing nanocomposite films is the result of both solvent evaporation and the presence of a filler in the polymer matrix. The nanocomposites with the addition of CE had a lower roughness value than PVC/1% GN for the higher dispersion of the filler in the PVC matrix [63,64].

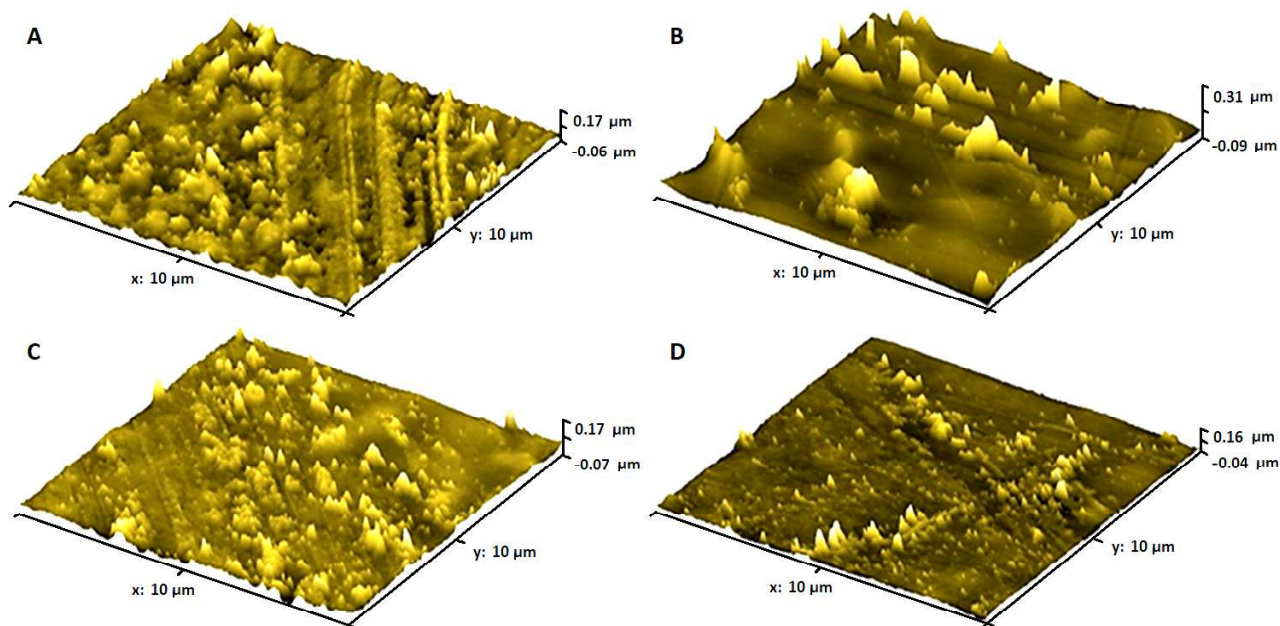


Figure 4. AFM 3D images of (A) PVC, (B) PVC/1% GN, (C) PVC + CE, and (D) PVC/1% GN + CE.

The improved dispersion of graphene in PVC nanocomposites, due to the *Curcuma longa* L. rhizome extract, was also confirmed in our previous studies. In [65], structure analysis by Raman spectroscopy showed better dispersion of the filler, which was presented in the nanocomposites in the form of few-layer sheets.

2.3. Thermal Properties of PVC/GN Nanocomposites

Next, thermogravimetric analysis was performed. Figure 5 presents TGA curves of a nanocomposite containing 0.1 wt.% of GN and PVC with the addition of CE and, for comparison, unmodified poly(vinyl chloride). The thermograms show mass loss at a temperatures up to 170 °C, which is related to the evaporation of residual THF [29,66]. The residual solvent in the films, regardless of their composition, was also found on the basis of the Raman spectrum [65]; its content was about 5.7% (Table 1) despite the applied evaporation and drying methods. This temperature range was proposed based on an earlier study, where a higher temperature would lead to the degradation of the material [67].

Therefore, the thermal degradation of poly(vinyl chloride) and nanocomposites is divided into two steps and is related to the decomposition of poly(vinyl chloride). The first step (from 200 to 375 °C) is related to the dehydrochlorination of the polymer matrix and the formation of a conjugated polyene structure. The second major mass loss in the range of 375 to 600 °C corresponds to thermal cracking of the carbonaceous conjugated polyene sequences and the formation of residual chars [22,29,66]. Based on the residual differential thermogravimetry (DTG) [24,68], the first and second decomposition steps were used to analyze the thermal stability of the obtained material, and the residual mass after the nanocomposite heating process was assessed. The results are summarized in Table 1 (standard deviation of the obtained mean values in brackets). The conducted thermogravimetric analysis proved a lack of statistically significant changes in the thermal

stability of the obtained nanocomposite materials compared with unmodified PVC. The addition of CE also did not affect the thermal stability of PVC/GN nanocomposites.

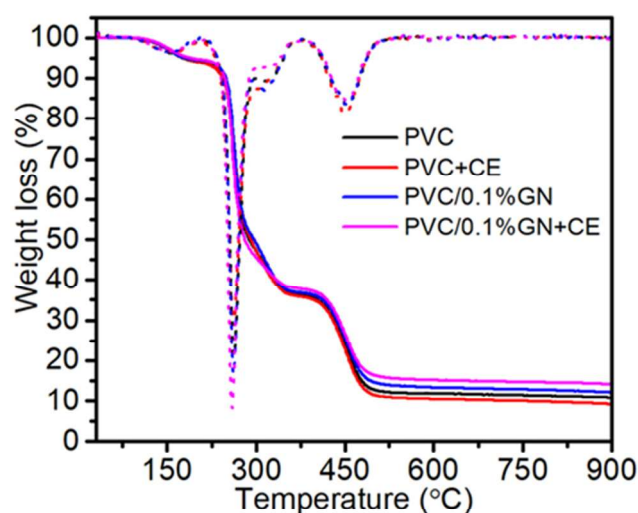


Figure 5. TGA thermograms of PVC, PVC + CE and PVC/0.1% GN, and PVC/0.1% GN + CE nanocomposites.

Table 1. Thermal properties.

Material	Cont. of THE, %	Max. DTG I, °C	Max. DTG II, °C	Residual Mass, %	Congo Red Test, Min	T _g , °C
PVC	5.3 (0.9)	268.4 (5.5)	456.5 (7.2)	8.7 (0.4)	3.0 (0.3)	74.3 (0.04)
PVC + CE	5.8 (0.2)	267.4 (4.9)	455.6 (8.1)	8.6 (1.2)	5.1 (0.8)	74.4 (0.2)
PVC/0.01% GN	5.9 (0.1)	268.2 (5.0)	459.0 (5.5)	9.5 (1.1)	2.5 (0.5)	74.5 (0.4)
PVC/0.01% GN + CE	5.8 (0.5)	264.3 (6.7)	456.1 (6.6)	11.0 (2.9)	5.7 (0.1)	76.3 (0.2)
PVC/0.1% GN	5.7 (0.2)	268.2 (5.7)	461.6 (4.2)	10.8 (1.2)	2.2 (0.2)	74.6 (0.2)
PVC/0.1% GN + CE	5.6 (0.3)	268.7 (8.6)	461.1 (3.6)	11.0 (2.8)	6.9 (0.3)	75.4 (0.1)
PVC/0.5% GN	5.8 (0.5)	267.5 (3.3)	460.4 (4.7)	10.8 (1.4)	4.0 (0.5)	73.3 (0.3)
PVC/0.5% GN + CE	5.7 (0.5)	263.4 (4.0)	459.5 (5.4)	11.9 (2.1)	5.7 (0.6)	75.3 (0.3)
PVC/1% GN	5.9 (0.9)	267.6 (7.1)	457.6 (7.8)	11.5 (1.8)	3.9 (0.2)	73.3 (0.2)
PVC/1% GN + CE	5.6 (0.3)	269.0 (6.1)	459.8 (6.6)	12.7 (0.9)	5.5 (0.2)	74.4 (0.3)

Poly(vinyl chloride) is sensitive to heat, so it can undergo thermomechanical degradation processes under processing due to the progressive dehydrochlorination that can take place according to various mechanisms [16]. The determination of the thermal stability of PVC is extremely important due to the correct selection of processing parameters. A commonly used method for assessing thermal stability is the Congo red test, which was applied to determine the thermal stability time of the obtained nanocomposites. The results presented in Table 1 show that the introduction of graphene at an amount above 0.5 wt.% results in a slight improvement in the thermal stability of materials with no CE content. On the other hand, a small concentration of graphene in the PVC matrix accelerates the dehydrochlorination process. The authors [68] indicated that the lower stability of PVC/GN composites may be due to the fact that GN nanoflakes act as a reinforcing particulate filler that attracts Cl. The addition of *Curcuma longa* L. extract significantly extended the thermal stability time of poly(vinyl chloride) nanocomposites containing graphene, which is similar, regardless of the GN content. The improvement in thermal stability was attributed to the antioxidant properties of curcuminoids containing the phenolic -OH group effectively neutralizing free radicals [69]. The mechanism preventing the propagation of HCl release from PVC, thanks to the use of antioxidants, is applied to improve its thermal stability [70].

2.4. Swelling Behavior of PVC/GN Nanocomposites

Numerous studies confirm the chemical resistance of poly(vinyl chloride) against various types of compounds [22,71,72]. However, PVC may swell or even dissolve if contacted with ketones, ethers, and aromatic or chlorinated hydrocarbons [39]. PVC dissolves completely in THF and cyclohexanone, and it undergoes limited swelling when contacted with acetone.

Therefore, in this work, the chemical resistance of the proposed PVC/GN nanocomposites was tested by analyzing the swelling process in acetone. Swelling curves, that is, the dependence of the swelling degree as a function of time, are shown in Figure 6.

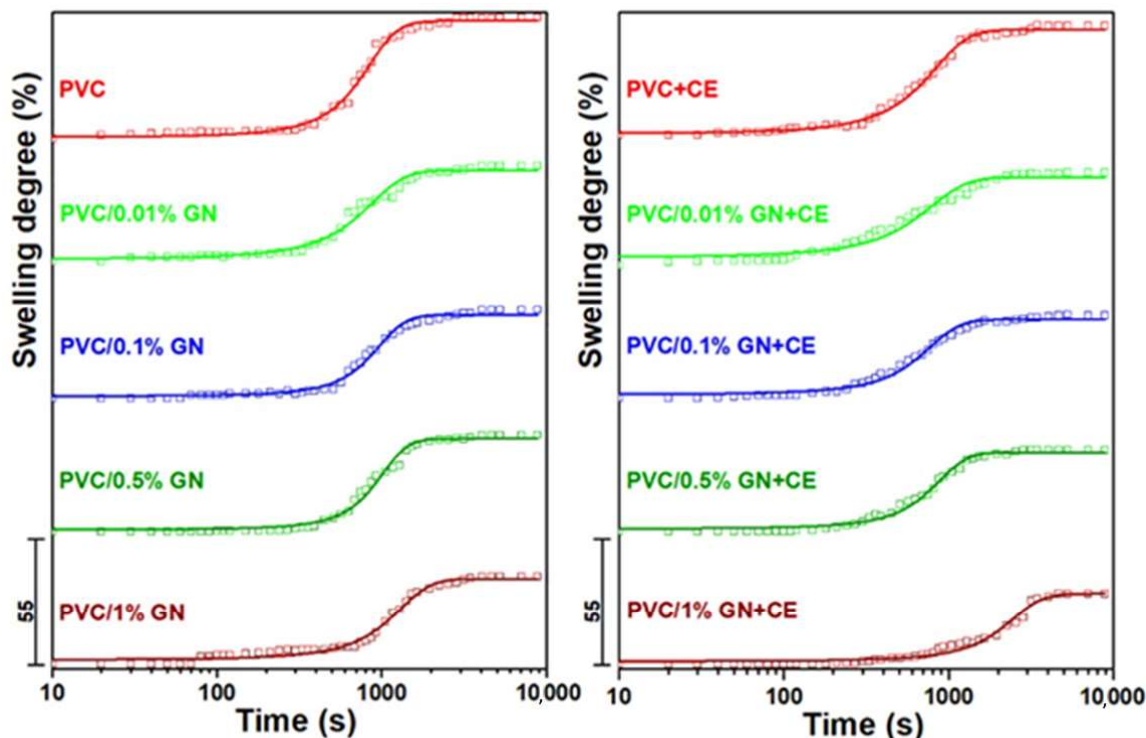


Figure 6. Swelling degree of PVC and PVC/GN nanocomposites vs. time.

On the basis of the obtained results, it was found that all the obtained materials undergo limited swelling, while the dependence of the swelling degree on the exposure time to the swelling agent has a shape of a sigmoid function. Therefore, Equation (1) was used to approximate the swelling curves [73]:

$$S_d = \frac{S_E}{1 + 10^{(t_M - t)p}} \quad (1)$$

where

S_d —swelling degree, %;

S_E —equilibrium swelling, upper asymptote, %;

t_M —time in which the swelling occurs with a maximum rate, s;

t —time of exposure to the swelling agent, s;

p —comparison parameter, s^{-1} .

The parameters of the equation and the coefficient of determination R^2 describing the degree of matching of the experimental results to the assumed model are summarized in Table 2. The proposed model describes the experimental results with high accuracy, as evidenced by the high values of the coefficient of determination (close to one).

Table 2. Parameters of the model describing the swelling process.

Material	S_E , %	t_M , s	p , s^{-1}	R^2
PVC	53.3 (0.5)	725 (10)	0.002 (0.00007)	0.994
PVC + CE	48.6 (0.4)	672 (10)	0.0017 (0.00005)	0.995
PVC/0.01% GN	41.4 (0.6)	702 (19)	0.0016 (0.00008)	0.986
PVC/0.01% GN + CE	38.4 (0.7)	599 (24)	0.0016 (0.00001)	0.974
PVC/0.1% GN	36.3 (0.4)	859 (16)	0.0019 (0.00009)	0.990
PVC/0.1% GN + CE	34.2 (0.4)	643 (14)	0.002 (0.00009)	0.990
PVC/0.5% GN	40.4 (0.5)	903 (16)	0.0019 (0.00001)	0.991
PVC/0.5% GN + CE	34.4 (0.4)	753 (14)	0.0019 (0.00008)	0.991
PVC/1% GN	37.4 (0.5)	1086 (24)	0.0012 (0.00005)	0.988
PVC/1% GN + CE	30.1 (0.7)	2091 (67)	0.0006 (0.00004)	0.979

It was found that the addition of CE to poly(vinyl chloride) reduces the equilibrium swelling degree (S_E) by 8.8%. Materials with graphene, even at 0.01 wt.% of GN content, are characterized by a much lower S_E in comparison with PVC and PVC + CE. The values of the equilibrium swelling degree decreased, thanks to the use of GN in nanocomposites. PVC/1% GN + CE was determined by the lowest S_E , which means an improvement by 43.5% in comparison with PVC and by 38.1% in comparison with PVC + CE. It should also be emphasized that nanocomposites with *Curcuma longa* L. extract are characterized by a lower value of the discussed parameter compared with the corresponding materials without CE. This was attributed to the improved dispersion of the filler in the polymer matrix, which was confirmed by significantly lower values of the equilibrium swelling degree for materials with 0.5 and 1 wt.% of GN. As the graphene content of the nanocomposites increased, the t_M value was also increased, which confirmed the chemical resistance of nanocomposites to acetone. A similar effect can be achieved by additional chlorination of the polymer chain [73]; however, the use of graphene is an environmentally friendly solution, and it does not require a chemical change in the structure of poly(vinyl chloride). In the literature, it has been indicated that the increased chemical resistance of PVC, thanks to the use of carbon fillers, is the result of increasing its stiffness and reducing its free volume. As a consequence, this leads to less solvent access to the polymer chain [71]. In the case of the discussed materials, this mechanism is very likely, which can be explained by the improvement of the graphene dispersion in the polymer matrix compared with bare GN.

2.5. Dynamic Mechanical Thermal Analysis of PVC/GN Nanocomposites

In order to assess the influence of GN on the mobility of PVC macromolecule segments, the dynamic mechanical properties of nanocomposites were investigated using tensile testing. Figure 7 shows the changes in the storage modulus (E') and the loss coefficient ($\tan \delta$) of the obtained materials as a function of temperature.

On the basis of the obtained results, it was observed that the value of the storage modulus decreased with the increase in temperature for all nanocomposites, regardless of their composition, which resulted from the increase in the mobility of the polymer chain segments [26]. The E' values of composites with no CE content decrease with the increase in the filler content in PVC, which may be related to the crumpled morphology of the applied GN and, above all, to the heterogeneous dispersion of the filler in the matrix [25,40]. The use of the extract resulted in the increase in the storage modulus of nanocomposites in the temperature range below the glass transition temperature compared with both PVC and composites with no CE content. Additionally, for samples containing up to 0.5 wt.% of GN in the polymer matrix, an increase in E' in the matrix is observed. The increase in E' indicates strong interfacial interactions between GN and PVC because of the use of CE, as

well as the limitation of the mobility of polymer chain segments by a well-dispersed filler and, thus, an increase in the stiffness of nanocomposites [26,31,74].

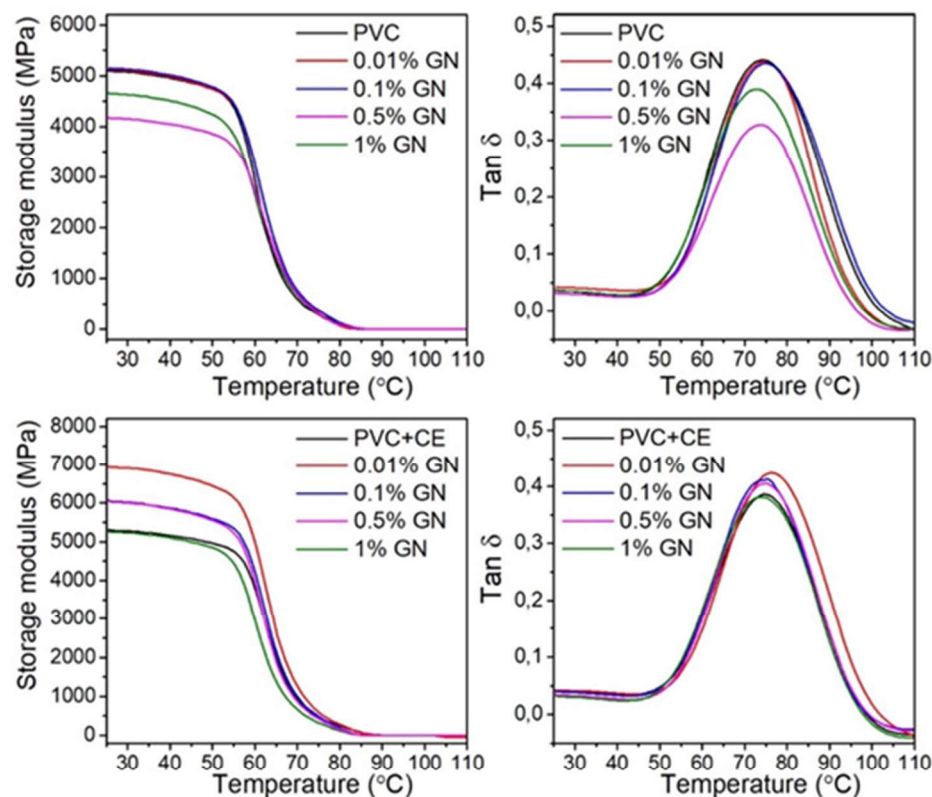


Figure 7. Storage modulus and $\tan \delta$ of PVC and PVC/GN nanocomposites.

The values of the glass transition temperature of nanocomposites and PVC as their matrices, determined on the basis of the dependence of $\tan \delta$ as a function of temperature, are summarized in Table 1. Extract from *Curcuma longa* L. had practically no effect on the T_g value of PVC with no filler. However, its application influenced the increase in T_g of PVC/GN + CE nanocomposites compared with both PVC and PVC/GN, while the highest value of this temperature was observed in the case of the PVC/0.01% GN + CE sample (increase by 2 °C compared with the T_g value of the matrix material). An increase in the concentration of graphene to 0.1 and 0.5 wt.% increases the T_g value about 1 °C what showing similar values to unmodified material. Therefore, it can be concluded that the amount of applied CE (1 wt.% based on PVC weight) is insufficient to increase filler–polymer interactions at higher GN contents.

In the composite without CE, no statistically significant effect of graphene at an amount up to 0.1 wt.% on the glass transition temperature of PVC was found. An increase in the content of graphene to 0.5 and 1 wt.% caused its decrease by 1 °C compared with the T_g value of unmodified PVC.

An increase in temperature associated with the maximum $\tan \delta$ value and an increase in the storage modulus in CE-containing materials indicate that well-dispersed graphene affects molecular dynamics, limiting the segmental movement of PVC polymer chains in nanocomposites. This leads to an increase in the glass transition temperature compared with unmodified PVC films.

2.6. Mechanical Properties of PVC/GN Nanocomposites

Figure 8 shows exemplary stress–strain curves of PVC and nanocomposites on the matrix and the determined tensile strength (TS). The results of the tests of mechanical properties are summarized in Table S1, included in the Supplementary Materials. The course of the stress–strain curve shows no yield point regardless of the material composition,

which is as expected. In the case of the film with no CE addition, an increase in the slope of the stress–strain curve can be observed, compared with the slope of the unmodified PVC curve. This is only in the case of the PVC/0.1% GN sample. The slope of the other curves is smaller.

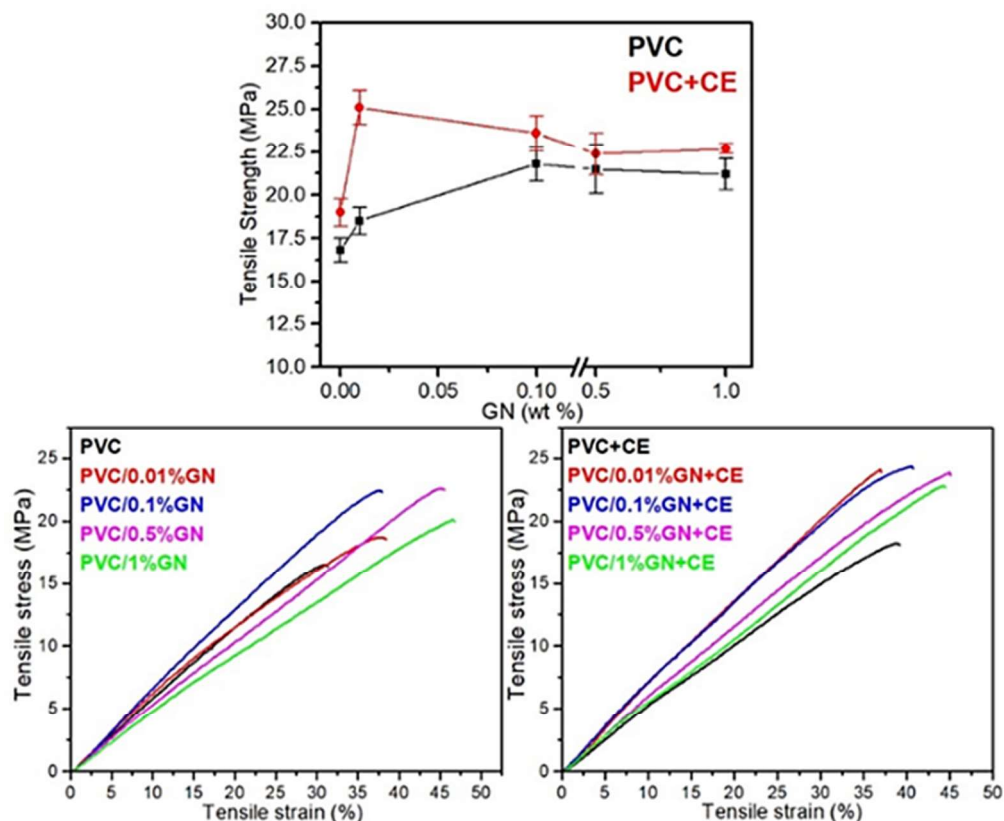


Figure 8. Mechanical properties of PVC and PVC/GN nanocomposites.

The slope of all stress–strain curves of a PVC/GN + CE foil is greater than the slope of the PVC + CE sample curve. A significant (and the largest) increase in the stress–strain curve slope was first observed for the sample containing as little as 0.01 wt.% of GN, indicating a higher stiffness of the materials, and improved the dispersion of the filler.

The presence of graphene flakes in the PVC matrix reduces the mobility of polymer chains, which leads to an increase in the stiffness of the material [64]. As the interfacial interactions in PVC/GN composites are of physical nature and may be insufficient to increase the stiffness of polymer chains at higher filler contents [25], the slope in the stress–strain curves decreases for PVC/0.5% GN and PVC/1% GN samples (Figure 8). The addition of CE caused an increase in interfacial interactions between the matrix and a nanofiller, as evidenced by the increase in stiffness of nanocomposites compared with the composites without CE.

Regardless of the composition of nanocomposites, the introduction of graphene into the PVC matrix resulted in an increase in tensile strength. The TS value of PVC with no dispersant was 16.8 MPa, and the addition of CE slightly increased this value (up to 19 MPa). The highest increase in tensile strength was observed for the samples of PVC/0.1% GN (by 29.8% as compared with PVC) and PVC/0.01% GN + CE (by 49.4% as compared with PVC and by 32.1% as compared with PVC + CE). A further increase in the content of graphene in nanocomposites, regardless of the presence of the dispersant, did not cause statistically significant changes in tensile strength, and the obtained mean values indicated a gradual decrease in TS. In [25,64,75], the authors indicated the presence of the percolation threshold, beyond which no significant increase in mechanical properties or even their deterioration was observed. This fact results from the secondary agglomeration

of graphene and the introduction of defects in the structure of nanocomposites along with the increasing content of the filler, for example, air bubbles sticking in the matrix. The presented results demonstrate the beneficial use of the extract from *Curcuma longa* L. as a graphene stabilizer in the PVC matrix, improving the mechanical properties of the nanocomposite. This is confirmed by an almost 35.7% increase in TS of a PVC/0.01% GN + CE film as compared with the material with the same content of graphene without CE. In the paper [65], it was indicated that the stabilization of the GN (using CE) dispersion in solutions and the poly(vinyl chloride) matrix occurs as a result of π - π interactions. As demonstrated in [35,38], intermolecular interactions can be successfully used to improve the filler-polymer interactions in PVC/GN nanocomposites. This effect was observed in the present research, but the constant amount of the applied dispersant (1 wt.%) was insufficient to increase the above-mentioned interactions at higher GN contents. This is evidenced by the lack of a statistically significant difference in the tensile strength values of nanocomposites with and without the addition of CE, containing 0.1 and 0.5 wt.% of graphene, respectively, and similar tensile strength values of films containing 1 wt.% of GN. In studies [25,31], it was pointed out that the use of additional nanocomposite components requires their correlation with the content of graphene.

To summarize, it can be clearly stated that the improvement of the mechanical properties of PVC/GN nanocomposites depends on the homogeneous dispersion of graphene in the polymer matrix. However, on the other hand, the dense GN network limits the penetration of poly(vinyl chloride) macromolecules between its layers, which makes the matrix discontinuous [25,30,64]. This explains the lack of a significant improvement in the mechanical properties of materials with significantly improved filler dispersion, for example, PVC/1% GN + CE. The filler-polymer interaction also has an impact on the limited improvement in these properties. The lack of oxygen-containing functional groups (the applied filler contained only 2.5% of oxygen—manufacturer's data) on the GN surface results in its high integrity and good mechanical properties, which directly determines the improvement of the mechanical properties of PVC/GN nanocomposites. However, the interfacial interactions in materials containing such fillers have the nature of physical bonds, too weak to improve tensile strength at high graphene contents in the composite [59,64,75]. As shown in the present study, the use of CE as a dispersant can improve interfacial interactions in nanocomposites. However, further research is needed to determine the appropriate extract content in relation to GN, which affects both the improvement of filler dispersion and the increase in filler-polymer interaction.

2.7. Electrical Properties of PVC/GN Nanocomposites

Literature reports [25,31,67] present that it is possible to modify the electrical properties of poly(vinyl chloride) with the use of graphene. The influence of GN on the resistivity or conductivity of PVC/GN nanocomposites is significantly related to the dispersion of the filler in the polymer matrix. Figure 9 shows the results of the resistivity tests of the obtained materials, which are summarized in Table S1 (Supplementary File).

The surface resistivity of poly(vinyl chloride) was determined to be 7.5×10^{15} , while in the case of PVC + CE, it equaled $4.5 \times 10^{15} \Omega$. The surface resistivity value decreases slightly for the nanocomposite without CE with the increase in graphene content to 0.1 wt.%, and its significant change occurs only when the filler concentration in the composites is 0.5 and 1 wt.%. The lowest resistivity, which equals $1.5 \times 10^7 \Omega$, is characteristic for the PVC/1% GN sample. This value allows the composite to be classified as an antistatic material [31,32]. Nanocomposites containing CE did not show such a sharp decrease in surface resistivity; after the decrease in its value to 1.7×10^{13} for the PVC/0.1% GN + CE sample, no further significant changes were observed. The volume resistivity of PVC/GN composites with no CE also decreases with the increase in graphene concentration in the matrix, and its step change occurs at 0.5 wt.% of the filler. The materials containing 1 wt.% of GN were characterized by the lowest resistivity, and it equaled $3.9 \times 10^5 \Omega \text{ m}$, which means a change by nine orders of magnitude compared with PVC (7.7×10^{14}). Considering

the significant agglomeration of graphene, such a large change in resistivity is, on the one hand, a surprising effect, and on the other hand, it indicates that the GN dispersion was sufficient to create conduction paths. PVC/GN + CE composites, as in the case of surface resistivity, did not show large changes in volume resistivity as the filler content in the matrix increased.

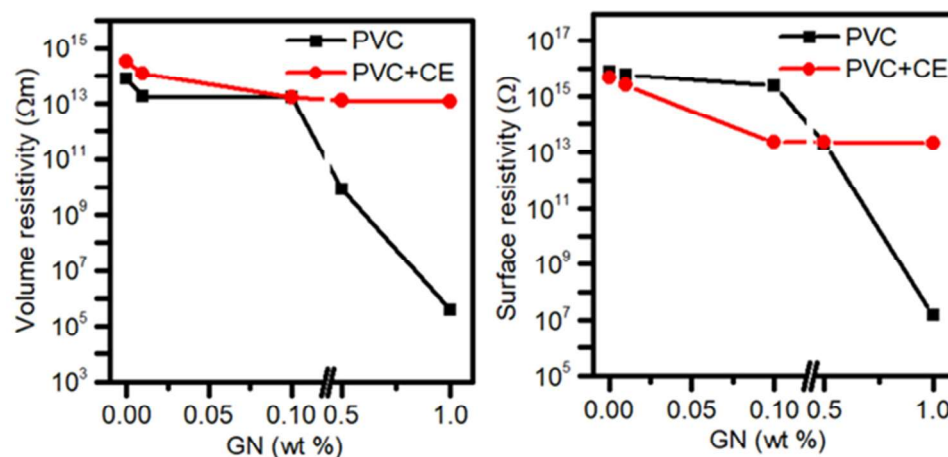


Figure 9. Surface and volume resistivity of PVC and nanocomposites.

No change in the resistivity of CE-containing materials, despite a significant improvement in GN dispersion, results from the π - π interactions between graphene and curcuminoids. Some studies show the disturbances in the displacement of π electrons on the graphene surface, leading to the significant deterioration of its electrical properties [35,67]. Nevertheless, the application of CE improves the interfacial interactions, leading to the well dispersion of GN in the polymer matrix.

3. Experimental Section

3.1. Materials

Graphene-based nanopowder with a flake thickness of 1.6 nm (maximum of 3 atomic monolayers), a flake length of 10 μ m, and a specific surface area of $400 \div 800 \text{ m}^2\text{g}^{-1}$ was purchased from USA Graphene Laboratories Inc. Graphene was dispersed in a poly(vinyl chloride) solution using unmodified suspensive poly(vinyl chloride) Neralit 601 (Czech Republic, Spolana s.r.o. Anwil S.A. group) with a K number of 59–61, a bulk density of $0.56\text{--}0.63 \text{ g cm}^{-3}$, a specific density of 1.39 g cm^{-3} , and 97% purity. As a solvent for PVC, tetrahydrofuran (THF) (Chempur, Piekary Śląskie, Poland) was used. *Curcuma longa* L. rhizome extract was used as a stabilizer of graphene in a PVC solution. Materials for the analysis of the extract with HPLC grade of methanol, acetonitrile, and water were purchased from Sigma-Aldrich (St. Louis, MO, USA). Acetic acid (99%), curcumin (99.5%), demethoxycurcumin (≥ 98), and bisdemethoxycurcumin (99%) were supplied from Sigma-Aldrich (USA).

3.2. Preparation of *Curcuma longa* L. Rhizome Extract

Curcuma longa L. extract was prepared by extraction in a B-811 Büchi Soxhlet extractor (Byrne, Switzerland), where 20 g of *Curcuma longa* L. rhizome powder (Heuschen & Schrouff, Landgraaf, The Netherlands) was placed in a glass thimble and extracted with methanol (Chempur, Poland). Extraction was performed in 80 °C for 3 h. Then, the solvent was evaporated from the extract at 60 °C for 24 h, pure extract. The methodology and analysis of the obtained extract are presented in the Supplementary Materials.

3.3. Preparation of PVC/GN Nanocomposites

In the first stage of preparation of the nanocomposites, poly(vinyl chloride) was dissolved in THF at 25 °C for ca. 48 h, yielding a solution with a concentration of 3 wt.% Next,

graphene was added to the solution and dispersed for 60 min at 20 °C. The dispersion of graphene flakes was enhanced ultrasonically with a frequency of 20 kHz and 40% amplitude, using a SONOPULS rod-shaped probe homogenizer from Bandelin. The suspension containing curcuma extract was prepared in the same way, adding 1% of CE to the PVC weight. The amount of graphene in the prepared dispersions was 0.01%, 0.1%, 0.5%, and 1% per the polymer weight.

Then, the thin films of PVC/GN nanocomposites were obtained by the solvent evaporation method onto Petri dishes having a diameter of 7 cm, where the solvent was evaporated at 50 °C for 24 h. To remove the THF residue, the film was dried in a vacuum drier under reduced pressure (max 20 mbar absolute) at 50 °C for 2 weeks. Films of unmodified PVC and PVC with 1 wt.% of CE were obtained under the same conditions. All samples were coded to take into account the graphene content and the presence of curcumin, for example, a sample containing only GN at a concentration of 0.01 wt.% as PVC/0.01% GN versus a sample containing the same graphene content and turmeric extract PVC/0.01% GN + CE.

3.4. Methods of *Curcuma longa* L. Rhizome Extract Analysis

The identification of *Curcuma longa* L. rhizome extract was carried out by Fourier-transform infrared spectroscopy (FTIR) using the ATR technique. The study was performed with an Alpha apparatus from Bruker in the range of 400–4000 cm^{-1} . A total of 32 scans at a resolution of 4 cm^{-1} were performed.

For HPLC analysis, the fresh turmeric extract for chromatographic determination was dissolved in methanol. The methanol solution was filtered through a 0.45 μm Acrodisc 13 mm nylon filter (Gelman, St. Louis, MO, USA). HPLC analysis was performed using a Shimadzu UFLCXR with a SPD-M30A photodiode array detector. The UV-vis spectra were taken in the range of 200–800 nm. A Phenomenex Luna 3 μ C18(2) 100A (150 \times 3.0 mm) column was used. The column temperature was set at 40 °C. The profile of the gradient elution was: (A) water (0.25% HOAc) and (B) acetonitrile 1, 0–17 min, 40–60% B; 17–28 min, 60–100% B; 28–35 min, 100% B; 35–40 min, 100–40% B, at a flow rate of 0.8 mL min^{-1} .

For the quantitative analysis of curcumin, demethoxycurcumin, bisdemethoxycurcumin, the following concentrations of each compound were prepared: 2, 10, 20, 40, and 80 $\mu\text{g mL}^{-1}$. A calibration curve and a correlation coefficient (R^2) were determined for each compound. The limit of detection (LOD) was defined as the signal-to-noise (S/N) ratio of 3. The limit of quantification (LOQ) was defined as S/N = 10. Concentrations of curcumin, demethoxycurcumin, and bisdemethoxycurcumin in the extract were calculated based on the regression equations.

The curcumin extract was also analyzed on an Agilent 7890B GC System gas chromatograph with an Agilent 5977B GC/MSD mass spectrometry detector with an HP-5MS column (0.25 mm \times 30 m \times 0.25 μm). The analyses were performed under the following chromatographic conditions: injector temperature of 250 °C, detector temperature of 280 °C, oven temperature program from 50 °C/4 min increase of 15 °C min^{-1} to 300 °C (maintained for 10 min). Helium was used as a carrier gas, flow 1 mL min^{-1} . The volume of the sample was 1 μL . The substances were identified by comparing the obtained MS spectra with the spectra of the NIST17.L Mass Spectrum Library.

3.5. Characterization of PVC/GN Nanocomposites

The structure of the prepared nanocomposites was studied using a ZEISS EVO 40 scanning electron microscope (SEM). The samples for SEM observation were fractured cryogenically and sputtered with gold nanometric layer.

The filler dispersion in the matrix was also determined by a Nanosurf atomic force microscope (AFM) (Liestal, Switzerland) in contact mode using a PPP-XYCONTR measuring probe (NANOSENSORS, Neuchatel, Switzerland), where the fillet radius of the aluminum-coated blade was 7 nm, while its line inclination angle was 20 degrees. The surface roughness was measured over a distance of 50 μm by collecting data from 50 measurement lines at 1 nm intervals. The number of measuring points per one line was

5000. The sample scan rate during surface evaluation by roughness measurement was $12.5 \mu\text{m s}^{-1}$. Three-dimensional images were made within an area of $10 \times 10 \mu\text{m}$. In order to determine the surface topography, 500 lines were measured in the given area (at 20 nm intervals), and the number of measuring points per one line was 5000. The sample scan rate was $5 \mu\text{m s}^{-1}$.

The thermal stability of the nanocomposites was assessed by the thermogravimetric method (TGA) using a TG 209 F3 Tarsus apparatus (Netzsch). The heating rate was about $10 \text{ }^\circ\text{C min}^{-1}$ in an open ceramic crucible under a nitrogen atmosphere in the temperature range of 30 to 900 $^\circ\text{C}$. The change in sample mass as a function of temperature was measured. Static thermal stability tests using the Congo red test at 200 $^\circ\text{C}$ measuring the thermal stability time, that is, the time when the sample shows no signs of destruction in the form of hydrogen chloride release and color changes of the indicator paper, were also performed [76].

The resistance of the obtained materials to swelling in acetone was tested in accordance with the method proposed in our earlier study [67]. The measurement consisted in determining the change in swelling degree (S_d) (see Equation (2)), depending on the immersion time in the swelling agent. The changes in the sample diameters were determined on the basis of photos using the NIS-Elements 4.0 software. The frequency of taking pictures depended on the exposure time to the swelling agent. The measurement temperature was 20 $^\circ\text{C}$, and the initial diameter of the samples was $h_0 = 10 \text{ mm}$,

$$S_d = \frac{h - h_0}{h_0} \cdot 100\% \quad (2)$$

where

h —sample diameter after time t (mm);

h_0 —initial sample diameter (mm).

Next, the thermomechanical and mechanical properties of nanocomposites were investigated. Thermal analysis of dynamic mechanical properties was performed on a DMA Artemis device (Netzsch Group, Selb, Germany). The values of the storage modulus (E') and the loss angle tangent ($\tan\delta$) as a function of temperature were determined. The position of the maximum $\tan\delta$ was assumed to be the glass transition temperature. The test was performed in the tensile mode (measuring length of 10 mm, sample width of 5 mm, thickness of $0.18 \pm 0.02 \text{ mm}$) with a deformation of 10 μm in the temperature range of 25–110 $^\circ\text{C}$ and with a heating rate of 2 $^\circ\text{C min}^{-1}$. The deformation was determined with a frequency of 1 Hz. A relatively small amplitude and low frequency of deformation allow for measurement in the linear viscoelastic range [77,78].

A study of tensile properties was carried out with the use of an in-house built tensile tester equipped with a Zemic H3-C3-25 kg-3B strain gauge beam characterized by a measuring range of 25 kg and a maximum measurement error of 0.02%. The tests were carried out on samples with a thickness of $0.18 \pm 0.02 \text{ mm}$ and a width of $2 \pm 0.1 \text{ mm}$, while the length of the measuring section L_0 was 1.5 mm. The materials were stretched at a constant rate of 0.1 mm s^{-1} , and the mechanical properties of the nanocomposites were determined on the basis of the measurement data. The force from the strain gauge beam was recorded with an accuracy of 0.001 N every 0.014 s [79,80].

Electrical properties of nanocomposites were determined by examining surface and volume resistivity. The measurement was performed with a measuring system consisting of a 6517A electrometer and a 8009 measuring chamber (Keithley Instrument Inc., Cleveland, OH, USA). Measurements of volume and surface resistivity were carried out on film samples with a diameter of 70 mm in air at a temperature of 23 $^\circ\text{C}$ and humidity of 50% at a voltage of 10 V.

In order to analyze the obtained results, the Origin 8.6 Pro software with implemented statistical analysis modules was used. ANOVA with Tukey's post hoc test was used to compare the significance of the difference for the mean values of the obtained results.

The normal distribution was confirmed by the Shapiro–Wilk test, and the homogeneity of variance by Levene’s test. All analyses were performed assuming a significance level below 0.05.

4. Conclusions

In this work, a nanocomposite based on poly(vinyl chloride) and graphene stabilized with *Curcuma longa* L. extract was proposed. The use of the environmentally friendly plant extract significantly improved the dispersion of GN in the PVC matrix, which was confirmed by SEM and AFM. CE did not affect the thermal stability of PVC measured by the TGA method, but improved the thermal stability time (determined by means of the Congo red test) due to the antioxidant properties of this dispersant. The enhancement of the stability time indicates promising potential for its application for the production of nanocomposites by the melt mixing method. Moreover, a significant improvement in mechanical and thermomechanical properties at a very low content of GN (0.01 wt.%) is noteworthy, which indicates an increase in the filler–polymer interfacial interactions resulting from the use of CE. The use of the extract causes a significant deterioration of the electrical properties of graphene, resulting in the lack of changes in the resistivity of nanocomposites.

Curcuma longa L. extract has great potential to be used as a dispersant in PVC/GN nanocomposites, mainly because of its lack of negative impact on health and the environment. However, its application requires further research aimed at developing an optimal composition of certain composites in which the amount of CE will be correlated with the content of GN.

Supplementary Materials: The following supporting information can be downloaded at: <https://www.mdpi.com/article/10.3390/molecules27228081/s1>, Figure S1: Mass spectrum of Ar-curcumene; Figure S2: Mass spectrum of (-)-zingiberene; Figure S3: Mass spectrum of β -sesquiphellandrene; Figure S4: Mass spectrum of Ar-turmerone; Figure S5: Mass spectrum of α -turmerone; Figure S6: Mass spectrum of β -turmerone; Figure S7: Mass spectrum of (6R,7R)-bisabolene; Figure S8: Mass spectrum of (E)-atlantone; Table S1: Mechanical and electrical properties of PVC/GN nanocomposites.

Author Contributions: Conceptualization, S.W., K.S. and J.T.; methodology, S.W., K.S., K.L. and J.T.; validation, S.W., K.S., J.T., K.L., W.S., M.O., P.J., H.G. and A.D.; formal analysis, S.W., K.S. and K.L.; investigation, S.W., K.S., K.L., W.S., P.J., H.G. and A.D.; resources, S.W., K.S. and J.T.; data curation, S.W., K.S., K.L., W.S., P.J., H.G. and A.D.; writing—original draft preparation, S.W., K.S., J.T., K.L., W.S. and M.O.; visualization, S.W. and K.L.; supervision, J.T. and M.O.; project administration, S.W. All authors have read and agreed to the published version of the manuscript.

Funding: This work was supported by the Ministry of Education and Science of Poland.

Institutional Review Board Statement: Not applicable.

Informed Consent Statement: Not applicable.

Data Availability Statement: The data that support the findings of this study are available in the Supplementary Materials of this article or from the corresponding author upon reasonable request.

Conflicts of Interest: The authors declare that they have no known competing financial interest or personal relationship that could have appeared to influence the work reported in this paper.

Sample Availability: Samples of the compounds are not available from the authors.

References

1. Saleem, H.; Haneef, M.; Abbasi, H.Y. Synthesis route of reduced graphene oxide via thermal reduction of chemically exfoliated graphene oxide. *Mater. Chem. Phys.* **2018**, *204*, 1–7. [[CrossRef](#)]
2. Johnson, D.W.; Dobson, B.P.; Coleman, K.S. A manufacturing perspective on graphene dispersions. *Curr. Opin. Colloid Interface Sci.* **2015**, *20*, 367–382. [[CrossRef](#)]
3. Abdel Ghany, N.A.; Elsherif, S.A.; Handal, H.T. Revolution of Graphene for different applications: State-of-the-art. *Surf. Interfaces* **2017**, *9*, 93–106. [[CrossRef](#)]

4. Drewniak, S.; Muzyka, R.; Stolarczyk, A.; Pustelny, T.; Kotyczka-Morańska, M.; Setkiewicz, M. Studies of reduced graphene oxide and graphite oxide in the aspect of their possible application in gas sensors. *Sensors* **2016**, *16*, 103. [[CrossRef](#)] [[PubMed](#)]
5. Mikhailov, S. *Physics and Applications of Graphene-Experiments*; InTech: Singapore, 2011; ISBN 9789533071527.
6. Punetha, V.D.; Rana, S.; Yoo, H.J.; Chaurasia, A.; McLeskey, J.T.; Ramasamy, M.S.; Sahoo, N.G.; Cho, J.W. Functionalization of carbon nanomaterials for advanced polymer nanocomposites: A comparison study between CNT and graphene. *Prog. Polym. Sci.* **2017**, *67*, 1–47. [[CrossRef](#)]
7. Galpaya, D.; Wang, M.; Liu, M.; Motta, N.; Waclawik, E.; Yan, C. Recent Advances in Fabrication and Characterization of Graphene-Polymer Nanocomposites. *Graphene* **2012**, *01*, 30–49. [[CrossRef](#)]
8. Sreenivasulu, B.; Ramji, B.R.; Nagaral, M. A Review on Graphene Reinforced Polymer Matrix Composites. *Mater. Today Proc.* **2018**, *5*, 2419–2428. [[CrossRef](#)]
9. Phiri, J.; Gane, P.; Maloney, T.C. General overview of graphene: Production, properties and application in polymer composites. *Mater. Sci. Eng. B Solid State Mater. Adv. Technol.* **2017**, *215*, 9–28. [[CrossRef](#)]
10. Mohan, V.B.; Lau, K.; Hui, D.; Bhattacharyya, D. Graphene-based materials and their composites: A review on production, applications and product limitations. *Compos. Part B Eng.* **2018**, *142*, 200–220. [[CrossRef](#)]
11. Münch, F.; Höllerer, C.; Klapproth, A.; Eckert, E.; Ruffer, A.; Cesnjevar, R.; Göen, T. Effect of phospholipid coating on the migration of plasticizers from PVC tubes. *Chemosphere* **2018**, *202*, 742–749. [[CrossRef](#)]
12. Brostow, W.; Lu, X.; Osmanson, A.T. Nontoxic bio-plasticizers for PVC as replacements for conventional toxic plasticizers. *Polym. Test.* **2018**, *69*, 63–70. [[CrossRef](#)]
13. Yousif, E.; Salimon, J.; Salih, N. New photostabilizers for PVC based on some diorganotin(IV) complexes. *J. Saudi Chem. Soc.* **2015**, *19*, 133–141. [[CrossRef](#)]
14. Borowska, A.; Sterzyński, T.; Piszczek, K. Ocena degradacji PVC-U poddanego przyspieszonemu starzeniu fotooksydacyjnemu. *Polimery* **2010**, *55*, 306–313. [[CrossRef](#)]
15. Piszczek, K. *Żelowanie Suspensyjnego, Nieplastyfikowanego Poli(Chlorku Winyłu)*; Wydawnictwa Uczelniane Uniwersytetu Technologiczno-Przyrodniczego: Bydgoszcz, Poland, 2009.
16. Klapiszewski, Ł.; Tomaszewska, J.; Skórczewska, K.; Jesionowski, T. Preparation and characterization of eco-friendly Mg(OH)₂/lignin hybrid material and its use as a functional filler for poly(vinyl chloride). *Polymers* **2017**, *9*, 258. [[CrossRef](#)] [[PubMed](#)]
17. Feng, A.; Wu, G.; Wang, Y.; Pan, C. Synthesis, preparation and mechanical property of wood fiber-reinforced poly(vinyl chloride) composites. *J. Nanosci. Nanotechnol.* **2017**, *17*, 3859–3863. [[CrossRef](#)]
18. Taha, T.A.; Azab, A.A. Thermal, optical, and dielectric investigations of PVC/La_{0.95}Bi_{0.05}FeO₃ nanocomposites. *J. Mol. Struct.* **2019**, *1178*, 39–44. [[CrossRef](#)]
19. Qiu, F.; He, G.; Hao, M.; Zhang, G. Enhancing the mechanical and electrical properties of poly(vinyl chloride)-based conductive nanocomposites by zinc oxide nanorods. *Materials* **2018**, *11*, 2139. [[CrossRef](#)]
20. Sterzyński, T.; Tomaszewska, J.; Piszczek, K.; Skórczewska, K. The influence of carbon nanotubes on the PVC glass transition temperature. *Compos. Sci. Technol.* **2010**, *70*, 966–969. [[CrossRef](#)]
21. Lu, Y.; Khanal, S.; Ahmed, S.; Xu, S. Mechanical and thermal properties of poly(vinyl chloride) composites filled with carbon microspheres chemically modified by a biopolymer coupling agent. *Compos. Sci. Technol.* **2019**, *172*, 29–35. [[CrossRef](#)]
22. Deshmukh, K.; Joshi, G.M. Thermo-mechanical properties of poly (vinyl chloride)/graphene oxide as high performance nanocomposites. *Polym. Test.* **2014**, *34*, 211–219. [[CrossRef](#)]
23. Nawaz, K.; Ayub, M.; Ul-Haq, N.; Khan, M.B.; Niazi, M.B.K.; Hussain, A. The Effect of Graphene Nanosheets on the Mechanical Properties of Polyvinylchloride. *Polym. Compos.* **2016**, *37*, 1572–1576. [[CrossRef](#)]
24. Mindivan, F.; Göktas, M. Preparation of new PVC composite using green reduced graphene oxide and its effects in thermal and mechanical properties. *Polym. Bull.* **2020**, *77*, 1929–1949. [[CrossRef](#)]
25. Li, Q.; Shen, F.; Zhang, Y.; Huang, Z.; Muhammad, Y.; Hu, H.; Zhu, Y.; Yu, C.; Qin, Y. Graphene incorporated poly(vinyl chloride) composites prepared by mechanical activation with enhanced electrical and thermo-mechanical properties. *J. Appl. Polym. Sci.* **2020**, *137*, 21–23. [[CrossRef](#)]
26. Akhina, H.; Gopinathan Nair, M.R.; Kalarikkal, N.; Pramoda, K.P.; Hui Ru, T.; Kailas, L.; Thomas, S. Plasticized PVC graphene nanocomposites: Morphology, mechanical, and dynamic mechanical properties. *Polym. Eng. Sci.* **2018**, *58*, E104–E113. [[CrossRef](#)]
27. Wang, H.; Xie, G.; Fang, M.; Ying, Z.; Tong, Y.; Zeng, Y. Mechanical reinforcement of graphene/poly(vinyl chloride) composites prepared by combining the in-situ suspension polymerization and melt-mixing methods. *Compos. Part B Eng.* **2017**, *113*, 278–284. [[CrossRef](#)]
28. Wang, H.; Xie, G.; Yang, C.; Zheng, Y.; Ying, Z.; Ren, W.; Zeng, Y. Enhanced Toughness of Multilayer Graphene-Filled Poly(vinyl chloride) Composites Prepared Using Melt-Mixing Method. *Polym. Compos.* **2017**, *38*, 138–146. [[CrossRef](#)]
29. Hasan, M.; Banerjee, A.N.; Lee, M. Enhanced thermo-optical performance and high BET surface area of graphene@PVC nanocomposite fibers prepared by simple facile deposition technique: N₂ adsorption study. *J. Ind. Eng. Chem.* **2015**, *21*, 828–834. [[CrossRef](#)]
30. Wang, L.; Wei, X.; Wang, G.; Zhao, S.; Cui, J.; Gao, A.; Zhang, G.; Yan, Y. A facile and industrially feasible one-pot approach to prepare graphene-decorated PVC particles and their application in multifunctional PVC/graphene composites with segregated structure. *Compos. Part B Eng.* **2020**, *185*, 107775. [[CrossRef](#)]

31. Wang, H.; Xie, G.; Fang, M.; Ying, Z.; Tong, Y.; Zeng, Y. Electrical and mechanical properties of antistatic PVC films containing multi-layer graphene. *Compos. Part B Eng.* **2015**, *79*, 444–450. [[CrossRef](#)]
32. Wei, Z.B.; Zhao, Y.; Wang, C.; Kuga, S.; Huang, Y.; Wu, M. Antistatic PVC-graphene Composite through Plasticizer-mediated Exfoliation of Graphite. *Chin. J. Polym. Sci.* **2018**, *36*, 1361–1367. [[CrossRef](#)]
33. Ma, J.; Liu, J.; Zhu, W.; Qin, W. Solubility study on the surfactants functionalized reduced graphene oxide. *Colloids Surf. A Physicochem. Eng. Asp.* **2018**, *538*, 79–85. [[CrossRef](#)]
34. Dai, J.; Wang, G.; Ma, L.; Wu, C. Study on the surface energies and dispersibility of graphene oxide and its derivatives. *J. Mater. Sci.* **2015**, *50*, 3895–3907. [[CrossRef](#)]
35. Tkalya, E.E.; Ghislandi, M.; De With, G.; Koning, C.E. The use of surfactants for dispersing carbon nanotubes and graphene to make conductive nanocomposites. *Curr. Opin. Colloid Interface Sci.* **2012**, *17*, 225–232. [[CrossRef](#)]
36. Kuila, T.; Bose, S.; Mishra, A.K.; Khanra, P.; Kim, N.H.; Lee, J.H. Chemical functionalization of graphene and its applications. *Prog. Mater. Sci.* **2012**, *57*, 1061–1105. [[CrossRef](#)]
37. Ma, F.; Yuan, N.; Ding, J. The conductive network made up by the reduced graphene nanosheet/polyaniline/polyvinyl chloride. *J. Appl. Polym. Sci.* **2013**, *128*, 3870–3875. [[CrossRef](#)]
38. Li, P.; Chen, X.; Zeng, J.-B.; Gan, L.; Wang, M. Enhancement of Interfacial Interaction between Poly(vinyl chloride) and Zinc Oxide Modified Reduced Graphene Oxide. *RSC Adv.* **2016**, *6*, 5784–5791. [[CrossRef](#)]
39. Khaleghi, M.; Didehban, K.; Shabaniyan, M. Simple and fast preparation of graphene oxide@melamine terephthaldehyde and its PVC nanocomposite via ultrasonic irradiation: Chemical and thermal resistance study. *Ultrason. Sonochem.* **2018**, *43*, 275–284. [[CrossRef](#)]
40. Hu, J.; Jia, X.; Li, C.; Ma, Z.; Zhang, G.; Sheng, W.; Zhang, X.; Wei, Z. Effect of interfacial interaction between graphene oxide derivatives and poly(vinyl chloride) upon the mechanical properties of their nanocomposites. *J. Mater. Sci.* **2014**, *49*, 2943–2951. [[CrossRef](#)]
41. Khaleghi, M.; Didehban, K.; Shabaniyan, M. Effect of new melamine-terephthaldehyde resin modified graphene oxide on thermal and mechanical properties of PVC. *Polym. Test.* **2017**, *63*, 382–391. [[CrossRef](#)]
42. Hatamie, S.; Ahadian, M.M.; Irajizad, A.; Akhavan, O.; Jokar, E. Photoluminescence and electrochemical investigation of curcumin-reduced graphene oxide sheets. *J. Iran. Chem. Soc.* **2018**, *15*, 351–357. [[CrossRef](#)]
43. Hatamie, S.; Akhavan, O.; Sadrezaad, S.K.; Ahadian, M.M.; Shirolkar, M.M.; Wang, H.Q. Curcumin-reduced graphene oxide sheets and their effects on human breast cancer cells. *Mater. Sci. Eng. C* **2015**, *55*, 482–489. [[CrossRef](#)]
44. Navik, R.; Gai, Y.; Wang, W.; Zhao, Y. Curcumin-assisted ultrasound exfoliation of graphite to graphene in ethanol. *Ultrason. Sonochem.* **2018**, *48*, 96–102. [[CrossRef](#)]
45. Rohman, A.; Sudjadi, D.; Ramadhani, D.; Nugroho, A. Analysis of curcumin in curcuma longa and Curcuma xanthorrhiza using FTIR spectroscopy and chemometrics. *Res. J. Med. Plant* **2015**, *9*, 179–186. [[CrossRef](#)]
46. Bagchi, A. Extraction of Curcumin. *IOSR J. Environ. Sci. Toxicol. Food Technol.* **2012**, *1*, 1–16. [[CrossRef](#)]
47. Priyadarsini, K.I. The chemistry of curcumin: From extraction to therapeutic agent. *Molecules* **2014**, *19*, 20091–20112. [[CrossRef](#)]
48. Lestari, M.; Indrayanto, G. Curcumin. *Profiles Drug Subst. Excipients Relat. Methodol.* **2014**, *39*, 113–204. [[CrossRef](#)]
49. Saltos, J.A.; Shi, W.; Mancuso, A.; Sun, C.; Park, T.; Averick, N.; Punia, K.; Fatab, J.; Raja, K. Curcumin-derived green plasticizers for Poly(vinyl) chloride. *RSC Adv.* **2014**, *4*, 54725–54728. [[CrossRef](#)]
50. Larrañeta, E.; Imízcoz, M.; Toh, J.X.; Irwin, N.J.; Ripolin, A.; Perminova, A.; Domínguez-Robles, J.; Rodríguez, A.; Donnelly, R.F. Synthesis and Characterization of Lignin Hydrogels for Potential Applications as Drug Eluting Antimicrobial Coatings for Medical Materials. *ACS Sustain. Chem. Eng.* **2018**, *6*, 9037–9046. [[CrossRef](#)]
51. Velho, S.; Brum, L.; Petter, C.; dos Santos, J.H.; Šimunić, Š.; Kappa, W.H. Development of structured natural dyes for use into plastics. *Dye. Pigment.* **2017**, *136*, 248–254. [[CrossRef](#)]
52. Mohan, P.R.K.; Sreelakshmi, G.; Muraleedharan, C.V.; Joseph, R. Water soluble complexes of curcumin with cyclodextrins: Characterization by FT-Raman spectroscopy. *Vib. Spectrosc.* **2012**, *62*, 77–84. [[CrossRef](#)]
53. Sofyan, N.; Situmorang, F.W.; Ridhova, A.; Yuwono, A.H.; Udhiarto, A. Visible light absorption and photosensitizing characteristics of natural yellow 3 extracted from Curcuma Longa, L. for Dye-Sensitized solar cell. *IOP Conf. Ser. Earth Environ. Sci.* **2018**, *105*, 1–6. [[CrossRef](#)]
54. He, X.G.; Lin, L.Z.; Lian, L.Z.; Lindenmaier, M. Liquid chromatography-electrospray mass spectrometric analysis of curcuminoids and sesquiterpenoids in turmeric (*Curcuma longa*). *J. Chromatogr. A* **1998**, *818*, 127–132. [[CrossRef](#)]
55. Singh, G.; Kapoor, I.P.S.; Singh, P.; de Heluani, C.S.; de Lampasona, M.P.; Catalan, C.A.N. Comparative study of chemical composition and antioxidant activity of fresh and dry rhizomes of turmeric (*Curcuma longa* Linn.) *Food Chem. Tox.* **2010**, *48*, 1026–1031. [[CrossRef](#)]
56. Xu, L.L.; Shang, Z.P.; Lu, Y.Y.; Li, P.; Sun, L.; Guo, Q.L.; Bo, T.; Le, Z.Y.; Bai, Z.L.; Zhang, X.L.; et al. Analysis of curcuminoids and volatile components in 160 batches of turmeric samples in China by high-performance liquid chromatography and gas chromatography mass spectrometry. *J. Pharm. Biomed. Anal.* **2020**, *188*, 113465. [[CrossRef](#)]
57. Li, R.; Xiang, C.; Zhang, X.; An Guo, D.-; Ye, M. Chemical Analysis of the Chinese Herbal Medicine Turmeric (*Curcuma longa* L.). *Curr. Pharm. Anal.* **2010**, *6*, 256–268. [[CrossRef](#)]
58. Asgarzadeh, Z.; Naderi, G. Morphology and properties of unvulcanized and dynamically vulcanized PVC/NBR blend reinforced by graphene nanoplatelets. *Int. Polym.* **2018**, *33*, 497–505. [[CrossRef](#)]

59. Wang, H.; Xie, G.; Zhu, Z.; Ying, Z.; Zeng, Y. Enhanced tribological performance of the multi-layer graphene filled poly(vinyl chloride) composites. *Compos. Part A Appl. Sci. Manuf.* **2014**, *67*, 268–273. [[CrossRef](#)]
60. Wang, H.; Xie, G.; Ying, Z.; Tong, Y.; Zeng, Y. Enhanced mechanical properties of multi-layer graphene filled poly(vinyl chloride) composite films. *J. Mater. Sci. Technol.* **2015**, *31*, 340–344. [[CrossRef](#)]
61. Godínez-García, A.; Vallejo-Arenas, D.D.; Salinas-Rodríguez, E.; Gómez-Torres, S.A.; Ruíz, J.C. Spraying synthesis and ion permeation in polyvinyl chloride/graphene oxide membranes. *Appl. Surf. Sci.* **2019**, *489*, 962–975. [[CrossRef](#)]
62. Kugler, S.; Spychaj, T. Nanostruktury węglowe i błony lub powłoki polimerowe z ich udziałem: Cz. II. Błony i powłoki polimerowe z udziałem nanostruktur węglowych. *Polimery* **2013**, *58*, 177–180. [[CrossRef](#)]
63. Deshmukh, K.; Khatake, S.M.; Joshi, G.M. Surface properties of graphene oxide reinforced polyvinyl chloride nanocomposites. *J. Polym. Res.* **2013**, *20*, 286. [[CrossRef](#)]
64. Vadukumpully, S.; Paul, J.; Mahanta, N.; Valiyaveetil, S. Flexible conductive graphene/poly(vinyl chloride) composite thin films with high mechanical strength and thermal stability. *Carbon* **2011**, *49*, 198–205. [[CrossRef](#)]
65. Wilczewski, S.; Skórczewska, K.; Tomaszewska, J.; Lewandowski, K.; Szulc, J.; Runka, T. Manufacturing homogenous PVC/graphene nanocomposites using a novel dispersion agent. *Polym. Test.* **2020**, *91*, 106868. [[CrossRef](#)]
66. Hasan, M.; Lee, M. Enhancement of the thermo-mechanical properties and efficacy of mixing technique in the preparation of graphene/PVC nanocomposites compared to carbon nanotubes/PVC. *Prog. Nat. Sci. Mater. Int.* **2014**, *24*, 579–587. [[CrossRef](#)]
67. Wilczewski, S.; Skórczewska, K.; Tomaszewska, J.; Lewandowski, K. Structure and properties of poly (vinyl chloride)/graphene nanocomposites. *Polym. Test.* **2020**, *81*, 106282. [[CrossRef](#)]
68. Mindivan, F.; Göktaş, M.; Dike, A.S. Mechanical, thermal, and micro- and nanostructural properties of polyvinyl chloride/graphene nanoplatelets nanocomposites. *Polym. Compos.* **2020**, *9*, 3707–3716. [[CrossRef](#)]
69. Ak, T.; Gülçin, I. Antioxidant and radical scavenging properties of curcumin. *Chem. Biol. Interact.* **2008**, *174*, 27–37. [[CrossRef](#)]
70. Brostow, W.; Hnatchuk, N.; Kim, T. Preventing thermal degradation of PVC insulation by mixtures of cross-linking agents and antioxidants. *J. Appl. Polym. Sci.* **2020**, *137*, 48816. [[CrossRef](#)]
71. Broza, G.; Piszczek, K.; Schulte, K.; Sterzynski, T. Nanocomposites of poly(vinyl chloride) with carbon nanotubes (CNT). *Compos. Sci. Technol.* **2007**, *67*, 890–894. [[CrossRef](#)]
72. Brostow, W.; Hagg Lobland, H.E. *Materials: Introduction and Applications*; John Wiley and Sons: New York, NY, USA, 2017; ISBN 978-0-470-52379-7.
73. Xu, C.; Wang, S.; Shao, L.; Zhao, J.; Feng, Y. Structure and properties of chlorinated polyvinyl chloride graft copolymer with higher property. *Polym. Adv. Technol.* **2012**, *23*, 470–477. [[CrossRef](#)]
74. Lee, K.W.; Chung, J.W.; Kwak, S.Y. Flexible Poly(vinyl chloride) Nanocomposites Reinforced with Hyperbranched Polyglycerol-Functionalized Graphene Oxide for Enhanced Gas Barrier Performance. *ACS Appl. Mater. Interfaces* **2017**, *9*, 33149–33158. [[CrossRef](#)]
75. Ahmed, R.M.; Ibrahim, A.A.; El-Bayoumi, A.S.; Atta, M.M. Structural, mechanical, and dielectric properties of polyvinylchloride/graphene nano platelets composites. *Int. J. Polym. Anal. Charact.* **2021**, *26*, 68–83. [[CrossRef](#)]
76. Lewandowski, K.; Skórczewska, K.; Piszczek, K.; Urbaniak, W. Recycled glass fibres from wind turbines as a filler for poly(Vinyl chloride). *Adv. Polym. Technol.* **2019**, *2019*, 8960503. [[CrossRef](#)]
77. Ferry, J.D. *Viscoelastic Properties of Polymers*; John Wiley and Sons: New York, NY, USA, 1980; ISBN 0471048941.
78. Ward, I.M.; Sweeney, J. *Mechanical Properties of Solid Polymers*; John Wiley and Sons: New York, NY, USA, 2013; ISBN 9781444319507.
79. Jarzabek, D.M.; Dziekoński, C.; Dera, W.; Chrzanowska, J.; Wojciechowski, T. Influence of Cu coating of SiC particles on mechanical properties of Ni/SiC co-electrodeposited composites. *Ceram. Int.* **2018**, *44*, 21750–21758. [[CrossRef](#)]
80. Jarzabek, D.M. The impact of weak interfacial bonding strength on mechanical properties of metal matrix–Ceramic reinforced composites. *Compos. Struct.* **2018**, *201*, 352–362. [[CrossRef](#)]

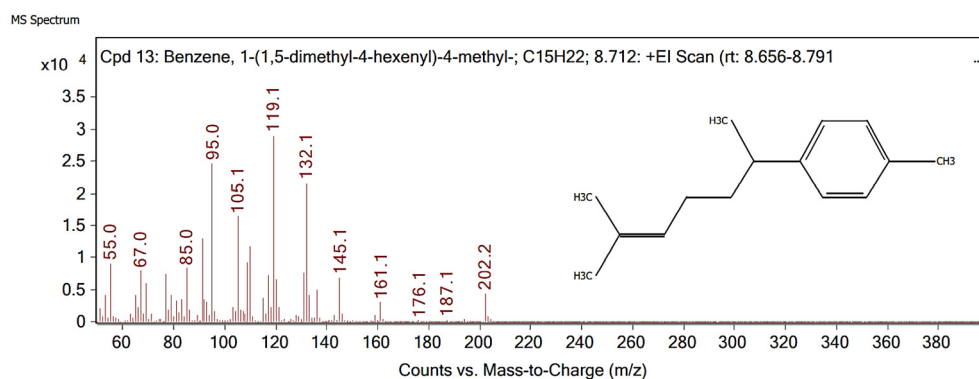


Figure S1. Mass spectrum of Ar-Curcumene

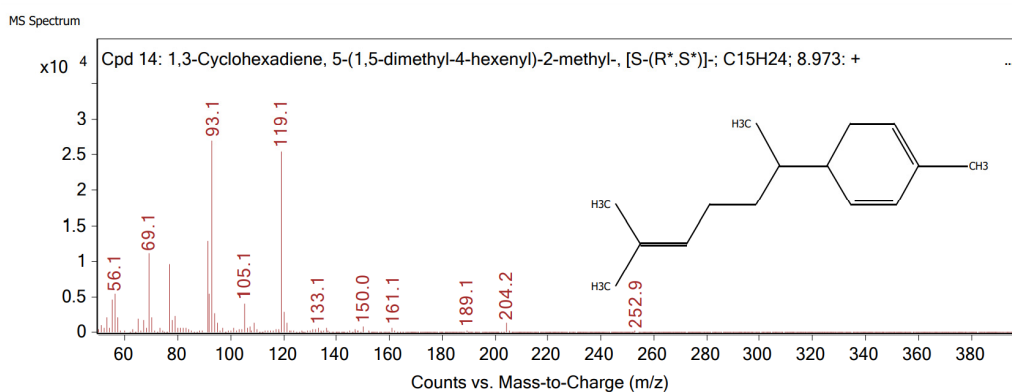


Figure S2. Mass spectrum of (-)-Zingiberene

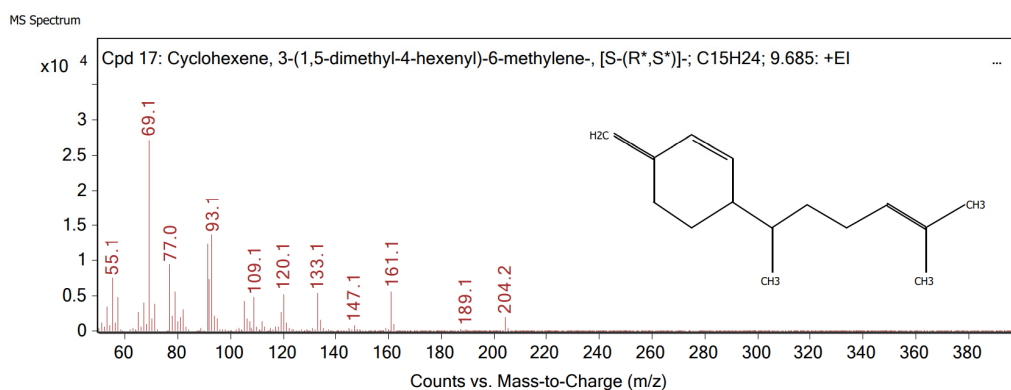


Figure S3. Mass spectrum of β -Sesquiphelandrene

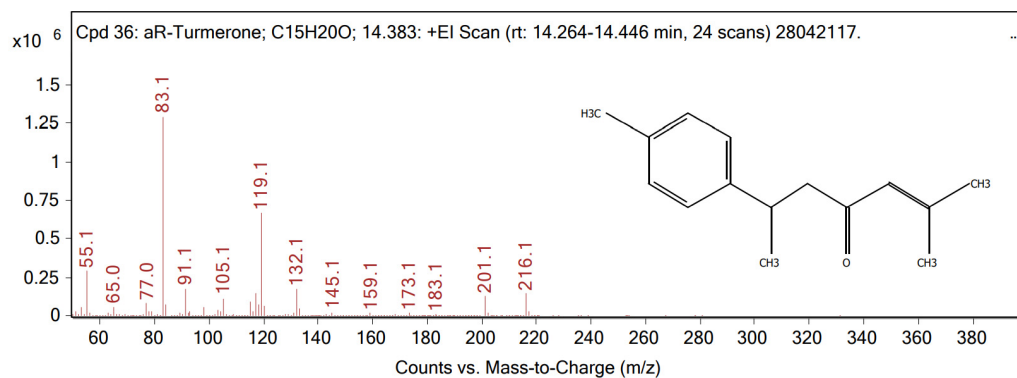


Figure S4. Mass spectrum of Ar-turmerone

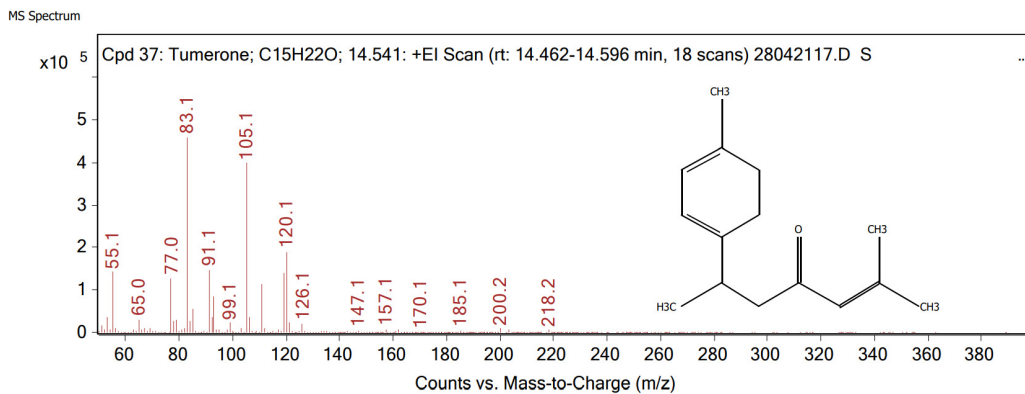


Figure S5. Mass spectrum of α -turmerone

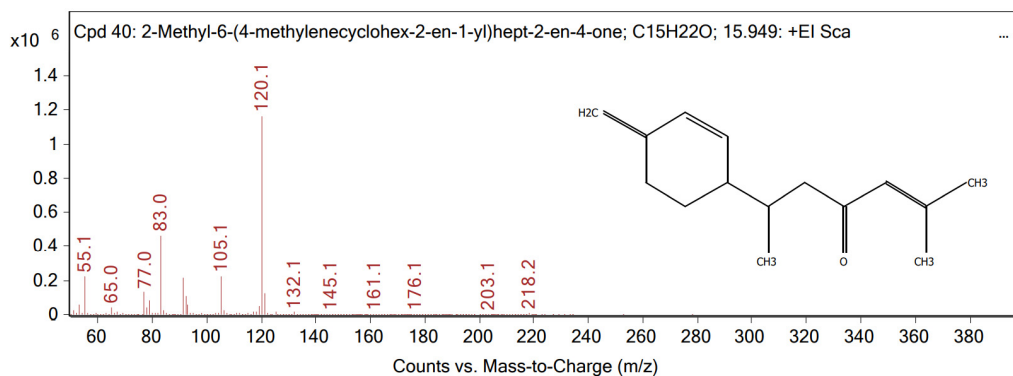


Figure S6. Mass spectrum of β -turmerone

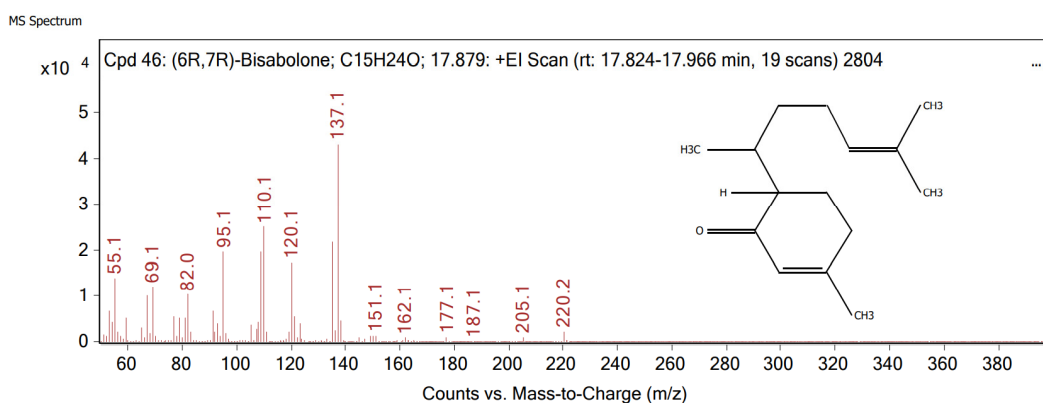


Figure S7. Mass spectrum of (6R,7R)-Bisabolone

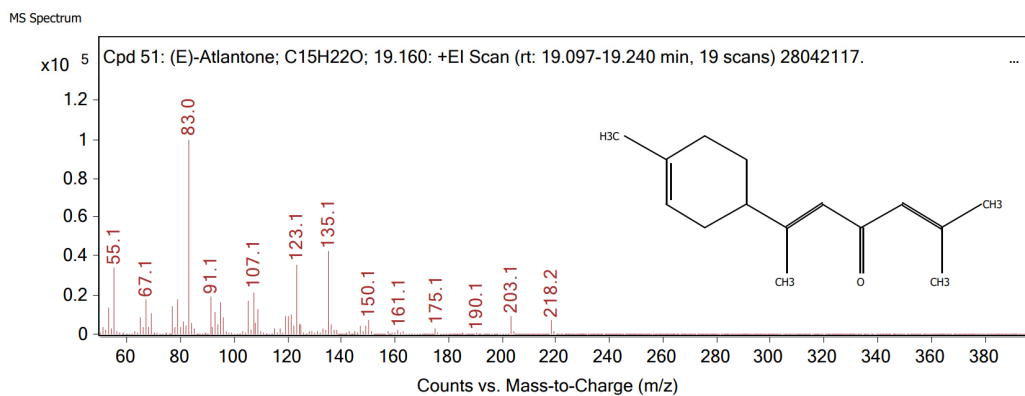


Figure S8. Mass spectrum of (E)-atlantone

Table S1. Mechanical and electrical properties of PVC/GN nanocomposites

Material	Tensile strength, MPa	Volume resistivity, Ωm	Surface resistivity, Ω
PVC	16.8 (0.7)	7.7×10^{14} (3.8×10^{11})	7.5×10^{15} (6.7×10^{13})
PVC+CE	19.0 (0.8)	3.1×10^{14} (2.2×10^{11})	4.5×10^{15} (3.9×10^{13})
PVC/0.01%GN	18.5 (0.8)	1.9×10^{13} (1.5×10^{11})	5.8×10^{15} (6.9×10^{13})
PVC/0.01%GN+CE	25.1 (1.0)	1.2×10^{14} (8.2×10^{11})	2.5×10^{15} (1.9×10^{13})
PVC/0.1%GN	21.8 (1.0)	1.6×10^{13} (9.8×10^{10})	2.4×10^{15} (1.9×10^{13})
PVC/0.1%GN+CE	23.6 (1.0)	1.7×10^{13} (1.7×10^{11})	2.3×10^{13} (2.7×10^{11})
PVC/0.5%GN	21.5 (1.4)	8.4×10^9 (8.4×10^7)	2.0×10^{13} (1.8×10^{11})
PVC/0.5%GN+CE	22.4 (1.2)	1.2×10^{13} (1.2×10^{11})	2.2×10^{13} (4.2×10^{11})
PVC/1%GN	21.2 (0.9)	3.9×10^5 (3.5×10^4)	1.5×10^7 (2.1×10^5)
PVC/1%GN+CE	22.7 (0.3)	1.2×10^{13} (9.9×10^{10})	2.11×10^{13} (4.9×10^{11})

Publikacja [P4]

Graphene modification by curcuminoids as an effective method to improve the dispersion and stability of PVC/graphene nanocomposites

Article

Graphene Modification by Curcuminoids as an Effective Method to Improve the Dispersion and Stability of PVC/Graphene Nanocomposites

Sławomir Wilczewski ^{1,*}, Katarzyna Skórczewska ^{1,*}, Jolanta Tomaszewska ¹, Magdalena Osiał ²,
Agnieszka Dąbrowska ^{3,4}, Kostiantyn Nikiforow ⁵, Piotr Jenczyk ² and Hubert Grzywacz ²

¹ Faculty of Chemical Technology and Engineering, Bydgoszcz University of Science and Technology, Seminaryjna 3 Street, 85-326 Bydgoszcz, Poland; jolanta.tomaszewska@pbs.edu.pl

² Institute of Fundamental Technological Research, Polish Academy of Sciences, Pawińskiego 5B Street, 02-106 Warsaw, Poland; mosial@ippt.pan.pl (M.O.)

³ Faculty of Chemistry, University of Warsaw, Pasteura 1 Street, 02-093 Warsaw, Poland

⁴ Biological and Chemical Research Centre, University of Warsaw, Żwirki i Wigury 101, 02-089 Warsaw, Poland

⁵ Institute of Physical Chemistry, Polish Academy of Sciences, Kasprzaka 44/52, 01-224 Warsaw, Poland

* Correspondence: slawomir.wilczewski@pbs.edu.pl (S.W.); katarzyna.skorczevska@pbs.edu.pl (K.S.)

Abstract: A large amount of graphene-related research is its use as a filler for polymer composites, including thin nanocomposite films. However, its use is limited by the need for large-scale methods to obtain high-quality filler, as well as its poor dispersion in the polymer matrix. This work presents polymer thin-film composites based on poly(vinyl chloride) (PVC) and graphene, whose surfaces were modified by curcuminoids. TGA, UV-vis, Raman spectroscopy, XPS, TEM, and SEM methods have confirmed the effectiveness of the graphene modification due to π - π interactions. The dispersion of graphene in the PVC solution was investigated by the turbidimetric method. SEM, AFM, and Raman spectroscopy methods evaluated the thin-film composite's structure. The research showed significant improvements in terms of graphene's dispersion (in solutions and PVC composites) following the application of curcuminoids. The best results were obtained for materials modified with compounds obtained from the extraction of the rhizome of *Curcuma longa* L. Modification of the graphene's surface with these compounds also increased the thermal and chemical stability of PVC/graphene nanocomposites.

Keywords: graphene; curcuminoids; poly(vinyl chloride); nanocomposites stability; polymer films



Citation: Wilczewski, S.; Skórczewska, K.; Tomaszewska, J.; Osiał, M.; Dąbrowska, A.; Nikiforow, K.; Jenczyk, P.; Grzywacz, H. Graphene Modification by Curcuminoids as an Effective Method to Improve the Dispersion and Stability of PVC/Graphene Nanocomposites. *Molecules* **2023**, *28*, 3383. <https://doi.org/10.3390/molecules28083383>

Academic Editors: Nadya Vasileva Dencheva and Zlatan Denchev

Received: 22 March 2023

Revised: 4 April 2023

Accepted: 7 April 2023

Published: 11 April 2023



Copyright: © 2023 by the authors. Licensee MDPI, Basel, Switzerland. This article is an open access article distributed under the terms and conditions of the Creative Commons Attribution (CC BY) license (<https://creativecommons.org/licenses/by/4.0/>).

1. Introduction

Research concerning the application of graphene materials is carried out in many areas, such as medicine, chemistry, materials engineering, energetics, and electronics. A large area of graphene-related research regards its use as a filler for polymer nanocomposites [1–5]. Graphene materials (graphene, multilayer graphene, graphene oxide) show a considerable variation regarding their dispersibility in the polymer matrix, depending on the number of defects and layers and the presence of oxygen-containing functional groups. Furthermore, studies have shown that adding graphene to the polymer matrix can positively change the physicochemical properties of plastics [6–10].

An interesting and still relatively unexplored group of polymer nanocomposites with graphene are poly(vinyl chloride)-based materials (PVC/GN). Analysis of the literature has shown that in these materials with relatively well-dispersed graphene, regardless of the method of preparation (melt mixing, solvent casting, in situ polymerization method), result in an increase in tensile strength and modulus of elasticity [11–16], as well as in increased impact strength [16,17]. Such materials are also characterized by higher thermal stability [13,18,19], swelling agent resistance [20–22] and glass transition temperature (T_g) [13–15,23,24], lower

volume and surface resistivity compared to matrix material [14,25,26]. However, the improvement of poly(vinyl chloride) properties using graphene has limitations, mainly due to the poor dispersibility of the filler in the matrix and insufficient interactions at the filler–polymer interface. Depending on the method of filler introduction, maximum properties are obtained in materials containing between 0.1 and 0.5 wt.% graphene. Filler agglomeration affects the deterioration of all the properties mentioned above of PVC/GN polymer nanocomposites.

The agglomerative behavior of graphene is due to strong π – π interactions and van der Waals forces [27–30]. The main preventive methods are based on covalent modification of chemical reactions with graphene's carbon atoms [2,27,29] and non-covalent modification based on the adsorption of particles onto the material's surface. Due to the functionalization mechanism, non-covalent methods to counteract graphene aggregation are divided into four main groups. The first includes methods related to π – π interactions [28,31–34]. The second stabilization mechanism is based on cation– π interactions [35,36]. Other methods apply hydrophilic–hydrophobic effects [2,27,29,37] and surface modifications of graphene with other nanoparticles [2,38,39]. Improving graphene's dispersion in the PVC matrix is also based on the above methods. However, the covalent solutions presented so far [40–44] use reagents harmful to health and the environment, such as aniline, N-methylpyrrolidone, hydrazine, and terephthalaldehyde. Non-covalent methods, on the other hand, are mainly based on the use of plasticizers [14,25], which alter the properties of poly(vinyl chloride). Soft varieties of PVC in terms of properties can be considered a different group of materials compared to rigid PVC, so they also have entirely different practical applications [45].

The π – π interactions refer to non-covalent interactions (overlapping orbitals) between the π bonds of aromatic rings. However, this is a misleading description, because the direct sandwich overlap is electrostatically repulsive. Instead, we are dealing with staggered stacking (parallel displaced) or π – π T-teeing (perpendicular T-shaped), which makes the described interactions electrostatically attractive. The displacement occurs due to the superposition of carbon atoms with partially negative charges over hydrogen atoms with partially positive charges. Similarly, T-type perpendicular overlap is electrostatically attractive because here, too, there is an overlap of different charges [32,33,46].

A promising method of graphene modification using π – π stacking is the modification of its surface with curcuminoids. The interaction between the aromatic rings of curcumin and the GN surface was used to obtain graphene by reducing graphene oxide, through ultrasonic exfoliation of graphite [31,34,47]. However, the most common use of the graphene–curcumin system is in drug delivery systems [48,49]. Curcuminoids, thanks to their high chemical and thermal stability (in combination with graphene, even up to 220 °C), are also attractive for applications in the modification of polymers, including PVC [50–52].

Therefore, the present work aimed to modify surface graphene with curcuminoids and to investigate the potential of this modification to improve graphene dispersion in poly(vinyl chloride)/graphene nanocomposites obtained by the solvent-casting method. In this work, we used a commercially available mixture of three types of curcumin (CU) (curcumin, demethoxycurcumin, and bisdemethoxycurcumin) and an extract of *Curcuma longa* L. (CE) obtained by extraction of the powdered rhizome of the plant, which was presented in our earlier work [22]. In addition to the aforementioned main ingredients, CE also contained Ar–curcumene, (–)–zingiberene, β –sesquiphellandrene, Ar–turmerone, α –turmerone, β –turmerone, (6R, 7R)–bisabolene and (E)–atlantone.

2. Results and Discussion

2.1. UV-Vis Spectroscopy

Before the morphology studies were conducted, the UV-vis studies were performed, in order to determine if the GN was successfully modified with curcuminoids. Figure 1 shows the UV-Vis spectra of graphene, curcumin, *Curcuma longa* L. extract, and GN–CU and GN–CE colloidal suspensions. The analysis showed that the maximum absorption for

graphene was observed at 272 nm, corresponding to π - π^* transitions of C=C bonds [53,54]. Two absorption bands were observed in the spectrum of curcumin; at 263 nm, with π - π^* and C=C bonds, and at 422 nm, which corresponds to n - π^* transitions of C=O bonds [54,55]. In the spectrum of the *Curcuma* extract, the described transitions were observed at 233 nm and 422 nm, respectively. The shift of the absorption maximum (233 nm) toward the ultraviolet spectrum is due to the presence of the other CE components. A maximum wavelength of 233 nm is characteristic of ar-turmerone [56,57]. Two absorption bands were observed on the GN-CU and GN-CE spectra at 269 nm and 414 nm, respectively, which were attributed to the π - π^* transitions of C=C bonds and n - π^* bonds of C=O. The presence of a band at 414 nm, characteristic of curcumin, indicates the effective functionalization of graphene [54,58]. In addition, the change in band position at 269 nm confirms the interaction of π - π graphene and curcuminoid-containing modifiers [21,55,59].

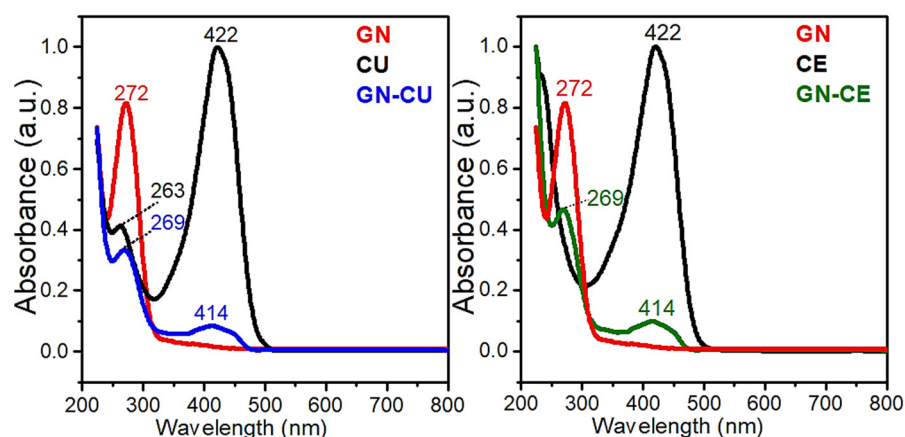


Figure 1. UV-Vis spectra of the GN, CE, CU and GN-CU, GN-CE dispersion in methanol.

2.2. XPS Analysis

Next, X-ray photoelectron spectroscopy (XPS) was used to characterize graphene surfaces' functionalization accurately. Figure 2 shows the XPS spectra of GN and curcuminoid-modified materials. In the image, one can see an increase in the intensity of the O1s band in materials after modification. It indicates the effective deposition of curcuminoids (which contain oxygen functional groups) onto the graphene surface [4,47]. Finally, the deconvolution of O1s and C1s peaks and the XPS characterization of GN, GN-CU, and GN-CE sheets are presented in Figure 3 and Table 1. Since graphene materials were modified, mainly sp^2 hybridization was expected. Unfortunately, it was impossible to match sp^2 in any way, so an additional sp^3 hybridization peak was used. This fact may be due to the partial defecting of the graphene used and its partial oxidation (according to the manufacturer, about 2.5% was oxidized) [31,47,60].

The distance between the C sp^2 and C sp^3 peaks at 0.8 eV, especially for the starting sample, agrees very well with literature data on peak distances of thin carbon films, which are, respectively, 0.7 eV for graphene oxide and reduced graphene oxide [61], 0.8 eV for diamond-like carbon films [62,63], and 0.9 eV for graphite and graphite-like materials [64–66]. Furthermore, the position of the C sp^2 peak around 284.5 eV is also characteristic of this type of material [64] and generally corresponds to values found in the literature (284.25–285 eV), including graphene materials [4,31,61,67].

The rest of the smaller carbon peaks (Figure 3, Table 1) of the carbon functional groups are characterized by the expected distance from the main peak C sp^2 [68]. Considering the literature data, the chemical compounds of turmeric are composed of carbon-oxygen groups [69–71]. The obtained spectra for the samples with CU and CE confirm an increase in the proportion of oxygen groups (O1s), which was 0.6 at.% for GN and 5.3 and 3.3 at.% for GN-CU and GN-CE, respectively, which confirms the deposition of curcuminoids on the graphene's surface. However, the changes in the π electrons (Table 1 C1s spectra)

indicate the physical nature of their interactions as a result of non-covalent π - π stacking modification [63,72].

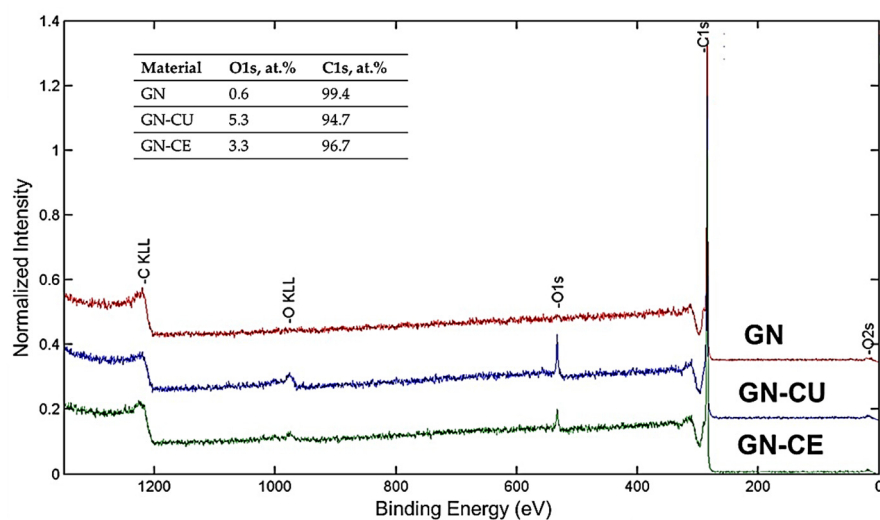


Figure 2. XPS spectra of the GN, GN-CU and GN-CE.

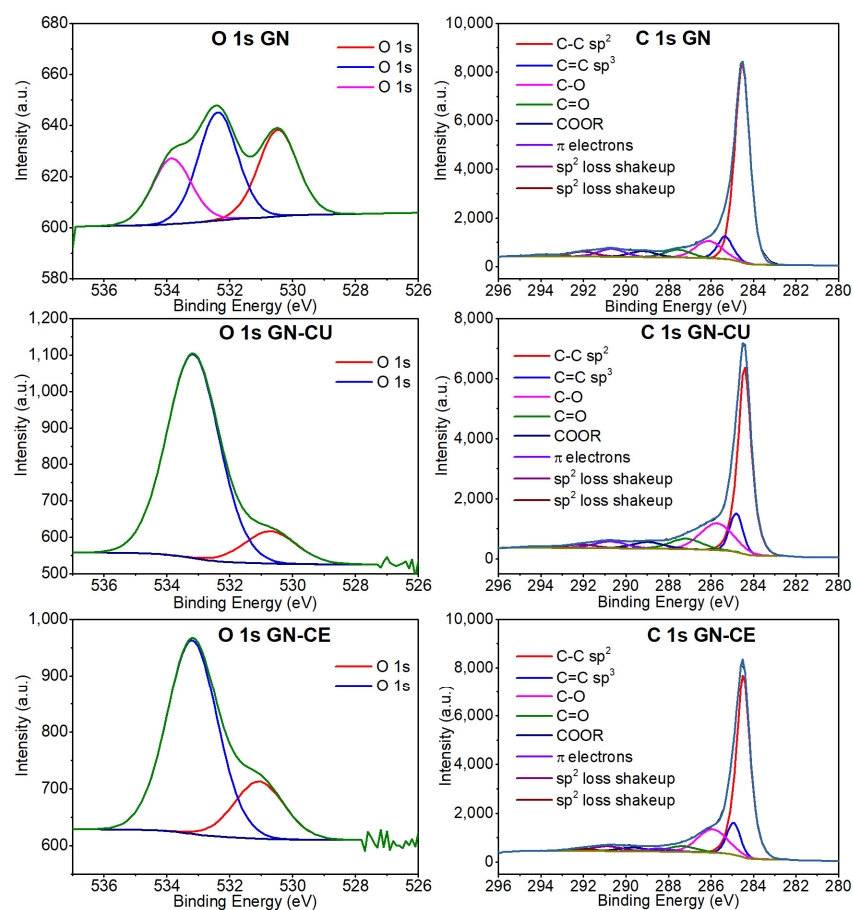


Figure 3. Peaks deconvolution of O1s and C1s of the GN, GN-CU and GN-CE.

Table 1. XPS characterization of GN, GN-CU and GN-CE.

Binding Energy, eV	Chemical Bonds	FWHM	Atomic, %
GRAPHENE			
O1s			
530.47	O1s	1.47	0.2
532.38	O1s	1.47	0.2
533.84	O1s	1.47	0.2
			0.6
C1s			
284.53	C-C sp ²	0.82	65.3
285.33	C=C sp ³	0.82	7.5
286.11	C-O	1.49	10.0
287.56	C=O	1.49	4.5
289.21	COOR	1.49	3.5
290.68	π electrons	1.49	4.6
292.03	sp ² loss shakeup	1.49	2.8
293.87	sp ² loss shakeup	1.49	1.1
			99.4
			100.0
GRAPHENE-CURCUMIN			
O1s			
530.7	O1s	1.95	0.7
533.17	O1s	1.95	4.6
			5.3
C1s			
284.42	C-C sp ²	0.73	50.9
284.81	C=C sp ³	0.73	9.6
285.72	C-O	1.82	16.5
287.18	C=O	1.82	6.4
288.99	COOR	1.82	4.0
290.73	π electrons	1.82	4.2
292.14	sp ² loss shakeup	1.82	2.1
294.15	sp ² loss shakeup	1.82	1.0
			94.7
			100
GRAPHENE-Curcuma Longa L. EXTRACT			
O1s			
531.06	O1s	1.87	0.8
533.19	O1s	1.87	2.5
			3.3

Table 1. Cont.

Binding Energy, eV	Chemical Bonds	FWHM	Atomic, %
C1s			
284.48	C-C sp ²	0.76	59.4
284.94	C=C sp ³	0.76	9.4
285.92	C-O	1.65	15.2
287.35	C=O	1.65	3.7
289.66	COOR	1.65	2.4
288.45	π electrons	1.65	2.0
290.88	sp ² loss shakeup	1.65	3.2
292.16	sp ² loss shakeup	1.65	1.5
			96.7
			100.0

2.3. Thermogravimetric Analysis (TGA)

A thermogravimetric analysis was performed to determine the modifier's content on the graphene surface. The test was carried out in the temperature range from 30 to 700 °C. The analysis results (Figure 4) showed that the graphene was thermally stable over the entire temperature range, in good agreement with the literature data [34,73]. The extract from *Curcuma longa* L was stable up to about 175 °C, and its degradation occurred between 175 °C and about 450 °C (Figure 4A) while the curcumin was stable up to 250 °C, and its decomposition occurred at temperatures ranging from 250 to 550 °C (Figure 4B). The differences in the thermal stability of these modifiers are due to the presence of additional components in the extract. Their decomposition, up to a temperature of about 320 °C, is related to the degradation of the –OH and –OCH₃ groups. Furthermore, the curcuminoids are decomposed [74–76].

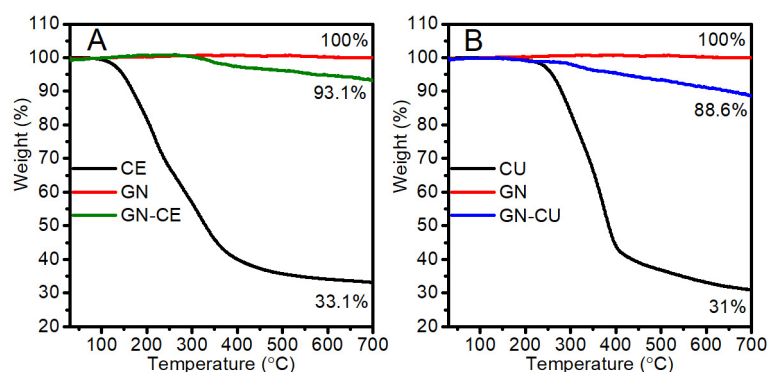


Figure 4. TGA of curcumin, GN, GN-CU (A), and *Curcuma longa* L extract and GN, GN-CE (B).

Both GN-CU and GN-CE showed thermal stability up to about 340 °C, and their decomposition was associated with the degradation of the organic modifier [34,73]. It is worth noting that the thermal stability of the modified graphene is well above the processing temperature of PVC (below 200 °C) [77–79]. This indicates that the proposed modification can also be used to obtain poly(vinyl chloride)/graphene nanocomposites by the melt mixing method. From the mass differences at 700 °C, the modifier's content on the GN surface was determined by comparing the reference GN sample with the mass loss for GN-CU and GN-CE, respectively. The calculations showed that the mass of curcumin on the graphene surface was 11.4% (Figure 4B), while the mass of the extract was 6.9% (Figure 4A).

2.4. Morphology Characterization

The morphology of the materials was observed by transmission electron microscopy (Figure 5A–C) and scanning electron microscopy (Figure 5(A1–C1)). The observations showed that the modified graphene was a material composed of several layers, which was characterized by a crumpled morphology. This is typical of types of graphene with several layers and relatively large, flake diameters (according to the manufacturer, three-layered graphene with a diameter of up to 10 μm) [1,60,80].

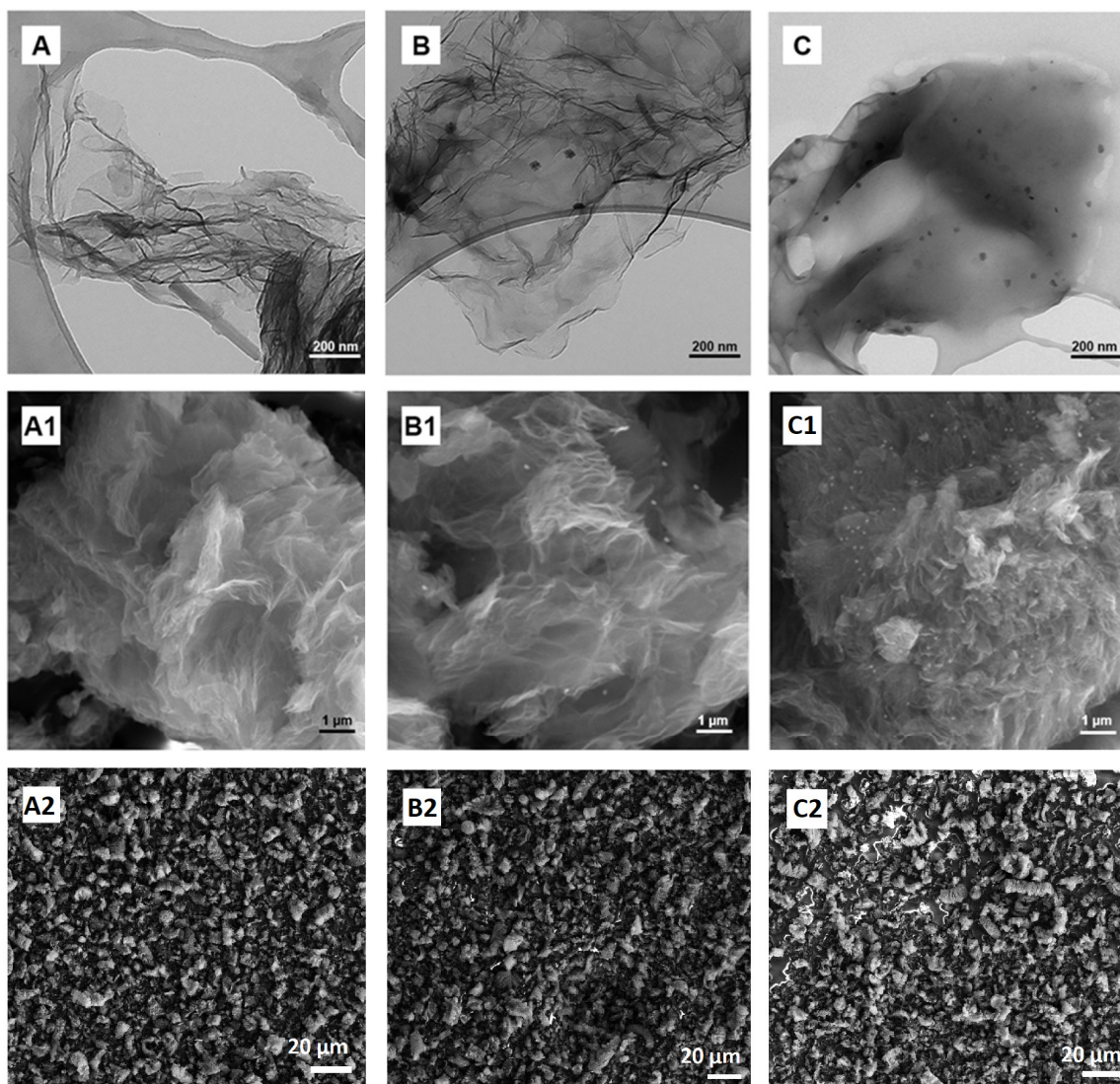


Figure 5. TEM images of GN, GN-CU, GN-CE (A–C), SEM images of GN, GN-CU, GN-CE (A1,B1,C1) with scale bar 1 μm , and GN, GN-CU, GN-CE (A2,B2,C2) with scale bar 20 μm (survey images).

Spherical curcuminoid particles (brighter white dots) can be seen in the SEM images (Figure 5(B1,C1)) of the modified graphene [81,82]. Simultaneously, they have a smaller diameter than those in GN-CU (Figure 5(B1)). On the other hand, in TEM images, it can be seen that both modifiers, CU and CE, on the graphene's surface have a floral-spherical shape (Figure 5B,C) [83,84]. As in the SEM images, the curcuminoids from the extract (Figure 5C) were much better deposited on the graphene surface. They are well-dispersed, as present in all SEM pictures of the specimen, and have a smaller diameter. Figure 5(A2–C2) shows the uniform distribution of the flakes in the whole volume as a survey image. Based on the SEM images, it can be argued that CU and CE mainly cover the edges of the graphene

flakes, but the TEM images, especially that of GN-CE, indicate that the modifier can cover the surface of graphene to a greater extent.

2.5. Raman Spectroscopy

The following step was the evaluation of the structure of graphene materials using Raman spectroscopy, an effective method for studying carbon materials [85]. Recorded spectra presented in Figure 6 for GN, GN-CU and GN-CE reveal the presence of the D-band, which is characteristic of graphene with a disordered carbon structure, and the G-band, typical for graphite materials, which, in the case of graphene, is also associated with the number of layers [5,86]. To estimate the size of graphene domains, the D- and G-band intensity (I_D/I_G) ratio was used, where this quantity is inversely proportional to the size of the crystallites [15,27,86,87]. In our materials, it was 1.5–1.6 (depending on the background treatment) for all fillers, indicating a high level of defects in curcuminoid-modified materials, which can increase their wettability by the polymer matrix. Furthermore, the intensity ratio $2D:G < 1$ confirms the presence of multilayered, and not structuralized, material. The 2D band is broad and weak, and is slightly shifted towards higher frequencies ($\sim 2700\text{ cm}^{-1}$), which indicates the residual compression stress in the material. The RBS parameter (Raman Band Separation) is relatively high and equals 287 (GN-CE) to 293 (GN-CU), whereas non modified filler has a value of ~ 291 . This confirms the different mechanisms of carbon structure modification by both curcuminoids.

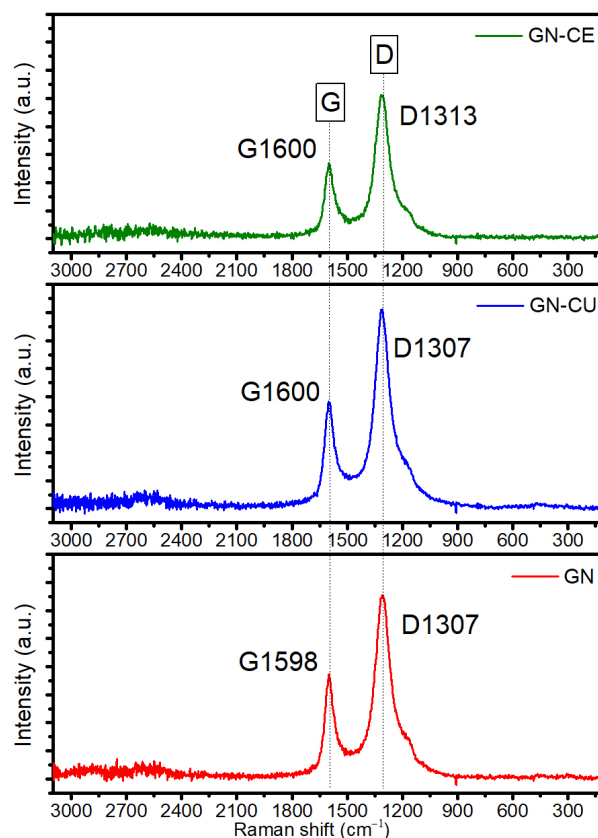


Figure 6. Raman spectra of GN, GN-CU and GN-CE.

In paper [31], it was shown that the stacking of more graphene layers causes a shift of the G-band peak towards higher frequencies, and the Rs for the monolayer is generally higher than for a bilayer. In curcuminoid-modified materials, a shift toward higher wavenumbers was observed, from 1598 cm^{-1} for GN to 1600 cm^{-1} for graphene modified with curcumin and *Curcuma longa* L. extract, further confirming the better foliation of the

material after surface functionalization with curcuminoids. Bands typical for disordered carbons are not visible (360 cm^{-1} , 1620 cm^{-1}).

2.6. Dispersion Stability Analysis

As we pointed out in our earlier work [21], in nanocomposites obtained by solvent casting, the critical step in determining the homogeneity of graphene dispersion in the PVC matrix is obtaining a stable filler dispersion in the polymer solution. Therefore, the stability of GN, GN-CU, and GN-CE dispersions in a 3% poly(vinyl chloride) solution was evaluated, from which thin polymer films were obtained after THF evaporation. The test was carried out using the multiple light-scattering method (used in the Turbiscan Lab Toulouse, France). Figure 7 shows the change in the percentage of backscattered and transmitted light as a function of the height of the measuring cell over 24 h. This time is sufficient to obtain a polymer film from a PVC solution at room temperature.

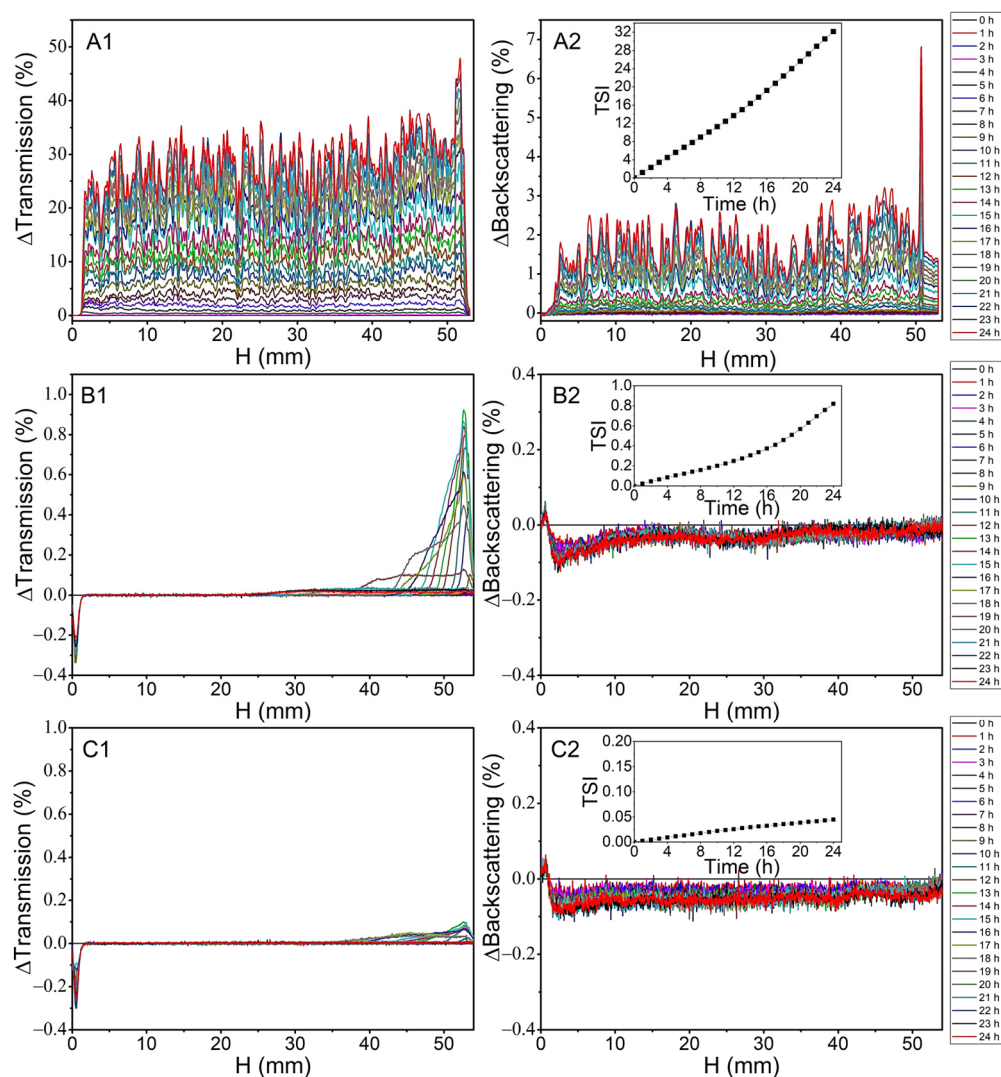


Figure 7. Δ Transmission and Δ Backscattering of GN (A1,A2), GN-CU (B1,B2) and GN-CE (C1,C2) dispersion.

The analysis shows that the destabilization and stratification of graphene dispersion occur due to re-agglomeration and sedimentation of the filler [88,89]. The study demonstrated that the unmodified graphene does not form stable dispersions in PVC solution (Figure 7(A1,A2)), as evidenced by changes in transmitted and backscattered light [88,90]. Functionalization of the GN's surface with curcuminoids improved its stability in PVC

solution. Neither GN–CU nor GN–CE re-agglomerated, as evidenced by the absence of significant changes in backscattered light (Figure 7(B2,C2)) [89]. However, in Figure 7(B1,C1), we can see an increase in the solution's transparency after about 16 h, especially for GN–CU. This is due to the gravitational descent of the filler particles.

The Turbiscan Stability Index (TSI) (a specific Turbiscan parameter) was determined to compare the destabilization kinetics of the prepared systems, in particular, the differences between the CU and CE effect. TSI is an efficient method of comparing several systems, where the higher its value is, the less stable the system is [91,92]. Other sources [21,28] distinguish a more precise division of TSI values, indicating that the dispersion is stable when TSI is less than five. When its value is between 5 and 20, we are dealing with a partially stable system; above 20, the dispersion is sedimentary. The results presented in Figure 7(A2–C2) show that the GN dispersion is stable for only 4 h, while modifying its surface resulted in extending this time to 24 h. TSI analysis proved that the most stable systems are formed by GN–CE, for which the discussed value, even after 24 h, was below 0.05.

2.7. Graphene Dispersion in Nanocomposites

The structure of nanocomposite polymer thin films obtained by solvent casting was studied using Raman spectroscopy and atomic force microscopy. In addition, the morphologies of the obtained materials were also observed on a macro- and micrometer scale, using images from digital photography and SEM. As mentioned in the introduction, the problem with graphene aggregation occurs in materials containing about 0.5 wt.% filler or more, so the structure evaluation was carried out for materials with 1 wt.% GN.

Regarding the Raman spectra of the nanocomposites (Figure 8), D- and G-bands typical of graphene and peaks originating from poly(vinyl chloride) were observed. Signals were assigned to the following chemical groups: a band at about 360 cm^{-1} to C–Cl in the trans configuration of the polymer [93], bands at 635 and 695 cm^{-1} to C–Cl stretching [93,94], a band at approximately 1113 cm^{-1} to C–C stretching [93], a band at ~ 1430 and 1498 cm^{-1} to C–H symmetrical stretching in CH_2 group [21] and a band at approximately 2916 cm^{-1} to C–H asymmetrical stretching in CH_2 group [21,93]. In addition, a peak was observed in PVC/1% GN–CU and PVC/1% GN–CE at about 1185 cm^{-1} . It was attributed to the C–O bonds of curcuminoids [95]. The study did not reveal any new chemical bonds in PVC, which indicates the physical nature of filler–polymer interactions. Analysis of the graphene–derived bands showed changes in the fillers' structures, due to their dispersion in the poly(vinyl chloride) matrix. Firstly, the RBS decreased for all materials, with 243 (GN–CE), 247 GN, and 249 (GN–CU), but it increased in the same way from GN–CE to GN–CU. Raman shifts of G bands decreased in all samples below 1600 cm^{-1} (1592 cm^{-1} , 1597 cm^{-1} , 1598 cm^{-1}), being the lowest in GN–CE and the highest in GN–CU. This can be explained by the layer-stacking enhancement in the matrix's presence. Thus, the best filler dispersion was observed in GN–CU. Contrarily, the D-bands have been shifted towards higher R_s (1349 cm^{-1} in modified materials and 1350 cm^{-1} in GN). The D (first-order peak) moves towards lower frequencies in the case of tensile stress and towards higher ones in the presence of compressive stress, as observed in nanocomposites. Additionally, the I_D to I_G ratio decreases, especially in the case of the GN–CU, indicating better structural ordering. However, the sheer increase in the intensity of the PVC-derived band (2916 cm^{-1}) in the materials after its functionalization may indicate better dispersion of these materials and deposition inside the polymer matrix [93] (the spectrum is collected from the polymer, not from the agglomerate on the surface of the thin polymer film).

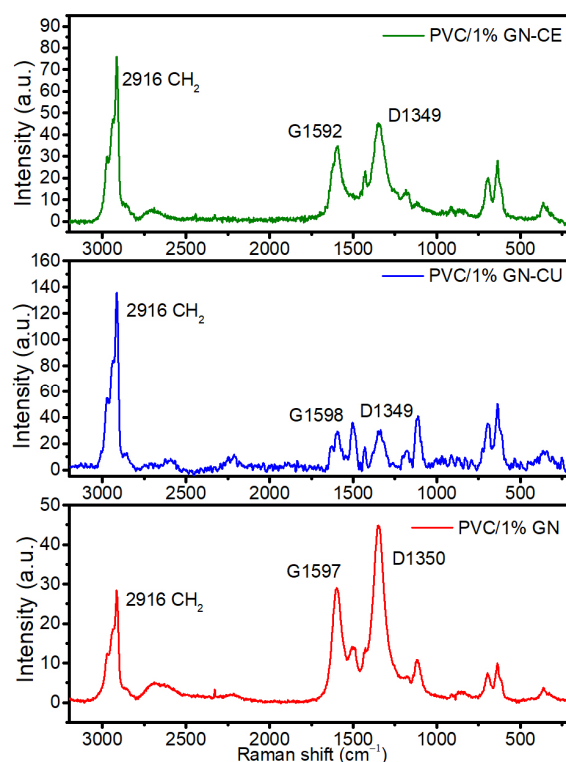


Figure 8. Raman spectra of PVC/1%GN, PVC/1%GN-CU and PVC/1%GN-CE.

AFM also investigated the surface structure of the obtained nanocomposites in contact with a surface (the upper side of the surface that was not in contact with glass during THF evaporation, forming a polymer film). AFM allows for the direct evaluation of the dispersion of graphene in the PVC matrix and the determination of roughness [94,96]. Figure 9 shows 2D and 3D images of nanocomposites containing modified and unmodified graphene.

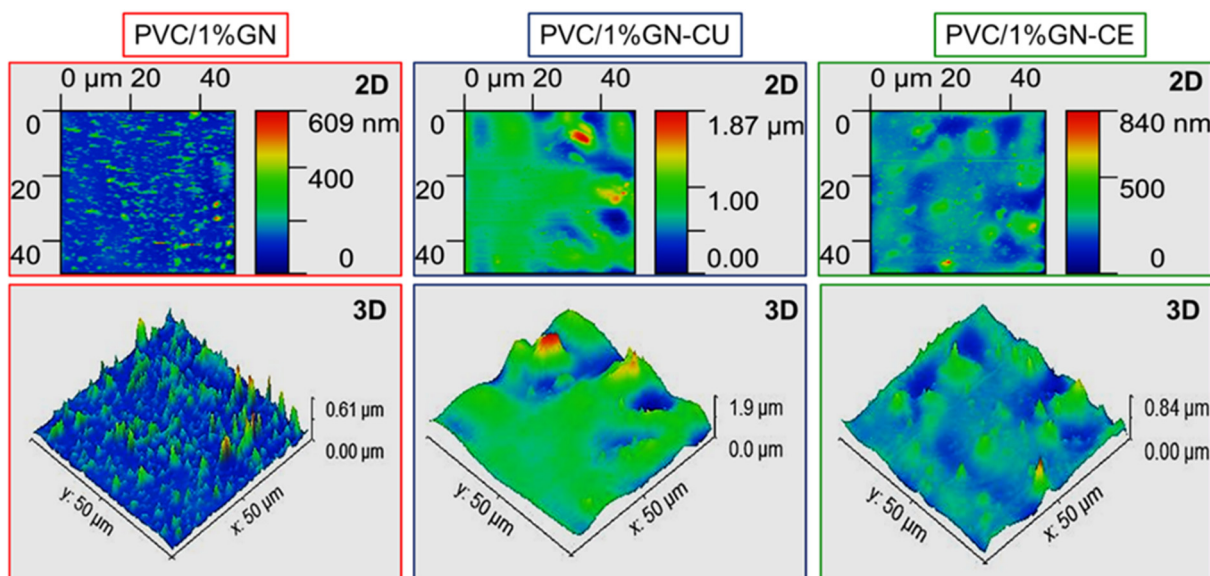


Figure 9. AFM 2D and 3D images of PVC/1%GN, PVC/1%GN-CU and PVC/1%GN-CE.

The image of the surface topography of the nanocomposites shows some corrugation of the samples due to the evaporation of solvent during the formation of the polymer film [22]. AFM PVC/1%GN shows extreme inhomogeneity of the material, and the 3D image shows

a large number of pointed tops, resulting from the presence of agglomerates. Additionally, the 2D image shows a lack of homogeneity of the material; the filler is distributed point-wise, and the sample is flat outside the place of its presence. In PVC/1%GN-CU nanocomposites, an increase in the homogeneity of the material was observed (no pointed vertices, no significant differences in roughness). At the same time, the roughness of the whole material increased significantly, which is a normal phenomenon in materials containing large amounts of dispersed filler [15,94,97]. However, the surface topography analysis showed the best dispersion in PVC films containing GN-CE; its material is homogeneous, and at the same time, its roughness is reduced compared to PVC/1%GN-CU.

The observations made earlier were confirmed by analyzing the homogeneity of the polymer films on a macroscopic scale. The presented digital images of nanocomposites containing 1 wt.% GN, GN-CU, and GN-CE Figure 10A–C, respectively, showed that the obtained materials had no visual defects in terms of their structure or the presence of pores. At the same time, it can be noted that the composite with unmodified GN is heterogeneous, and the filler is present in the form of agglomerates. Modifying the GN's surface with curcuminoids significantly enhances the homogeneity of the nanocomposites, where the PVC/1% GN-CE material is characterized by the best graphene dispersion (the two phases in the material cannot be distinguished).

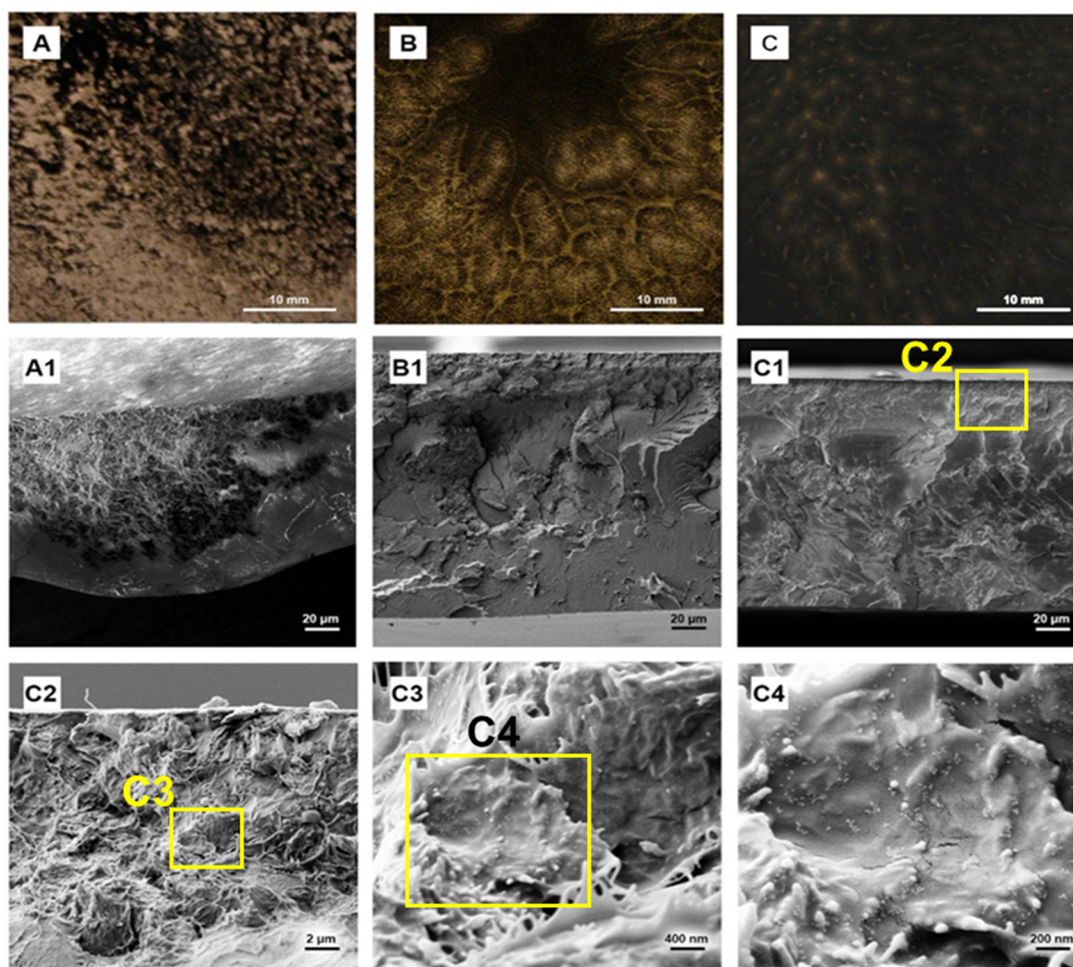


Figure 10. Digital photos of PVC/1% GN, PVC/1%GN-CU and PVC/1% GN-CE (A–C), SEM images of those materials (A1,B1,C1) and zoomed in structure of PVC/1%GN-CE (C2–C4).

The same observations were confirmed by SEM imaging on the surface of the PVC/1%GN cryogenic breakthrough (Figure 10(A1)); we observed two phases in the material, and a graphene agglomerate is surrounded by a polymer matrix. A significant improvement in

GN dispersion characterizes the PVC/1%GN–CU nanocomposites, but areas without filler can be observed on the surface of the cryogenic breakthrough (Figure 10(B1)). The image of the PVC/1% GN–CE breakthrough (Figure 10(C1)) is homogeneous throughout, and no areas of unmodified PVC can be seen, indicating the best filler dispersion [16,17,21,24]. At the same time, we can see that the structure of the nanocomposite differs significantly from that typically observed in unmodified poly(vinyl chloride) [20–22]. Its image may resemble balls of wool (Figure 10(C2)). Further zooming in on the structure (Figure 10(C3,C4)) shows the polymer matrix's thorough coverage of individual graphene flakes, which may translate into a good filler–polymer interfacial interaction. At the same time, we can see that the modifier in the form of CE remains on the graphene flakes and does not pass into the PVC in significant amounts. The Figure 10(C4) image shows curcuminoid particles having spherical shapes [81,82] on the surface of the flakes. These spheres were not observed in the expanded ends of the polymer. The jaggedness of the PVC/GN–CE confirms that good filler dispersion further affects the fracture ductility of modified PVC.

Observations of the structure demonstrated the best improvement in the dispersion of graphene in materials modified by *Curcuma longa* L. extract. Therefore, the CE-modified filler was used to study the effect of the applied modification on the properties of poly(vinyl chloride)/graphene nanocomposites. Materials containing 0.01, 0.1, 0.5, and 1 wt% GN were produced.

2.8. Thermal and Mechanical Properties of Nanocomposites

Thermal properties were determined by the thermogravimetric method and the Congo Red test, with which the thermal stability time was measured. The results obtained are summarized in Table 2 and are shown in Figure 11. The TGA thermograms (Figure 11A) show mass losses at temperatures up to 170 °C, which are related to the evaporation of residual THF [20,23]. The content of solvent was about 6% (Table 2), despite the applied evaporation and drying methods (reduced pressure at 50 °C for 2 weeks). Earlier studies have shown that higher evaporation temperature would lead to the degradation of the material [20].

Thermal degradation of PVC and PVC/GN nanocomposites takes place in two stages related to the decomposition of the polymer. The first step occurs at 200 °C to 375 °C, and is related to the dehydrochlorination of PVC and the formation of conjugated polyene structures. The second step in the range from 375 °C to 600 °C corresponds to thermal cracking of the carbonaceous, conjugated polyene sequences and the formation of residual chars [11,23].

Table 2. Thermal properties of PVC/GN and PVC/GN–CE nanocomposites.

Material	Cont. of THF, %	Max. DTG I, °C	Max. DTG II, °C	Residual Mass, %	Congo Red Test, min
PVC	5.2 (0.4)	269.8 (2.1)	452.4 (1.5)	7.7 (0.2)	3.5 (0.02)
PVC/0.01%GN	5.8 (0.1)	269.0 (0.6)	450.9 (0.6)	7.8 (0.4)	3.1 (0.04)
PVC/0.01%GN–CE	5.5 (0.1)	273.5 (0.3)	449.9 (1.1)	8.2 (0.1)	3.3 (0.08)
PVC/0.1%GN	5.8 (0.4)	273.0 (0.3)	454.2 (0.4)	7.5 (0.2)	3.1 (0.04)
PVC/0.1%GN–CE	6.4 (0.1)	274.9 (0.8)	452.9 (1.4)	8.3 (0.2)	2.8 (0.03)
PVC/0.5%GN	5.7 (0.6)	274.7 (2.0)	446.8 (0.6)	7.2 (0.4)	2.8 (0.04)
PVC/0.5%GN–CE	6.1 (0.2)	278.3 (0.8)	451.4 (1.5)	8.6 (0.1)	2.4 (0.03)
PVC/1%GN	6.8 (0.5)	270.6 (0.5)	438.1 (2.9)	8.0 (0.7)	2.6 (0.08)
PVC/1%GN–CE	6.6 (0.2)	278.5 (0.7)	453.5 (1.3)	9.9 (0.3)	2.3 (0.03)

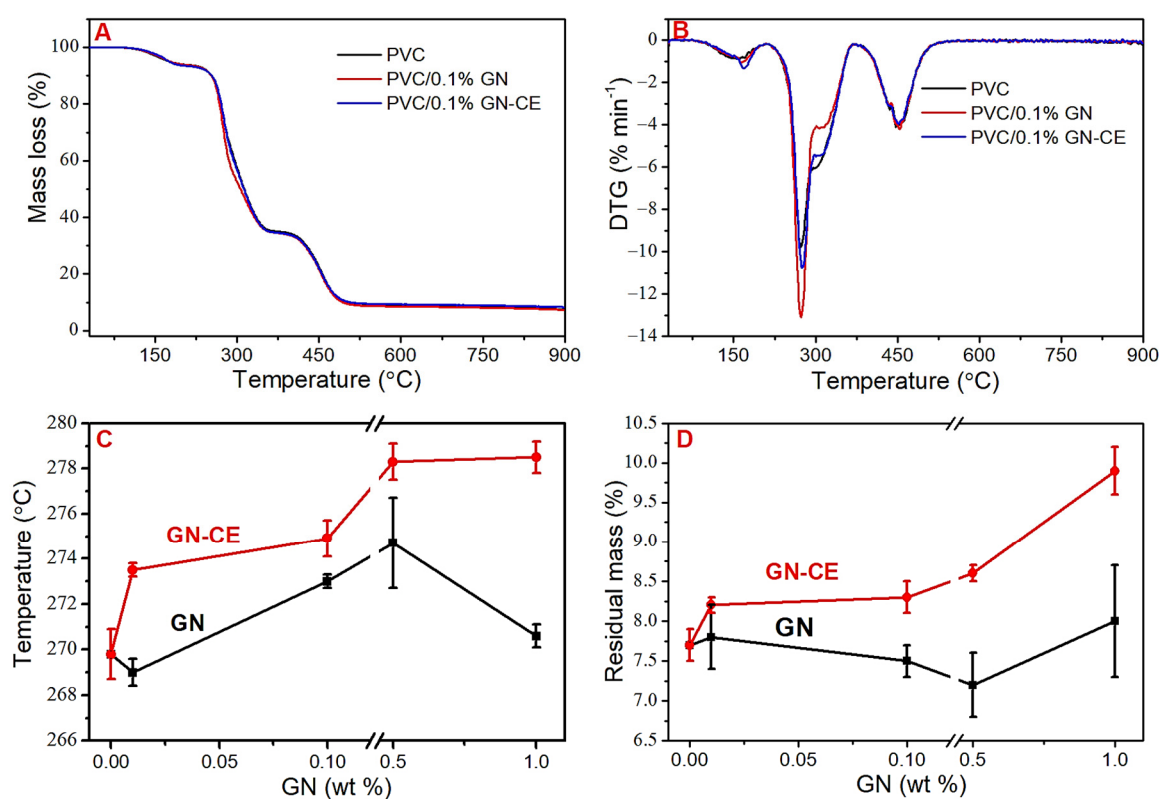


Figure 11. (A) Example TGA thermograms, (B) Example DTG curves, (C) Max. DTG I analysis, (D) Residual mass analysis.

Due to the presence of residual THF in PVC, the nanocomposite films' thermal stability was evaluated based on the differential thermogravimetry (DTG) [13,19]. DTG maxima of the first (max. DTG I) and second (max. DTG II) stages of decomposition, as well as the residual mass after the heating process, were used to analyze the thermal stability of the PVC/GN nanocomposites. The examples of thermogravimetric and DTG curves are presented in Figure 11A,B; all results are summarized in Table 2 (standard deviation of the obtained mean values in brackets). The max. DTG I analysis (Figure 11C) showed an increase in the thermal stability of graphene–CE modified materials, where the maximum temperature observed in the case of PVC/0.5%GN–CE was 8.5 °C higher compared to the unmodified matrix material. The introduction of GN–CE at a higher concentration does not cause a statistically significant change in thermal stability. In the case of nanocomposites with unmodified graphene, a significant improvement in stability was observed for materials with 0.1% GN; the temperature of the maximal degradation rate was in this case 3.2 °C higher than for poly(vinyl chloride). PVC/0.5%GN showed no statistically significant increase in this temperature, while an increase in standard deviation was observed. A further increase in the concentration of graphene filler to 1% had the effect of lowering the thermal stability of the nanocomposite materials. It can be assumed that the increase in standard deviation and decrease in thermal stability is due to the agglomeration of nanoparticles in the matrix material.

The max. DTG II analysis (Table 2) showed no statistically significant change in the temperature of the maximal degradation rate for materials with GN–CE. In contrast, a decrease in thermal stability was observed for materials with the unmodified graphene for concentrations of 0.5% and 1%, which may be related to the non-uniform distribution of the filler in the matrix. Residual mass analysis (Figure 11D) showed increases of these values in graphene–CE modified materials, and no statistically significant change in nanocomposites with GN. The increase in residual mass in materials with GN–CE indicates that a well-dispersed filler can act protectively against the carbon chain of the polymer, by forming an insulating layer [24,98].

A commonly used method for assessing the thermal stability of PVC materials is the Congo Red test. The results presented in Table 2 show that the introduction of graphene into polymer matrix results accelerates the dehydrochlorination process, which can take place according to various mechanisms [77]. The authors [19] indicated that the lower stability of PVC/GN composites may be due to the fact that GN nano-flakes act as reinforcing particulate fillers that attract chloride from the PVC. Obtained nanocomposites are sensitive to heat so they can undergo thermomechanical degradation processes under processing. Therefore, the use of thermal stabilizers will be required in the manufacture of these materials by conventional processing methods.

At the same time, it should be emphasized that discrepancies in the results of thermal stability measured by two methods are not unusual, due to the conditions under which the tests were conducted. Thermal stability by the Congo Red method is determined at a constant temperature that is close to the upper temperature range of PVC processing. In the TGA method, the sample is heated under a nitrogen atmosphere at a specified heating rate, over a wide temperature range, usually up to about 900 °C.

Figure 12 shows exemplary stress–strain curves for PVC with the nanocomposites on its matrix, and the determined tensile strength (TS) vs. GN and GN–CE concentration. The course of the stress–strain curves shows no yield point regardless of the material composition, which is as expected. The PVC/GN–CE nanocomposites had, compared to PVC/GN materials, a slightly higher mean TS value and a lower standard deviation, which is due to the better dispersion of the modified filler in the PVC matrix. However, the introduction of graphene into the PVC matrix, regardless of the graphene modification, did not result in a statistically significant change in the tensile strength of PVC nanocomposites.

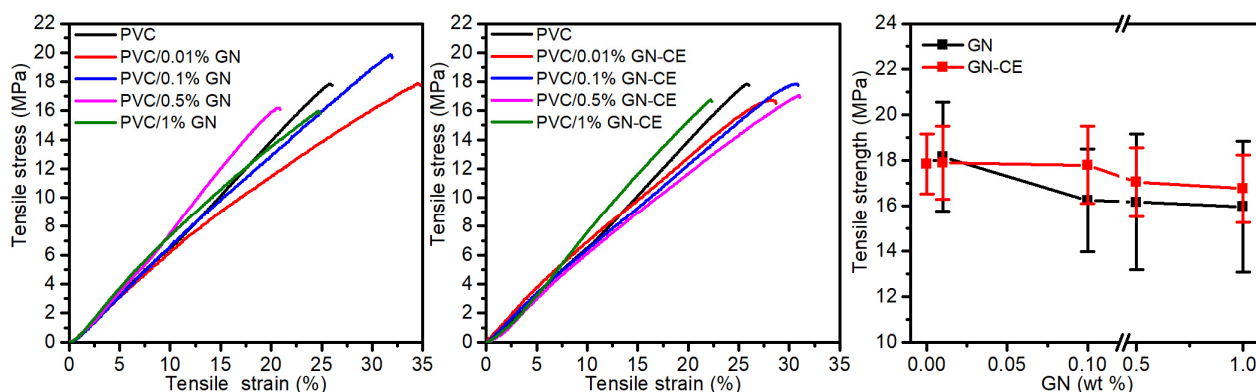


Figure 12. Mechanical properties of PVC, PVC/GN and PVC/GN-CE nanocomposites.

An improvement of the mechanical properties of PVC/GN nanocomposites depends on the homogeneous dispersion of graphene in the polymer matrix and the structure of the filler. The lack of defects on the GN surface results in its high integrity and good mechanical properties, which directly determines the improvement of the mechanical properties of nanocomposites [26,99,100]. On the other hand, the dense GN network limits the penetration of poly(vinyl chloride) macromolecules between its layers, which makes the matrix discontinuous [14,24,100]. This explains the lack of a significant improvement in the mechanical properties of materials with GN–CE, where filler dispersion was improved.

2.9. Electrical Properties of Nanocomposites

Figure 13 shows the results of the resistivity tests of the obtained materials. The surface resistivity of poly(vinyl chloride) was determined to be $4.7 \times 10^{14} \Omega$, and significant change occurs when the GN concentration in the composites is 0.5% and 1%. The lowest resistivity, which equals $1.4 \times 10^7 \Omega$, is characteristic of the PVC/1%GN sample, which makes it possible to conclude that it is an antistatic material [25,101]. Nanocomposites containing

GN–CE did not show a decrease in surface resistivity, and the lowest value ($1.5 \times 10^{14} \Omega$) was shown by the sample PVC/1%GN–CE.

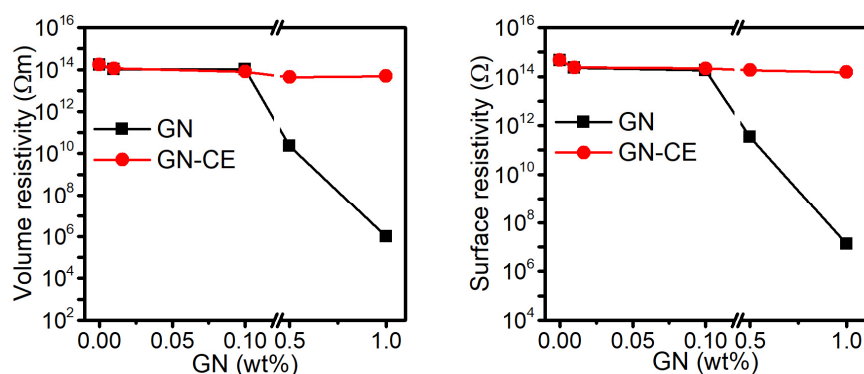


Figure 13. Surface and volume resistivity of PVC, PVC/GN and PVC/GN–CE nanocomposites.

The volume resistivity of PVC/GN composites also decreases with the increase in graphene concentration in the matrix. The materials containing 1% of GN were characterized by the lowest resistivity, and equaled $9.8 \times 10^5 \Omega\text{m}$. Such a large change in resistivity (for PVC was $1.7 \times 10^{14} \Omega\text{m}$) indicates that the dispersion of the GN was sufficient to create conduction paths. The PVC/GN–CE composites, as in the case of surface resistivity, did not show large changes in volume resistivity as the filler content in the matrix increased.

References [14,101] present that the influence of GN on the resistivity or conductivity of PVC/GN nanocomposites is significantly related to the dispersion of the filler in the polymer's matrix. Although the modification of graphene with turmeric significantly improved the homogeneity of the structure of PVC/GN–CE nanocomposites, the expected improvement in electrical properties was not found. Graphene surface modification with curcuma extract is possible by π – π interactions. Some studies have shown the disturbances in the displacement of π electrons on the graphene's surface, leading to the significant deterioration of its electrical properties [20,29]. This explains the lack of change regarding the resistivity of GN–CE-containing materials, despite a significant improvement of the graphene's dispersion in the PVC matrix.

2.10. Swelling Behaviour of Nanocomposites

The numerous applications of poly(vinyl chloride) are due to its resistance to solvents [19,102,103]. However, PVC dissolves completely in THF and cyclohexanone, and it undergoes limited swelling when contacted with acetone. In this work, the chemical resistance of the proposed PVC/GN nanocomposites was tested by analyzing the swelling process in acetone. Swelling curves, i.e., the dependence of the degree of swelling as a function of time, are shown in Figure 14.

It was found that all the obtained materials undergo limited swelling, while the dependence of swelling degree on the exposure time to the swelling agent has a shape of a sigmoid function. Therefore, Equation (1) was used to approximate the swelling curves [20,22].

$$S_d = \frac{S_E}{1 + 10^{(t_M - t)p}} \quad (1)$$

where:

S_d is swelling degree, %,

S_E is equilibrium swelling, upper asymptote, %,

t_M is time in which the swelling occurs with a maximum rate, s,

t is time of exposure to the swelling agent, s,

p is comparison parameter, 1 s^{-1} .

The parameters of the equation and the coefficient of determination R^2 are summarized in Table 3. The proposed model describes the experimental results with high accuracy, as evidenced by the high values of the coefficient of determination.

Table 3. Parameters of the model describing the swelling process.

Material	S_E , %	t_M , s	p , s^{-1}	R^2
PVC	48.2 (0.3)	348 (4)	0.007 (0.0004)	0.994
PVC/0.01% GN	43.8 (0.4)	477 (7)	0.004 (0.0002)	0.994
PVC/0.01% GN-CE	42.9 (0.3)	570 (7)	0.003 (0.0001)	0.996
PVC/0.1% GN	43.9 (0.4)	307 (6)	0.006 (0.0004)	0.990
PVC/0.1% GN-CE	42.1 (0.2)	262 (3)	0.010 (0.0005)	0.996
PVC/0.5% GN	49.5 (0.2)	262 (2)	0.009 (0.0003)	0.998
PVC/0.5% GN-CE	32.1 (0.3)	498 (8)	0.004 (0.0003)	0.992
PVC/1% GN	43.5 (0.1)	267 (1)	0.010 (0.0002)	0.999
PVC/1% GN-CE	27.3 (0.2)	443 (4)	0.007 (0.0003)	0.997

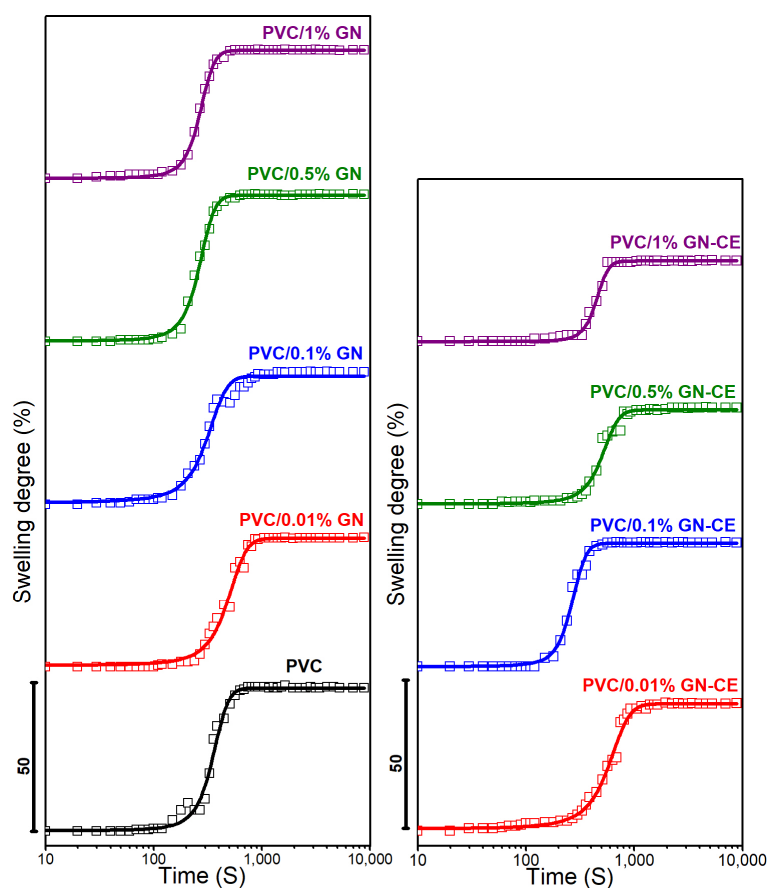


Figure 14. Swelling degree of PVC, PVC/GN and PVC/GN-CE nanocomposites vs. time.

PVC/GN nanocomposites were found to have a lower equilibrium swelling ratio compared to unmodified PVC; the lowest S_E value observed for PVC/1%GN, i.e., 43.5%, shows an improvement of about 5% in terms of the chemical resistance on the polymer matrix. Materials obtained with the addition of extract-modified graphene were characterized by a lower value of S_E compared to corresponding materials with unmodified graphene. This effect was attributed to the better dispersion of the filler in the polymer matrix, as evidenced by significantly lower S_E values for materials with 0.5 and 1% GN-CE. They

were 32.1 and 27.3%, respectively, which represents a reduction in the equilibrium degree of swelling relative to PVC of 14.1%, in the case of PVC/0.5%GN–CE, and of 20.9%, in PVC/1%GN–CE. In addition, it should be noted that the agglomeration of the filler in the polymer matrix can lead to lower resistance to solvents in the form of acetone, which was observed in PVC/0.5%GN, where the SE was 1.3% higher relative to PVC. As the GN–CE content of the nanocomposites increases, the time in which the swelling occurs with a maximum rate (t_M) also increases, which further confirms the correlation between acetone resistance of the materials and filler surface modifications. In materials with unmodified GN, a decrease in t_M values was observed with an increase in its content in the PVC matrix.

An increase in the chemical resistance of PVC, by using carbon fillers, occurs as a result of a decrease in its free volume. Consequently, this leads to a reduced access of solvents to the polymer chain [22,103]. In the case of the materials in question, this mechanism is very likely, as confirmed by the higher resistance of nanocomposites containing GN–CE, characterized by a better dispersion of graphene in the polymer matrix.

3. Materials and Methods

3.1. Materials

Graphene-based nanopowder with a flake thickness of 1.6 nm (maximum of 3 atomic monolayers), a flake length of 10 μm , and a specific surface area of $400 \div 800 \text{ m}^2\text{g}^{-1}$ was purchased from USA Graphene Laboratories Inc. Graphene was dispersed in a poly(vinyl chloride) solution using unmodified suspensive poly(vinyl chloride) Neralit 601 (Czech Republic, Spolana s.r.o. Anwil S.A. group), with a K number of 59–61, a bulk density of 0.56–0.63 g cm^{-3} , a specific density of 1.39 g cm^{-3} , and 97% purity. As a solvent for PVC and an environment used for graphene modification, tetrahydrofuran (THF) (Chempur, Piekary Śląskie, Poland) was used. Curcumin from *Curcuma longa* L. turmeric powder (Sigma-Aldrich, St. Louis, MO, USA) and *Curcuma longa* L. rhizome extract (made in-house [22]) was used to modify the surface of graphene. Methanol (Chempur, Piekary Śląskie, Poland) was used to wash modified graphene.

3.2. Graphene Modification

In order to functionalize the graphene's surface with curcuminoids in the first step, 100 cm^3 solutions of CU and CE in THF with a concentration of 2.25 mg cm^{-3} were prepared by ultrasound (frequency of 20 kHz, 40% amplitude, time 10 min, temperature 23 °C) using a SONOPULS rod-shaped probe homogenizer from Bandelin. Graphene was then introduced into the solution, which was prepared so that the dispersion concentration was 1.5 mg cm^{-3} . Next, GN was sonicated under the same conditions as curcuminoids for 2 h. It was then stirred with a magnetic stirrer for 15 h at 200 rpm. After this time, the material was centrifuged 4 times at 12,000 rpm for 4 min and washed after each step with methanol, in order to remove the undeposited modifier. After centrifugation, the graphene was dried at 45 °C for 65 h to evaporate residual solvents.

3.3. Preparation of PVC/GN Dispersions and Nanocomposites

In the first step, poly(vinyl chloride) was dissolved in THF at 25 °C for about 48 h, yielding a solution of 3 wt%. Then, the dry graphene was added to the solution and dispersed using ultrasound (conditions as in Section 2.2) for 60 min. The amount of graphene in the prepared dispersions for dispersion stability testing was 1 wt% per polymer mass.

Thin films of PVC/GN, PVC/GN–CU, and PVC/GN–CE nanocomposites containing 1% filler for structure test were obtained by solvent evaporation, where the dispersions were poured onto Petri dishes with a diameter of 7 cm, and the solvent was evaporated at 50 °C for 24 h. Nanocomposites for testing properties were dried in a vacuum drier under a reduced pressure (max 20 mbar absolute) at 50 °C for 2 weeks, in order to remove the THF residue from the polymer films. All samples were coded to take into account the graphene content and the presence of CE, e.g., a sample containing GN at a concentration of 0.01 wt.% was coded as PVC/1%GN, whereas a sample containing the same graphene

modified by *Curcuma longa* L. rhizome extract was coded as PVC/1%GN-CE, and that modified by Curcumin from *Curcuma longa* L. turmeric powder was consequently coded as PVC/1%GN-CU.

3.4. Characterization

Absorption studies were conducted using a UV-vis/NIR spectrometer (Perkin Elmer Lambda 1050+) in a quartz cuvette. For this purpose, solutions of CU, CE in methanol with a concentration of 0.008 mg cm^{-3} and dispersions of GN, GN-CU, and GN-CE with a concentration of 0.03 mg cm^{-3} were prepared. The study was conducted in the 210–800 nm range. The experimental results were normalized in the range 0–1 using the OriginLab software.

X-ray photoelectron spectroscopy: a PHI 5000 VersaProbe (ULVAC-PHI Inc., Hagisono, Japan) spectrometer was used to conduct XPS measurements under the following conditions: monochromatic Al K α radiation ($h\nu = 1486.6 \text{ eV}$), an X-ray source operating at 25 W, 15 kV, 100 μm spot, pass energy of 23.5 eV, energy step of 0.1 eV. Obtained XPS spectra were analyzed with CasaXPS software, using the set of the sensitivity factors native for the hardware. Shirley background and Gaussian-Lorentzian peak shape were used for deconvolution of all spectra.

The thermal stability of the fillers and nanocomposites was assessed by the thermogravimetric method using a TG 209 F3 Tarsus apparatus (Netzsch). The heating rate was about $10 \text{ }^\circ\text{C min}^{-1}$ in an open ceramic crucible, under a nitrogen atmosphere, at 30 to 700 $^\circ\text{C}$ for fillers and at 30 to 900 $^\circ\text{C}$ for nanocomposites. In addition, static thermal stability tests were determined for the nanocomposite materials using the Congo Red test. The test was carried out at 200 $^\circ\text{C}$, measuring the thermal stability time, i.e., the time during which the sample shows no signs of degradation in the form of hydrogen chloride release and color change of the indicator paper.

Raman spectra were collected with a Raman DXR microscope (Thermo Fisher Scientific, Waltham, MA, USA) using two laser lines, 532 nm and 780 nm, where the shorter wavelength was used for polymer composites, and fillers were studied using the longer wavelength line. The specimens were measured with 50 repetitions of 50 s each (20 in successive control measurements). The aperture was 50 μm , the lenses were 10 and 50 mm, and the laser beam power was 0.1 mW for 780 nm and 1 mW for 532 nm. Each sample was measured at least dozens of times (from 80 to >300) at different locations, and the final signal was obtained as an average and statistically representative one. The morphology of the samples was studied using scanning electron microscopy (SEM), and a Zeiss Cross-beam 350 microscope; in the case of polymer nanocomposites, cryogenic breakthroughs with a sputtered gold layer were observed. As a second technique, a Zeiss Libra 120 Plus transmission electron microscope (TEM) (Stuttgart, Germany) operating at 120 kV was used, where the aqueous suspension was placed on a copper grid coated with a formvar polymer layer. Finally, the sample was left in the air (under a fume hood) to dry.

Stability testing of the obtained graphene dispersions in PVC solution was carried out by multiple light scattering using the Turbiscan Lab apparatus (Formulation SA, Toulouse, France), where suspensions of GN, GN-CU and GN-CE in 3% PVC solution in THF were placed in glass cylindrical test tubes, with a working height of 54 mm. The samples were then placed in a Turbiscan Lab instrument and scanned with light at approximately 880 nm. Scanning was carried out every 1 h for 24 h at room temperature (23 $^\circ\text{C}$). The Turbiscan Stability Index (TSI) was determined from the results.

Filler dispersion in the matrix was also determined using an atomic force microscope Nanosurf (Liestal, Switzerland) in contact mode with the PPP-XYCONTR probe (NANOSENSORS, Neuchatel, Switzerland), where the radius of the aluminum-coated blade was 7 nm, while the line angle was 20 degrees. 2D and 3D images were taken within a $50 \times 50 \mu\text{m}$ area. To determine the surface topography of the area, 500 lines were measured (at 20 nm intervals), and the number of measurement points per line was 5000. The scanning speed of the sample was $5 \mu\text{m s}^{-1}$.

A study of tensile properties was carried out using an in-house-built tensile tester, with the parameters presented in our earlier work [22]. The tests were carried out on samples with a thickness of 0.2 ± 0.07 mm and a width of 2 ± 0.1 mm, while the length of the measuring section L0 was 1.5 mm. The materials were stretched at a constant speed of 0.1 mm s^{-1} .

The electrical properties of nanocomposites were determined by measuring system consisting of a 6517A electrometer and a 8009 measuring chamber (Keithley Instrument Inc., Cleveland, OH, USA). The surface and volume resistivity were measured. The tests were carried out on film samples with a diameter of 70 mm in air, at a temperature of 23°C and humidity of 50%, and at a voltage of 10 V.

The resistance of the obtained materials to swelling in acetone was tested in accordance with the method proposed in our earlier study [20]. The change in the swelling degree (S_d) was determined (see Equation (2)), depending on the immersion time in the swelling agent. The changes in the samples' diameters were set on the basis of photos using the NIS Elements 4.0 software. The frequency picture-taking depended on the exposure time to the swelling agent. The measurement temperature was 20°C and the initial diameter of the samples $h_0 = 10$ mm.

$$S_d = \frac{h - h_0}{h_0} \times 100\% \quad (2)$$

where:

h is sample diameter after time t (mm),

h_0 is initial sample diameter (mm).

In order to analyse the obtained results, Origin 8.6 Pro software with implemented statistical analysis modules was used. ANOVA with Tukey's post-hoc test was used to compare the significance of the difference for the mean values of the obtained results. The normal distribution was confirmed by the Shapiro–Wilk test, and the homogeneity of variance by the Levene's test. All analyses were performed assuming a significance level below 0.05.

4. Conclusions

Graphene is one of the most promising nanofillers of nanocomposites, improving their performance. However, its uniform distribution in the polymer matrix is challenging. Several studies refer the need to reduce the agglomeration of GN and its derivatives during nanocomposite fabrication, in order to achieve improved properties [104–107]. In the present work, an environmentally safe method of graphene surface modification is presented, using curcumin and an extract derived from the powdered rhizome of *Curcuma longa* L.

Observations of the modified materials' morphology showed better CE dispersion on the graphene's surface. Spectroscopic studies have shown that modification occurs via a π – π stacking mechanism. TGA analysis revealed a higher amount of deposited curcumin on GN flakes i.e., 11.4 wt.%, while for the extract it was 6.9 wt.%. In addition, it is worth noting that the modified materials have a high thermal stability of about 340°C . The analysis of the stability of GN, GN–CU, and GN–CE dispersions, as well as observations of the polymer films structure obtained after solvent evaporation from the dispersions, showed a significant improvement in the homogeneity of the nanocomposites after modification by curcuminoids. At the same time, extract-modified graphene showed better dispersion improvement in PVC. That indicates that not only the amount of modifier deposited on the graphene surface, but also its size and dispersion important in improving PVC/GN homogeneity. The analysis of the properties of nanocomposites with GN–CE has shown a better thermal and chemical stability of these materials. On the other hand, based on the results of the Congo Red test, it was stated that the proposed nanocomposites will require thermal stabilization at the processing stage by traditional methods, which is a well-known phenomenon in the field of the PVC technology.

Summarizing, the proposed naturally derived compounds in the form of CE can be an alternative to previously proposed modifications of graphene for use in PVC and other polymer composites. In addition, the high thermal stability of the proposed modification, as well as the relatively low cost and possibility of obtaining the modifier on a large scale, provide opportunities for the technological use of CE in the future production of graphene polymer nanocomposites, through traditional processing methods at high temperatures.

Author Contributions: Conceptualization, S.W., K.S. and J.T.; methodology, S.W., K.S., J.T., M.O., A.D., K.N., P.J. and H.G.; validation, S.W., K.S. and J.T.; formal analysis, S.W. and K.S.; investigation, S.W., K.S., M.O., A.D., K.N., P.J. and H.G.; resources, J.T.; data curation, S.W., K.N. and A.D.; writing—original draft preparation, S.W., K.S., J.T., M.O., A.D. and K.N.; writing—review and editing, S.W., K.S., J.T., M.O., A.D. and K.N.; visualization, S.W.; supervision, J.T. and K.S.; project administration, S.W. All authors have read and agreed to the published version of the manuscript.

Funding: This work was supported by the Ministry of Education and Science of Poland.

Institutional Review Board Statement: Not applicable.

Informed Consent Statement: Not applicable.

Data Availability Statement: The data that support the findings of this study are available from the corresponding author upon reasonable request.

Conflicts of Interest: The authors declare that they have no known competing financial interest or personal relationship that could have appeared to influence the work reported in this paper.

References

1. Saleem, H.; Haneef, M.; Abbasi, H.Y. Synthesis route of reduced graphene oxide via thermal reduction of chemically exfoliated graphene oxide. *Mater. Chem. Phys.* **2018**, *204*, 1–7. [[CrossRef](#)]
2. Johnson, D.W.; Dobson, B.P.; Coleman, K.S. A manufacturing perspective on graphene dispersions. *Curr. Opin. Colloid Interface Sci.* **2015**, *20*, 367–382. [[CrossRef](#)]
3. Abdel Ghany, N.A.; Elsherif, S.A.; Handal, H.T. Revolution of Graphene for different applications: State-of-the-art. *Surf. Interfaces* **2017**, *9*, 93–106. [[CrossRef](#)]
4. Drewniak, S.; Muzyka, R.; Stolarczyk, A.; Pustelny, T.; Kotyczka-Morańska, M.; Setkiewicz, M. Studies of reduced graphene oxide and graphite oxide in the aspect of their possible application in gas sensors. *Sensors* **2016**, *16*, 103. [[CrossRef](#)] [[PubMed](#)]
5. Mikhailov, S. *Physics and Applications of Graphene-Experiments*; InTech: Rijeka, Croatia, 2011; ISBN 9789533071527.
6. Punetha, V.D.; Rana, S.; Yoo, H.J.; Chaurasia, A.; McLeskey, J.T.; Ramasamy, M.S.; Sahoo, N.G.; Cho, J.W. Functionalization of carbon nanomaterials for advanced polymer nanocomposites: A comparison study between CNT and graphene. *Prog. Polym. Sci.* **2017**, *67*, 1–47. [[CrossRef](#)]
7. Galpaya, D.; Wang, M.; Liu, M.; Motta, N.; Waclawik, E.; Yan, C. Recent Advances in Fabrication and Characterization of Graphene-Polymer Nanocomposites. *Graphene* **2012**, *1*, 30–49. [[CrossRef](#)]
8. Sreenivasulu, B.; Ramji, B.R.; Nagaral, M. A Review on Graphene Reinforced Polymer Matrix Composites. *Mater. Today Proc.* **2018**, *5*, 2419–2428. [[CrossRef](#)]
9. Phiri, J.; Gane, P.; Maloney, T.C. General overview of graphene: Production, properties and application in polymer composites. *Mater. Sci. Eng. B Solid-State Mater. Adv. Technol.* **2017**, *215*, 9–28. [[CrossRef](#)]
10. Mohan, V.B.; Lau, K.; Hui, D.; Bhattacharyya, D. Graphene-based materials and their composites: A review on production, applications and product limitations. *Compos. Part B Eng.* **2018**, *142*, 200–220. [[CrossRef](#)]
11. Deshmukh, K.; Joshi, G.M. Thermo-mechanical properties of poly (vinyl chloride)/graphene oxide as high performance nanocomposites. *Polym. Test.* **2014**, *34*, 211–219. [[CrossRef](#)]
12. Nawaz, K.; Ayub, M.; Ul-Haq, N.; Khan, M.B.; Niazi, M.B.K.; Hussain, A. The Effect of Graphene Nanosheets on the Mechanical Properties of Polyvinylchloride. *Polym. Compos.* **2016**, *37*, 1572–1576. [[CrossRef](#)]
13. Mindivan, F.; Gökaş, M. Preparation of new PVC composite using green reduced graphene oxide and its effects in thermal and mechanical properties. *Polym. Bull.* **2020**, *77*, 1929–1949. [[CrossRef](#)]
14. Li, Q.; Shen, F.; Zhang, Y.; Huang, Z.; Muhammad, Y.; Hu, H.; Zhu, Y.; Yu, C.; Qin, Y. Graphene incorporated poly(vinyl chloride) composites prepared by mechanical activation with enhanced electrical and thermo-mechanical properties. *J. Appl. Polym. Sci.* **2020**, *137*, 21–23. [[CrossRef](#)]
15. Akhina, H.; Gopinathan Nair, M.R.; Kalarikkal, N.; Pramoda, K.P.; Hui Ru, T.; Kailas, L.; Thomas, S. Plasticized PVC graphene nanocomposites: Morphology, mechanical, and dynamic mechanical properties. *Polym. Eng. Sci.* **2018**, *58*, E104–E113. [[CrossRef](#)]
16. Wang, H.; Xie, G.; Fang, M.; Ying, Z.; Tong, Y.; Zeng, Y. Mechanical reinforcement of graphene/poly(vinyl chloride) composites prepared by combining the in-situ suspension polymerization and melt-mixing methods. *Compos. Part B Eng.* **2017**, *113*, 278–284. [[CrossRef](#)]

17. Wang, H.; Xie, G.; Yang, C.; Zheng, Y.; Ying, Z.; Ren, W.; Zeng, Y. Enhanced Toughness of Multilayer Graphene-Filled Poly(vinyl chloride) Composites Prepared Using Melt-Mixing Method. *Polym. Compos.* **2017**, *38*, 138–146. [[CrossRef](#)]
18. Abd El-Kader, M.F.H.; Awwad, N.S.; Ibrahim, H.A.; Ahmed, M.K. Graphene oxide fillers through polymeric blends of PVC/PVDF using laser ablation technique: Electrical behavior, cell viability, and thermal stability. *J. Mater. Res. Technol.* **2021**, *13*, 1878–1886. [[CrossRef](#)]
19. Mindivan, F.; Göktaş, M.; Dike, A.S. Mechanical, thermal, and micro- and nanostructural properties of polyvinyl chloride/graphene nanoplatelets nanocomposites. *Polym. Compos.* **2020**, *41*, 3707–3716. [[CrossRef](#)]
20. Wilczewski, S.; Skórczewska, K.; Tomaszewska, J.; Lewandowski, K. Structure and properties of poly (vinyl chloride)/ graphene nanocomposites. *Polym. Test.* **2020**, *81*, 106282. [[CrossRef](#)]
21. Wilczewski, S.; Skórczewska, K.; Tomaszewska, J.; Lewandowski, K.; Szulc, J.; Runka, T. Manufacturing homogenous PVC/graphene nanocomposites using a novel dispersion agent. *Polym. Test.* **2020**, *91*, 106868. [[CrossRef](#)]
22. Wilczewski, S.; Skórczewska, K.; Tomaszewska, J.; Lewandowski, K.; Studziński, W.; Osial, M.; Jencyk, P.; Grzywacz, H.; Domańska, A. *Curcuma longa* L. Rhizome Extract as a Poly(vinyl chloride)/Graphene Nanocomposite Green Modifier. *Molecules* **2022**, *27*, 8081. [[CrossRef](#)]
23. Hasan, M.; Banerjee, A.N.; Lee, M. Enhanced thermo-optical performance and high BET surface area of graphene@PVC nanocomposite fibers prepared by simple facile deposition technique: N₂ adsorption study. *J. Ind. Eng. Chem.* **2015**, *21*, 828–834. [[CrossRef](#)]
24. Wang, L.; Wei, X.; Wang, G.; Zhao, S.; Cui, J.; Gao, A.; Zhang, G.; Yan, Y. A facile and industrially feasible one-pot approach to prepare graphene-decorated PVC particles and their application in multifunctional PVC/graphene composites with segregated structure. *Compos. Part B Eng.* **2020**, *185*, 107775. [[CrossRef](#)]
25. Wei, Z.B.; Zhao, Y.; Wang, C.; Kuga, S.; Huang, Y.; Wu, M. Antistatic PVC-graphene Composite through Plasticizer-mediated Exfoliation of Graphite. *Chin. J. Polym. Sci.* **2018**, *36*, 1361–1367. [[CrossRef](#)]
26. Ahmed, R.M.; Ibrahim, A.A.; El-Bayoumi, A.S.; Atta, M.M. Structural, mechanical, and dielectric properties of polyvinylchloride/graphene nano platelets composites. *Int. J. Polym. Anal. Charact.* **2021**, *26*, 68–83. [[CrossRef](#)]
27. Ma, J.; Liu, J.; Zhu, W.; Qin, W. Solubility study on the surfactants functionalized reduced graphene oxide. *Colloids Surf. A Physicochem. Eng. Asp.* **2018**, *538*, 79–85. [[CrossRef](#)]
28. Dai, J.; Wang, G.; Ma, L.; Wu, C. Study on the surface energies and dispersibility of graphene oxide and its derivatives. *J. Mater. Sci.* **2015**, *50*, 3895–3907. [[CrossRef](#)]
29. Tkalya, E.E.; Ghislandi, M.; de With, G.; Koning, C.E. The use of surfactants for dispersing carbon nanotubes and graphene to make conductive nanocomposites. *Curr. Opin. Colloid Interface Sci.* **2012**, *17*, 225–232. [[CrossRef](#)]
30. Kuila, T.; Bose, S.; Mishra, A.K.; Khanra, P.; Kim, N.H.; Lee, J.H. Chemical functionalization of graphene and its applications. *Prog. Mater. Sci.* **2012**, *57*, 1061–1105. [[CrossRef](#)]
31. Hatamie, S.; Akhavan, O.; Sadrezaad, S.K.; Ahadian, M.M.; Shirolkar, M.M.; Wang, H.Q. Curcumin-reduced graphene oxide sheets and their effects on human breast cancer cells. *Mater. Sci. Eng. C* **2015**, *55*, 482–489. [[CrossRef](#)]
32. Grimme, S. Do special noncovalent π - π stacking interactions really exist? *Angew. Chemie Int. Ed.* **2008**, *47*, 3430–3434. [[CrossRef](#)] [[PubMed](#)]
33. Wang, W.; Zhang, Y.; Wang, Y.B. Noncovalent π - π interaction between graphene and aromatic molecule: Structure, energy, and nature. *J. Chem. Phys.* **2014**, *140*, 094302. [[CrossRef](#)]
34. Navik, R.; Gai, Y.; Wang, W.; Zhao, Y. Curcumin-assisted ultrasound exfoliation of graphite to graphene in ethanol. *Ultrason. Sonochem.* **2018**, *48*, 96–102. [[CrossRef](#)]
35. Yang, Y.K.; He, C.E.; Peng, R.G.; Baji, A.; Du, X.S.; Huang, Y.L.; Xie, X.L.; Mai, Y.W. Non-covalently modified graphene sheets by imidazolium ionic liquids for multifunctional polymer nanocomposites. *J. Mater. Chem.* **2012**, *22*, 5666–5675. [[CrossRef](#)]
36. Jeong, S.Y.; Kim, S.H.; Han, J.T.; Jeong, H.J.; Jeong, S.Y.; Lee, G.W. Highly concentrated and conductive reduced graphene oxide nanosheets by monovalent cation- π interaction: Toward printed electronics. *Adv. Funct. Mater.* **2012**, *22*, 3307–3314. [[CrossRef](#)]
37. Texter, J. Graphene dispersions. *Curr. Opin. Colloid Interface Sci.* **2014**, *19*, 163–174. [[CrossRef](#)]
38. Achari, A.; Datta, K.; De, M.; Dravid, V.; Eswaramoorthy, M. Amphiphilic aminoclay-RGO hybrids: A simple strategy to disperse a high concentration of RGO in water. *Nanoscale* **2013**, *5*, 5316–5320. [[CrossRef](#)] [[PubMed](#)]
39. Kou, L.; Gao, C. Making silica nanoparticle-covered graphene oxide nanohybrids as general building blocks for large-area superhydrophilic coatings. *Nanoscale* **2011**, *3*, 519–528. [[CrossRef](#)]
40. Ma, F.; Yuan, N.; Ding, J. The conductive network made up by the reduced graphene nanosheet/polyaniline/polyvinyl chloride. *J. Appl. Polym. Sci.* **2013**, *128*, 3870–3875. [[CrossRef](#)]
41. Li, P.; Chen, X.; Zeng, J.-B.; Gan, L.; Wang, M. Enhancement of Interfacial Interaction between Poly(vinyl chloride) and Zinc Oxide Modified Reduced Graphene Oxide. *RSC Adv.* **2016**, *6*, 5784–5791. [[CrossRef](#)]
42. Khaleghi, M.; Didehban, K.; Shabaniyan, M. Simple and fast preparation of graphene oxide@ melamine terephthaldehyde and its PVC nanocomposite via ultrasonic irradiation: Chemical and thermal resistance study. *Ultrason. Sonochem.* **2018**, *43*, 275–284. [[CrossRef](#)] [[PubMed](#)]
43. Hu, J.; Jia, X.; Li, C.; Ma, Z.; Zhang, G.; Sheng, W.; Zhang, X.; Wei, Z. Effect of interfacial interaction between graphene oxide derivatives and poly(vinyl chloride) upon the mechanical properties of their nanocomposites. *J. Mater. Sci.* **2014**, *49*, 2943–2951. [[CrossRef](#)]

44. Khaleghi, M.; Didehban, K.; Shabaniyan, M. Effect of new melamine-terephthaldehyde resin modified graphene oxide on thermal and mechanical properties of PVC. *Polym. Test.* **2017**, *63*, 382–391. [[CrossRef](#)]
45. Piszczek, K. *Żelowanie Suspensyjnego, Nieplastyfikowanego Poli(chloroku winylu)*; Wydawnictwa Uczelniane Uniwersytetu Technologiczno-Przyrodniczego: Bydgoszcz, Poland, 2009.
46. Thakuria, R.; Nath, N.K.; Saha, B.K. The Nature and Applications of π - π Interactions: A Perspective. *Cryst. Growth Des.* **2019**, *19*, 523–528. [[CrossRef](#)]
47. Hatamie, S.; Ahadian, M.M.; Irajizad, A.; Akhavan, O.; Jokar, E. Photoluminescence and electrochemical investigation of curcumin-reduced graphene oxide sheets. *J. Iran. Chem. Soc.* **2018**, *15*, 351–357. [[CrossRef](#)]
48. Aliboland, M.; Mohammadi, M.; Taghdisi, S.M.; Ramezani, M.; Abnous, K. Fabrication of aptamer decorated dextran coated nano-graphene oxide for targeted drug delivery. *Carbohydr. Polym.* **2017**, *155*, 218–229. [[CrossRef](#)] [[PubMed](#)]
49. Bani, F.; Adeli, M.; Movahedi, S.; Sadeghizadeh, M. Graphene-polyglycerol-curcumin hybrid as a near-infrared (NIR) laser stimuli-responsive system for chemo-photothermal cancer therapy. *RSC Adv.* **2016**, *6*, 61141–61149. [[CrossRef](#)]
50. Saltos, J.A.; Shi, W.; Mancuso, A.; Sun, C.; Park, T.; Averick, N.; Punia, K.; Fatab, J.; Raja, K. Curcumin-derived green plasticizers for Poly(vinyl) chloride. *RSC Adv.* **2014**, *4*, 54725–54728. [[CrossRef](#)]
51. Larrañeta, E.; Imízcoz, M.; Toh, J.X.; Irwin, N.J.; Ripolin, A.; Perminova, A.; Domínguez-Robles, J.; Rodríguez, A.; Donnelly, R.F. Synthesis and Characterization of Lignin Hydrogels for Potential Applications as Drug Eluting Antimicrobial Coatings for Medical Materials. *ACS Sustain. Chem. Eng.* **2018**, *6*, 9037–9046. [[CrossRef](#)]
52. Velho, S.; Brum, L.; Petter, C.; dos Santos, J.H.; Šimunić, Š.; Kappa, W.H. Development of structured natural dyes for use into plastics. *Dye. Pigment.* **2017**, *136*, 248–254. [[CrossRef](#)]
53. Thema, F.T.; Moloto, M.J.; Dikio, E.D.; Nyangiwe, N.N.; Kotsedi, L.; Maaza, M.; Khenfouch, M. Synthesis and characterization of graphene thin films by chemical reduction of exfoliated and intercalated graphite oxide. *J. Chem.* **2013**, *3*, 150536. [[CrossRef](#)]
54. Marković, Z.M.; Kepić, D.P.; Matijašević, D.M.; Pavlović, V.B.; Jovanović, S.P.; Stanković, N.K.; Milivojević, D.D.; Spitalsky, Z.; Holclajtner-Antunović, I.D.; Bajuk-Bogdanović, D.V.; et al. Ambient light induced antibacterial action of curcumin/graphene nanomesh hybrids. *RSC Adv.* **2017**, *7*, 36081–36092. [[CrossRef](#)]
55. Barua, S.; Karak, N.; Chattopadhyay, P.; Islam, J.; Phukan, M.M.; Konwar, B.K. Biocompatible hyperbranched epoxy/silver-reduced graphene oxide-curcumin nanocomposite as an advanced antimicrobial material. *RSC Adv.* **2014**, *4*, 47797–47805. [[CrossRef](#)]
56. Husein, S.G.; Hamdani, S.; Rinaldi, K. Optimization of ar-Turmerone Isolation Method from Turmeric Oleoresin using Silica Gel Adsorbent. *Lett. Appl. NanoBioSci.* **2023**, *12*, 53. [[CrossRef](#)]
57. Kadam, P.V.; Yadav, K.N.; Bhingare, C.L.; Patil, M.J. Standardization and quantification of curcumin from *Curcuma longa* extract using UV visible spectroscopy and HPLC. *J. Pharmacogn. Phytochem.* **2018**, *7*, 1913–1918.
58. Pourhajibagher, M.; Parker, S.; Chiniforush, N.; Bahador, A. Photoexcitation triggering via semiconductor Graphene Quantum Dots by photochemical doping with Curcumin versus perio-pathogens mixed biofilms. *Photodiagn. Photodyn. Ther.* **2019**, *28*, 125–131. [[CrossRef](#)]
59. Malekmohammadi, S.; Hadadzadeh, H.; Farrokhpour, H.; Amirghofran, Z. Immobilization of Gold Nanoparticles on Folate-Conjugated Dendritic Mesoporous Silica-Coated Reduced Graphene Oxide Nanosheets: A New Nanoplatfor for Curcumin pH-Controlled and Targeted Delivery. *Soft Matter* **2018**, *14*, 2400–2410. [[CrossRef](#)]
60. Fu, C.; Zhao, G.; Zhang, H.; Li, S. Evaluation and characterization of reduced graphene oxide nanosheets as anode materials for lithium-ion batteries. *Int. J. Electrochem. Sci.* **2013**, *8*, 6269–6280.
61. Stobinski, L.; Lesiak, B.; Malolepszy, A.; Mazurkiewicz, M.; Mierzwa, B.; Zemek, J.; Jiricek, P.; Bieloshapka, I. Graphene oxide and reduced graphene oxide studied by the XRD, TEM and electron spectroscopy methods. *J. Electron Spectros. Relat. Phenomena* **2014**, *195*, 145–154. [[CrossRef](#)]
62. Henderson, A.E.; Fitzgerald, A.G.; Rickerby, D.S.; Starey, B.E. Electron spectroscopy and electron microscopy of a a-C:H films. *J. Electron Spectros. Relat. Phenomena* **1990**, *52*, 475–483. [[CrossRef](#)]
63. Mezzi, A.; Kaciulis, S. Surface investigation of carbon films: From diamond to graphite. *Surf. Interface Anal.* **2010**, *42*, 1082–1084. [[CrossRef](#)]
64. Jackson, S.T.; Nuzzo, R.G. Determining hybridization differences for amorphous carbon from the XPS C 1s envelope. *Appl. Surf. Sci.* **1995**, *90*, 195–203. [[CrossRef](#)]
65. Díaz, J.; Paolicelli, G.; Ferrer, S.; Comin, F. Separation of the sp³ and sp² components in the C1s photoemission spectra of amorphous carbon films. *Phys. Rev. B Condens. Matter Mater. Phys.* **1996**, *54*, 8064–8069. [[CrossRef](#)] [[PubMed](#)]
66. Haerle, R.; Riedo, E.; Pasquarello, A.; Baldereschi, A. sp²/sp³ hybridization ratio in amorphous carbon from C 1s core-level shifts: X-ray photoelectron spectroscopy and first-principles calculation. *Phys. Rev. B Condens. Matter Mater. Phys.* **2001**, *65*, 1–9. [[CrossRef](#)]
67. Fujimoto, A.; Yamada, Y.; Koinuma, M.; Sato, S. Origins of sp³C peaks in C1s X-ray Photoelectron Spectra of Carbon Materials. *Anal. Chem.* **2016**, *88*, 6110–6114. [[CrossRef](#)] [[PubMed](#)]
68. Butenko, Y.V.; Krishnamurthy, S.; Chakraborty, A.K.; Kuznetsov, V.L.; Dhanak, V.R.; Hunt, M.R.C.; Šiller, L. Photoemission study of onionlike carbons produced by annealing nanodiamonds. *Phys. Rev. B Condens. Matter Mater. Phys.* **2005**, *71*, 075420. [[CrossRef](#)]
69. Dosoky, N.S.; Setzer, W.N. Chemical composition and biological activities of essential oils of *Curcuma* species. *Nutrients* **2018**, *10*, 1196. [[CrossRef](#)]

70. Li, S. Chemical Composition and Product Quality Control of Turmeric (*Curcuma longa* L.). *Pharm. Crop.* **2011**, *5*, 28–54. [[CrossRef](#)]
71. Jantan, I.; Saputri, F.C.; Qaisar, M.N.; Buang, F. Correlation between chemical composition of *Curcuma domestica* and *Curcuma xanthorrhiza* and their antioxidant effect on human low-density lipoprotein oxidation. Evidence-based Complement. *Altern. Med.* **2012**, *2012*, 438356. [[CrossRef](#)]
72. Qu, S.; Li, M.; Xie, L.; Huang, X.; Yang, J.; Wang, N.; Yang, S. Noncovalent functionalization of graphene attaching [6,6]-phenyl-C61-butyric acid methyl ester (PCBM) and application as electron extraction layer of polymer solar cells. *ACS Nano* **2013**, *7*, 4070–4081. [[CrossRef](#)]
73. George, G.; Sisupal, S.B.; Tomy, T.; Kumaran, A.; Vadivelu, P.; Suvembala, V.; Sivaram, S.; Ragupathy, L. Facile, environmentally benign and scalable approach to produce pristine few layers graphene suitable for preparing biocompatible polymer nanocomposites. *Sci. Rep.* **2018**, *8*, 11228. [[CrossRef](#)]
74. Refat, M.S. Synthesis and characterization of ligational behavior of curcumin drug towards some transition metal ions: Chelation effect on their thermal stability and biological activity. *Spectrochim. Acta Part A Mol. Biomol. Spectrosc.* **2013**, *105*, 326–337. [[CrossRef](#)] [[PubMed](#)]
75. Mohan, P.R.K.; Sreelakshmi, G.; Muraleedharan, C.V.; Joseph, R. Water soluble complexes of curcumin with cyclodextrins: Characterization by FT-Raman spectroscopy. *Vib. Spectrosc.* **2012**, *62*, 77–84. [[CrossRef](#)]
76. Lestari, M.; Indrayanto, G. Chapter Three—Curcumin. *Profiles Drug Subst. Excip. Relat. Methodol.* **2014**, *39*, 113–204. [[CrossRef](#)] [[PubMed](#)]
77. Klapiszewski, L.; Tomaszewska, J.; Skórczewska, K.; Jesionowski, T. Preparation and characterization of eco-friendly Mg(OH)₂/lignin hybrid material and its use as a functional filler for poly(vinyl chloride). *Polymers* **2017**, *9*, 258. [[CrossRef](#)]
78. Tomaszewska, J.; Sterzyński, T.; Piszczek, K. Rigid Poly(vinyl chloride) Gelation in a Brabender Measuring Mixer. III. Transformation in the Torque Maximum. *J. Appl. Polym. Sci.* **2007**, *106*, 3158–3164. [[CrossRef](#)]
79. Lewandowski, K.; Skórczewska, K.; Piszczek, K.; Urbaniak, W. Recycled glass fibres from wind turbines as a filler for poly(Vinyl chloride). *Adv. Polym. Technol.* **2019**, *2019*, 8960503. [[CrossRef](#)]
80. Yang, G.; Li, L.; Lee, W.B.; Ng, M.C. Structure of graphene and its disorders: A review. *Sci. Technol. Adv. Mater.* **2018**, *19*, 613–648. [[CrossRef](#)] [[PubMed](#)]
81. Huang, X.; Huang, X.; Gong, Y.; Xiao, H.; McClements, D.J.; Hu, K. Enhancement of curcumin water dispersibility and antioxidant activity using core-shell protein-polysaccharide nanoparticles. *Food Res. Int.* **2016**, *87*, 1–9. [[CrossRef](#)] [[PubMed](#)]
82. Meabed, O.M.; Shamaa, A.; Abdelrahman, I.Y.; El-Sayyed, G.S.; Mohammed, S.S. The Effect of Nano-chitosan and Nano-curcumin on Radiated Parotid Glands of Albino Rats: Comparative Study. *J. Clust. Sci.* **2022**, *34*, 977–989. [[CrossRef](#)]
83. Gupta, V.; Aseh, A.; Ríos, C.N.; Aggarwal, B.B.; Mathur, A.B. Fabrication and characterization of silk fibroin-derived curcumin nanoparticles for cancer therapy. *Int. J. Nanomed.* **2009**, *4*, 115–122. [[CrossRef](#)] [[PubMed](#)]
84. Taha, S.; El-Sherbiny, I.; Enomoto, T.; Salem, A.; Nagai, E.; Askar, A.; Abady, G.; Abdel-Hamid, M. Improving the functional activities of curcumin using milk proteins as nanocarriers. *Foods* **2020**, *9*, 986. [[CrossRef](#)]
85. Gedde, U.W. *Polymer Physics*; Chapman & Hall: London, UK; Glasgow, UK; Weinheim, Germany; New York, NY, USA; Tokyo, Japan; Melbourne, Australia; Madras, India, 1995.
86. Lee, J.W.; Kim, S.W.; Cho, Y.L.; Jeong, H.Y.; Song, Y.I.; Suh, S.J. Characterization and dispersion stabilities of multi-layer graphene-coated copper prepared by electrical wire-explosion method. *J. Nanosci. Nanotechnol.* **2016**, *16*, 11286–11291. [[CrossRef](#)]
87. Ferralis, N. Probing mechanical properties of graphene with Raman spectroscopy. *J. Mater. Sci.* **2010**, *45*, 5135–5149. [[CrossRef](#)]
88. Delforce, L.; Hofmann, E.; Nardello-Rataj, V.; Aubry, J.M. TiO₂ nanoparticle dispersions in water and nonaqueous solvents studied by gravitation sedimentation analysis: Complementarity of Hansen Parameters and DLVO interpretations. *Colloids Surf. A Physicochem. Eng. Asp.* **2021**, *628*, 127333. [[CrossRef](#)]
89. Navarrete-Segado, P.; Tourbin, M.; Frances, C.; Grossin, D. Masked stereolithography of hydroxyapatite bioceramic scaffolds: From powder tailoring to evaluation of 3D printed parts properties. *Open Ceram.* **2022**, *9*, 100235. [[CrossRef](#)]
90. Yue, M.; Huang, M.; Zhu, Z.; Huang, T.; Huang, M. Effect of ultrasound assisted emulsification in the production of Pickering emulsion formulated with chitosan self-assembled particles: Stability, macro, and micro rheological properties. *LWT* **2022**, *154*, 112595. [[CrossRef](#)]
91. Santos, J.; Trujillo-Cayado, L.A.; Carrillo, F.; López-Castejón, M.L.; Alfaro-Rodríguez, M.C. Relation between Droplet Size Distributions and Physical Stability for Zein Microfluidized Emulsions. *Polymers* **2022**, *14*, 2195. [[CrossRef](#)] [[PubMed](#)]
92. Pascaud, K.; Mercé, M.; Roucher, A.; Destribats, M.; Backov, R.; Schmitt, V.; Sescousse, R.; Brouillet, F.; Sarda, S.; Ré, M.I. Pickering emulsion as template for porous bioceramics in the perspective of bone regeneration. *Colloids Surf. A Physicochem. Eng. Asp.* **2022**, *643*, 128748. [[CrossRef](#)]
93. Baibarac, M.; Stingescu, L.; Stroe, M.; Negrila, C.; Matei, E.; Cotet, L.C.; Anghel, I.; Şofran, I.E.; Baia, L. Poly(vinyl chloride) spheres coated with graphene oxide sheets: From synthesis to optical properties and their applications as flame-retardant agents. *Polymers* **2021**, *13*, 565. [[CrossRef](#)]
94. Godínez-García, A.; Vallejo-Arenas, D.D.; Salinas-Rodríguez, E.; Gómez-Torres, S.A.; Ruíz, J.C. Spraying synthesis and ion permeation in polyvinyl chloride/graphene oxide membranes. *Appl. Surf. Sci.* **2019**, *489*, 962–975. [[CrossRef](#)]
95. Dhakal, S.; Chao, K.; Schmidt, W.; Qin, J.; Kim, M.; Chan, D. Evaluation of Turmeric Powder Adulterated with Metanil Yellow Using FT-Raman and FT-IR Spectroscopy. *Foods* **2016**, *5*, 36. [[CrossRef](#)]

96. Kugler, S.; Spychaj, T. Nanostruktury węglowe i błony lub powłoki polimerowe z ich udziałem: Cz. II. Błony i powłoki polimerowe z udziałem nanostruktur węglowych. *Polimery/Polymers* **2013**, *58*, 177–180. [[CrossRef](#)]
97. Deshmukh, K.; Khatake, S.M.; Joshi, G.M. Surface properties of graphene oxide reinforced polyvinyl chloride nanocomposites. *J. Polym. Res.* **2013**, *20*, 286. [[CrossRef](#)]
98. Xiao, Y.; Xin, B.; Chen, Z.; Lin, L.; Liu, Y.; Hu, Z. Enhanced thermal properties of graphene-based poly (vinyl chloride) composites. *J. Ind. Text.* **2019**, *48*, 1348–1363. [[CrossRef](#)]
99. Wang, H.; Xie, G.; Zhu, Z.; Ying, Z.; Zeng, Y. Enhanced tribological performance of the multi-layer graphene filled poly(vinyl chloride) composites. *Compos. Part A Appl. Sci. Manuf.* **2014**, *67*, 268–273. [[CrossRef](#)]
100. Vadukumpully, S.; Paul, J.; Mahanta, N.; Valiyaveetil, S. Flexible conductive graphene/poly(vinyl chloride) composite thin films with high mechanical strength and thermal stability. *Carbon* **2011**, *49*, 198–205. [[CrossRef](#)]
101. Wang, H.; Xie, G.; Fang, M.; Ying, Z.; Tong, Y.; Zeng, Y. Electrical and mechanical properties of antistatic PVC films containing multi-layer graphene. *Compos. Part B Eng.* **2015**, *79*, 444–450. [[CrossRef](#)]
102. Brostow, W.; Hagg Lobland, H.E. *Materials: Introduction and Applications*; John Wiley & Sons: Hoboken, NJ, USA, 2017; ISBN 978-0-470-52379-7.
103. Broza, G.; Piszczek, K.; Schulte, K.; Sterzynski, T. Nanocomposites of poly(vinyl chloride) with carbon nanotubes (CNT). *Compos. Sci. Technol.* **2007**, *67*, 890–894. [[CrossRef](#)]
104. Sun, X.; Huang, C.; Wang, L.; Liang, L.; Cheng, Y.; Fei, W.; Li, Y. Recent Progress in Graphene/Polymer Nanocomposites. *Adv. Mater.* **2021**, *33*, 2001105. [[CrossRef](#)] [[PubMed](#)]
105. Govindaraj, P.; Sokolova, A.; Salim, N.; Juodkazis, S.; Fuss, F.K.; Fox, B.; Hameed, N. Distribution states of graphene in polymer nanocomposites: A review. *Compos. Part B Eng.* **2021**, *226*, 109353. [[CrossRef](#)]
106. Reis, T.M.C.; Castro, V.G.; Amurin, L.G.; Silva, G.G. Graphene oxide dispersion in epoxy resin prepared by direct phase transfer from ethanol: Rheology and aging. *Compos. Part C Open Access* **2023**, *10*, 100340. [[CrossRef](#)]
107. Sharma, A.; Sharma, S. Graphene-based polymer coatings for preventing marine corrosion: A review. *J. Coatings Technol. Res.* **2023**, *20*, 413–432. [[CrossRef](#)]

Disclaimer/Publisher's Note: The statements, opinions and data contained in all publications are solely those of the individual author(s) and contributor(s) and not of MDPI and/or the editor(s). MDPI and/or the editor(s) disclaim responsibility for any injury to people or property resulting from any ideas, methods, instructions or products referred to in the content.

12.2. OŚWIADCZENIE AUTORA ROZPRAWY DOKTORSKIEJ

Oświadczenie Autora rozprawy doktorskiej

Mgr inż. Sławomir Józef Wilczewski

(tytuł zawodowy, imiona i nazwisko autora rozprawy doktorskiej)

Politechnika Bydgoska im. Jana i Jędrzeja Śniadeckich

(miejsce pracy/afiliacja)

OŚWIADCZENIE

Oświadczam, iż mój wkład autorski w niżej wymienionych artykułach naukowych stanowiących cykl publikacji rozprawy doktorskiej był następujący*:

1. **Wilczewski Sławomir**, Skórczewska Katarzyna, Tomaszewska Jolanta, Lewandowski Krzysztof, *Structure and properties of poly(vinyl chloride)/graphene nanocomposites*, Polymer Testing (Elsevier), 2020, 81, 106282, DOI: 10.1016/j.polymeresting.2019.106282. pkt. MNISW 100, Impact Factor 4,282

- a) Opracowanie i rozwój koncepcji badawczej we współpracy z promotorami
- b) Planowanie metodologii prac badawczych
- c) Przeprowadzenie prac badawczych
- d) Weryfikacja oraz zapewnienie powtarzalności eksperymentów i wyników badawczych
- e) Stosowanie technik statystycznych, matematycznych, obliczeniowych i innych technik formalnych w celu analizy danych eksperymentalnych
- f) Kierowanie procesem badawczym, w szczególności przeprowadzaniem eksperymentów i doświadczeń, wykonaniem badań
- g) Zarządzanie danymi badawczymi: gromadzenie i przetwarzanie danych badawczych, tworzenie metadanych, wstępne opracowywanie danych oraz ich przechowywanie w celu analizy oraz późniejszego porównania z innymi wynikami
- h) Współudział w analizie wyników prac badawczych
- i) Współredakcja manuskryptu
- j) Współredakcja odpowiedzi na recenzje
- k) Wstępne opracowanie oraz korekta prezentacji danych badawczych
- l) Edycja końcowa manuskryptu

* W przypadku prac dwu- lub wieloautorских wymagane są oświadczenia kandydata do stopnia doktora oraz współautorów, wskazujące na ich merytoryczny wkład w powstanie każdej pracy (np. twórca hipotezy badawczej, pomysłodawca badań, wykonanie specyficznych badań – np. przeprowadzenie konkretnych doświadczeń, opracowanie i zebranie ankiet itp., wykonanie analizy wyników, przygotowanie manuskryptu artykułu i inne). Określenie wkładu danego autora, w tym kandydata do stopnia doktora, powinno być na tyle precyzyjne, aby umożliwić dokładną ocenę jego udziału i roli w powstaniu każdej pracy.

2. **Wilczewski Sławomir**, Skórczewska Katarzyna, Tomaszewska Jolanta, Lewandowski Krzysztof, Szulc Joanna, Runka Tomasz, Manufacturing homogenous PVC/graphene nanocomposites using a novel dispersion agent, *Polymer Testing (Elsevier)*, 2020, 91, 106868, DOI: 10.1016/j.polymertesting.2020.106868. pkt. MNiSW 100, Impact Factor 4,282

- a) Opracowanie i rozwój koncepcji badawczej we współpracy z promotorami
- b) Planowanie metodologii prac badawczych
- c) Przeprowadzenie prac badawczych
- d) Weryfikacja oraz zapewnienie powtarzalności eksperymentów i wyników badawczych
- e) Stosowanie technik statystycznych, matematycznych, obliczeniowych i innych technik formalnych w celu analizy danych eksperymentalnych
- f) Kierowanie procesem badawczym, w szczególności przeprowadzaniem eksperymentów i doświadczeń, wykonaniem badań
- g) Zarządzanie danymi badawczymi: gromadzenie i przetwarzanie danych badawczych, tworzenie metadanych, wstępne opracowywanie danych oraz ich przechowywanie w celu analizy oraz późniejszego porównania z innymi wynikami
- h) Współudział w analizie wyników prac badawczych
- i) Współredakcja manuskryptu
- j) Współredakcja odpowiedzi na recenzje
- k) Wstępne opracowanie oraz korekta prezentacji danych badawczych
- l) Edycja końcowa manuskryptu

3. **Wilczewski Sławomir**, Skórczewska Katarzyna, Tomaszewska Jolanta, Lewandowski Krzysztof, Studziński Waldemar, Osiał Magdalena, Jencyk Piotr, Grzywacz Hubert, Domańska Agata, Curcuma longa L. rhizome extract as a poly(vinyl chloride)/graphene nanocomposite green modifier, *Molecules (MDPI)*, 2022, 27, 8081, DOI: 10.3390/molecules27228081. pkt. MNiSW 140, Impact Factor 4,600

- a) Opracowanie i rozwój koncepcji badawczej we współpracy z promotorami
- b) Planowanie metodologii prac badawczych
- c) Przeprowadzenie prac badawczych
- d) Weryfikacja oraz zapewnienie powtarzalności eksperymentów i wyników badawczych
- e) Stosowanie technik statystycznych, matematycznych, obliczeniowych i innych technik formalnych w celu analizy danych eksperymentalnych
- f) Kierowanie procesem badawczym, w szczególności przeprowadzaniem eksperymentów i doświadczeń, wykonaniem badań
- g) Zarządzanie danymi badawczymi: gromadzenie i przetwarzanie danych badawczych, tworzenie metadanych, wstępne opracowywanie danych oraz ich przechowywanie w celu analizy oraz późniejszego porównania z innymi wynikami
- h) Współudział w analizie wyników prac badawczych
- i) Współredakcja manuskryptu
- j) Współredakcja odpowiedzi na recenzje
- k) Wstępne opracowanie oraz korekta prezentacji danych badawczych
- l) Edycja końcowa manuskryptu

4. **Wilczewski Sławomir, Skórczewska Katarzyna, Tomaszewska Jolanta, Osiał Magdalena, Dąbrowska Agnieszka, Nikoforow Kostiantyn, Jenczyk Piotr, Grzywacz Hubert.** Graphene modification by curcuminoids as an effective method to improve the dispersion and stability of PVC/graphene nanocomposites, *Molecules* (MDPI), 2023, 28, 3383, DOI: 10.3390/molecules28083383 Pkt. MNiSW 140, Impact Factor 4,600

- a) Opracowanie i rozwój koncepcji badawczej we współpracy z promotorami
- b) Planowanie metodologii prac badawczych
- c) Przeprowadzenie prac badawczych
- d) Weryfikacja oraz zapewnienie powtarzalności eksperymentów i wyników badawczych
- e) Stosowanie technik statystycznych, matematycznych, obliczeniowych i innych technik formalnych w celu analizy danych eksperymentalnych
- f) Kierowanie procesem badawczym, w szczególności przeprowadzaniem eksperymentów i doświadczeń, wykonaniem badań
- g) Zarządzanie danymi badawczymi: gromadzenie i przetwarzanie danych badawczych, tworzenie metadanych, wstępne opracowywanie danych oraz ich przechowywanie w celu analizy oraz późniejszego porównania z innymi wynikami
- h) Współudział w analizie wyników prac badawczych
- i) Współredakcja manuskryptu
- j) Współredakcja odpowiedzi na recenzje
- k) Wstępne opracowanie oraz korekta prezentacji danych badawczych
- l) Edycja końcowa manuskryptu

Bydgoszcz 25.08.2023
miejsowość, data

.....*Sławomir Wilczewski*.....
Podpis Autora rozprawy doktorskiej

.....*Tomasz Osiał*.....
Podpis promotora

12.3. OŚWIADCZENIA WSPÓLAUTORÓW ARTYKUŁÓW NAUKOWYCH

Oświadczenie Współautora

Dr hab. inż. Jolanta Tomaszewska, prof. PBS
(tytuł zawodowy, imiona i nazwisko współautora)

Pollitechnika Bydgoska im. Jana i Jędrzeja Śniadeckich
(miejsce pracy/afiliacja)

OŚWIADCZENIE

Oświadczam, iż mój wkład autorski w niżej wymienionym artykule naukowym był następujący*:

1. Wilczewski Sławomir, Skórczewska Katarzyna, **Tomaszewska Jolanta**, Lewandowski Krzysztof, *Structure and properties of poly(vinyl chloride)/graphene nanocomposites*, *Polymer Testing* (Elsevier), 2020, 81, 106282,
DOI: 10.1016/j.polymertesting.2019.106282. pkt. MNiSW 100, Impact Factor 4,282
 - a) Współudział w opracowaniu koncepcji i planowaniu badań
 - b) Opieka i wsparcie merytoryczne w trakcie realizacji prac badawczych oraz analizy wyników
 - c) Współudział w przygotowaniu publikacji oraz odpowiedzi na recenzje
2. Wilczewski Sławomir, Skórczewska Katarzyna, **Tomaszewska Jolanta**, Lewandowski Krzysztof, Szulc Joanna, Runka Tomasz, *Manufacturing homogenous PVC/graphene nanocomposites using a novel dispersion agent*, *Polymer Testing* (Elsevier), 2020, 91, 106868,
DOI: 10.1016/j.polymertesting.2020.106868. pkt. MNiSW 100, Impact Factor 4,282
 - a) Współudział w opracowaniu koncepcji i planowaniu badań
 - b) Opieka i wsparcie merytoryczne w trakcie realizacji prac badawczych oraz analizie wyników
 - c) Współudział w przygotowaniu publikacji oraz odpowiedzi na recenzje
3. Wilczewski Sławomir, Skórczewska Katarzyna, **Tomaszewska Jolanta**, Lewandowski Krzysztof, Studziński Waldemar, Osiał Magdalena, Jencyk Piotr, Grzywacz Hubert, Domańska Agata, *Curcuma longa L. rhizome extract as a poly(vinyl chloride)/graphene nanocomposite green modifier*, *Molecules* (MDPI), 2022, 27, 8081,
DOI: 10.3390/molecules27228081. pkt. MNiSW 140, Impact Factor 4,600
 - a) Współudział w opracowaniu koncepcji i planowaniu badań
 - b) Opieka i wsparcie merytoryczne w trakcie realizacji prac badawczych oraz analizy wyników
 - c) Współudział w przygotowaniu publikacji oraz odpowiedzi na recenzje

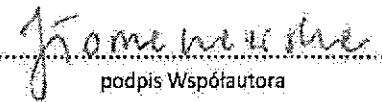
* W przypadku prac dwu- lub wieloautorских wymagane są oświadczenia kandydata do stopnia doktora oraz współautorów, wskazujące na ich merytoryczny wkład w powstanie każdej pracy (np. twórca hipotezy badawczej, pomysłodawca badań, wykonanie specyficznych badań – np. przeprowadzenie konkretnych doświadczeń, opracowanie i zebranie ankiet itp., wykonanie analizy wyników, przygotowanie manuskryptu artykułu i inne). Określenie wkładu danego autora, w tym kandydata do stopnia doktora, powinno być na tyle precyzyjne, aby umożliwić dokładną ocenę jego udziału i roli w powstaniu każdej pracy.

4. Wilczewski Sławomir, Skórczewska Katarzyna, Tomaszewska Jolanta, Osiał Magdalena, Dąbrowska Agnieszka, Nikoforow Kostiantyn, Jencyk Piotr, Grzywacz Hubert., Graphene modification by curcuminoids as an effective method to improve the dispersion and stability of PVC/graphene nanocomposites, *Molecules* (MDPI), 2023, 28, 3383, DOI: 10.3390/molecules28083383 Pkt. MNISW 140, Impact Factor 4,600

- a) Współdział w opracowaniu koncepcji i planowaniu badań
- b) Opieka i wsparcie merytoryczne w trakcie realizacji prac badawczych oraz analizy wyników
- c) Współdział w przygotowaniu publikacji oraz odpowiedzi na recenzje

Jednocześnie wyrażam zgodę na przedłożenie wyżej wymienionych prac przez mgr inż. Sławomira Wilczewskiego jako część rozprawy doktorskiej opartej na zbiorze opublikowanych i powiązanych tematycznie artykułów naukowych.

Bydgoszcz 25.08.2023.
miejscowość, data


.....
podpis Współautora

Oświadczenie Współautora

Dr. inż. Katarzyna Skórczewska

(tytuł zawodowy, imiona i nazwisko współautora)

Politechnika Bydgoska im. Jana i Jędrzeja Śniadeckich

miejsce pracy/afiliacja)

OŚWIADCZENIE

Oświadczam, iż mój wkład autorski w niżej wymienionym artykule naukowym był następujący*:

1. Wilczewski Sławomir, **Skórczewska Katarzyna**, Tomaszewska Jolanta, Lewandowski Krzysztof, *Structure and properties of poly(vinyl chloride)/graphene nanocomposites*, *Polymer Testing* (Elsevier), 2020, 81, 106282,
DOI: 10.1016/j.polymertesting.2019.106282. pkt. MNiSW 100, Impact Factor 4,282
 - a) Współudział w opracowaniu koncepcji i planowaniu badań
 - b) Przeprowadzenie analizy termicznej metodą termogravimetryczną
 - c) Opieka i wsparcie merytoryczne w trakcie realizacji prac badawczych oraz analizy wyników
 - d) Współudział w przygotowaniu publikacji oraz odpowiedzi na recenzje
2. Wilczewski Sławomir, **Skórczewska Katarzyna**, Tomaszewska Jolanta, Lewandowski Krzysztof, Szulc Joanna, Runka Tomasz, *Manufacturing homogenous PVC/graphene nanocomposites using a novel dispersion agent*, *Polymer Testing* (Elsevier), 2020, 91, 106868,
DOI: 10.1016/j.polymertesting.2020.106868. pkt. MNiSW 100, Impact Factor 4,282
 - a) Współudział w opracowaniu koncepcji i planowaniu badań
 - b) Opieka i wsparcie merytoryczne w trakcie realizacji prac badawczych oraz analizie wyników
 - c) Współudział w przygotowaniu publikacji oraz odpowiedzi na recenzje
3. Wilczewski Sławomir, **Skórczewska Katarzyna**, Tomaszewska Jolanta, Lewandowski Krzysztof, Studziński Waldemar, Osiał Magdalena, Jencyk Piotr, Grzywacz Hubert, Domańska Agata, *Curcuma longa L. rhizome extract as a poly(vinyl chloride)/graphene nanocomposite green modifier*, *Molecules* (MDPI), 2022, 27, 8081,
DOI: 10.3390/molecules27228081. pkt. MNiSW 140, Impact Factor 4,600
 - a) Współudział w opracowaniu koncepcji i planowaniu badań
 - b) Opieka i wsparcie merytoryczne w trakcie realizacji prac badawczych oraz analizy wyników
 - c) Współudział w przygotowaniu publikacji oraz odpowiedzi na recenzje

* W przypadku prac dwu- lub wieloautorskich wymagane są oświadczenia kandydata do stopnia doktora oraz współautorów, wskazujące na ich merytoryczny wkład w powstanie każdej pracy (np. twórca hipotezy badawczej, pomysłodawca badań, wykonanie specyficznych badań – np. przeprowadzenie konkretnych doświadczeń, opracowanie i zebranie ankiet itp., wykonanie analizy wyników, przygotowanie manuskryptu artykułu i inne). Określenie wkładu danego autora, w tym kandydata do stopnia doktora, powinno być na tyle precyzyjne, aby umożliwić dokładną ocenę jego udziału i roli w powstaniu każdej pracy.

4. Wilczewski Sławomir, Skórczewska Katarzyna, Tomaszewska Jolanta, Osiał Magdalena, Dąbrowska Agnieszka, Nikoforow Kostiantyn, Jencyk Piotr, Grzywacz Hubert., Graphene modification by curcuminoids as an effective method to improve the dispersion and stability of PVC/graphene nanocomposites, *Molecules* (MDPI), 2023, 28, 3383, DOI: 10.3390/molecules28083383 Pkt. MNiSW 140, Impact Factor 4,600

- a) Współdział w opracowaniu koncepcji i planowaniu badań
- b) Przeprowadzenie analizy termicznej metodą termogravimetryczną
- c) Opieka i wsparcie merytoryczne w trakcie realizacji prac badawczych oraz analizy wyników
- d) Współdział w przygotowaniu publikacji oraz odpowiedzi na recenzje

Jednocześnie wyrażam zgodę na przedłożenie wyżej wymienionych prac przez **mgr inż. Sławomira Wilczewskiego** jako część rozprawy doktorskiej opartej na zbiorze opublikowanych i powiązanych tematycznie artykułów naukowych.

Bydgoszcz 11.09.2023.
miejsowość, data


.....
podpis Współautora

Oświadczenie Współautora

dr inż. Krzysztof Lewandowski

(tytuł zawodowy, imiona i nazwisko współautora)

Politechnika Bydgoska im. Jana i Jędrzeja Śniadeckich

(miejsce pracy/afiliacja)

OŚWIADCZENIE

Oświadczam, iż mój wkład autorski w niżej wymienionych artykułach naukowych był następujący*:

1. Wilczewski Sławomir, Skórczewska Katarzyna, Tomaszewska Jolanta, **Lewandowski Krzysztof.**, *Structure and properties of poly(vinyl chloride)/graphene nanocomposites*, Polymer Testing (Elsevier), 2020, 81, 106282, DOI: 10.1016/j.polymertesting.2019.106282. pkt. MNiSW 100, Impact Factor 4,282

Wykonane zadania w ramach artykułu:

- a) Pomoc w analizie statystycznej oraz aproksymacji wyników pęcznienia w acetonie
- b) Współudział w redakcji artykułu w ww. zakresie prac

2. Wilczewski Sławomir, Skórczewska Katarzyna, Tomaszewska Jolanta, **Lewandowski Krzysztof**, Szulc Joanna, Runka Tomasz, *Manufacturing homogenous PVC/graphene nanocomposites using a novel dispersion agent*, Polymer Testing (Elsevier), 2020, 91, 106868, DOI: 10.1016/j.polymertesting.2020.106868. pkt. MNiSW 100, Impact Factor 4,282

Wykonane zadania w ramach artykułu:

- a) Konsultacja przeprowadzonych analiz oraz obliczeń matematycznych
- b) Współudział w redakcji artykułu

* W przypadku prac dwu- lub wieloautorskich wymagane są oświadczenia kandydata do stopnia doktora oraz współautorów, wskazujące na ich merytoryczny wkład w powstanie każdej pracy (np. twórca hipotezy badawczej, pomysłodawca badań, wykonanie specyficznych badań – np. przeprowadzenie konkretnych doświadczeń, opracowanie i zebranie ankiet itp., wykonanie analizy wyników, przygotowanie manuskryptu artykułu i inne). Określenie wkładu danego autora, w tym kandydata do stopnia doktora, powinno być na tyle precyzyjne, aby umożliwić dokładną ocenę jego udziału i roli w powstaniu każdej pracy.

3. Wilczewski Sławomir, Skórczewska Katarzyna, Tomaszewska Jolanta, **Lewandowski Krzysztof**, Studziński Waldemar, Osial Magdalena, Jencyk Piotr, Grzywacz Hubert, Domańska Agata., *Curcuma longa* L. rhizome extract as a poly(vinyl chloride)/graphene nanocomposite green modifier, *Molecules* (MDPI), 2022, 27, 8081, DOI: 10.3390/molecules27228081. pkt. MNiSW 140, Impact Factor 4,600

Wykonane zadania w ramach artykułu:

- a) Konsultacja wyników analizy statystycznej oraz aproksymacji wyników pęcznienia w acetonie
- b) Konsultacja analizy wyników wytrzymałości na rozciąganie

Jednocześnie wyrażam zgodę na przedłożenie wyżej wymienionych prac przez **mgr inż. Sławomira Wilczewskiego** jako część rozprawy doktorskiej opartej na zbiorze opublikowanych i powiązanych tematycznie artykułów naukowych.

B41060812 05.09.2023r.

.....
miejsowość, data


.....
podpis Współautora

Oświadczenie Współautora

dr inż. Joanna Szulc

(tytuł zawodowy, imiona i nazwisko współautora)

Politechnika Bydgoska im. Jana i Jędrzeja Śniadeckich

(miejsce pracy/afiliacja)

OŚWIADCZENIE

Oświadczam, iż mój wkład autorski w niżej wymienionym artykule naukowym był następujący*:

1. Wilczewski Sławomir, Skórczewska Katarzyna, Tomaszewska Jolanta, Lewandowski Krzysztof, **Szulc Joanna**, Runka Tomasz, Manufacturing homogenous PVC/graphene nanocomposites using a novel dispersion agent, Polymer Testing (Elsevier), 2020, 91, 106868, DOI: 10.1016/j.polymeresting.2020.106868. pkt. MNiSW 100, Impact Factor 4,282

Wykonane zadania w ramach artykułu:

- a) Przeprowadzenie ekstrakcji z kłącza *Curcuma longa L.*
- b) Pomoc w interpretacji wyników analizy składu otrzymanego ekstraktu na etapie redakcji artykułu i odpowiedzi na recenzje

Jednocześnie wyrażam zgodę na przedłożenie wyżej wymienionej pracy przez **mgr inż. Sławomira Wilczewskiego** jako część rozprawy doktorskiej opartej na zbiorze opublikowanych i powiązanych tematycznie artykułów naukowych.

Bydgoszcz, 04.09.2023
.....
miejsce, data

Joanna Szulc
.....
podpis Współautora

* W przypadku prac dwu- lub wieloautorskich wymagane są oświadczenia kandydata do stopnia doktora oraz współautorów, wskazujące na ich merytoryczny wkład w powstanie każdej pracy (np. twórca hipotezy badawczej, pomysłodawca badań, wykonanie specyficznych badań – np. przeprowadzenie konkretnych doświadczeń, opracowanie i zehrzenie ankiet itp., wykonanie analizy wyników, przygotowanie manuskryptu artykułu i inne). Określenie wkładu danego autora, w tym kandydata do stopnia doktora, powinno być na tyle precyzyjne, aby umożliwić dokładną ocenę jego udziału i roli w powstaniu każdej pracy.

Oświadczenie Współautora

dr hab. Tomasz Runka

(tytuł zawodowy, imiona i nazwisko współautora)

Instytut Badań Materiałowych i Inżynierii Kwantowej

Politechnika Poznańska

(miejsce pracy/afiliacja)

OŚWIADCZENIE

Oświadczam, iż mój wkład autorski w niżej wymienionym artykule naukowym był następujący*:

1. Wilczewski Sławomir, Skórczewska Katarzyna, Tomaszewska Jolanta, Lewandowski Krzysztof, Szulc Joanna, **Runka Tomasz**, Manufacturing homogenous PVC/graphene nanocomposites using a novel dispersion agent, Polymer Testing (Elsevier), 2020, 91, 106868, DOI: 10.1016/j.polymertesting.2020.106868. pkt. MNiSW 100, Impact Factor 4,282

Wykonane zadania w ramach artykułu:

- a) Przeprowadzenie analizy materiałów kompozytowych metodą spektroskopii Ramana
- b) Pomoc w interpretacji otrzymanych wyników na etapie redakcji artykułu naukowego

Jednocześnie wyrażam zgodę na przedłożenie wyżej wymienionej pracy przez **mgr inż. Sławomira Wilczewskiego** jako część rozprawy doktorskiej opartej na zbiorze opublikowanych i powiązanych tematycznie artykułów naukowych.

Poznań, 07.09.2023

.....
miejsce, data

Tomasz Runka

.....
podpis Współautora

* W przypadku prac dwu- lub wieloautorskich wymagane są oświadczenia kandydata do stopnia doktora oraz współautorów, wskazujące na ich merytoryczny wkład w powstanie każdej pracy (np. twórca hipotezy badawczej, pomysłodawca badań, wykonanie specyficznych badań – np. przeprowadzenie konkretnych doświadczeń, opracowanie i zebranie ankiet itp., wykonanie analizy wyników, przygotowanie manuskryptu artykułu i inne). Określenie wkładu danego autora, w tym kandydata do stopnia doktora, powinno być na tyle precyzyjne, aby umożliwić dokładną ocenę jego udziału i roli w powstaniu każdej pracy.

Oświadczenie Współautora

dr Magdalena Osiał

(tytuł zawodowy, imiona i nazwisko współautora)

Zakład Teorii Ośrodków Ciągłych i Nanostruktur

Instytut Podstawowych Problemów Techniki

Polskiej Akademii Nauk

(miejsce pracy/afiliacja)

OŚWIADCZENIE

Oświadczam, iż mój wkład autorski w niżej wymienionych artykułach naukowych był następujący*:

1. Wilczewski Sławomir, Skórczewska Katarzyna, Tomaszewska Jolanta, Lewandowski Krzysztof, Studziński Waldemar, **Osiał Magdalena**, Jencyk Piotr, Grzywacz Hubert, Domańska Agata., Curcuma longa L. rhizome extract as a poly(vinyl chloride)/graphene nanocomposite green modifier, *Molecules* (MDPI), 2022, 27, 8081, DOI: 10.3390/molecules27228081. pkt. MNiSW 140, Impact Factor 4,600

Wykonane zadania w ramach artykułu:

- a) Konsultacja wyników badań otrzymanych metodą chromatografii cieczowej oraz gazowej
- b) Współredagowaniu artykułu oraz odpowiedzi na recenzję

2. Wilczewski Sławomir, Skórczewska Katarzyna, Tomaszewska Jolanta, **Osiał Magdalena**, Dąbrowska Agnieszka, Nikoforow Kostiantyn, Jencyk Piotr, Grzywacz Hubert., Graphene modification by curcuminoids as an effective method to improve the dispersion and stability of PVC/graphene nanocomposites, *Molecules* (MDPI), 2023, 28, 3383, DOI: 10.3390/molecules28083383 Pkt. MNiSW 140, Impact Factor 4,600

Wykonane zadania w ramach artykułu:

- c) Konsultacja wyników badań (UV-vis, XPS)
- d) Współredagowaniu artykułu oraz odpowiedzi na recenzję

Jednocześnie wyrażam zgodę na przedłożenie wyżej wymienionej pracy przez **mgr inż. Sławomira Wilczewskiego** jako część rozprawy doktorskiej opartej na zbiorze opublikowanych i powiązanych tematycznie artykułów naukowych.

Warszawa 30/08/2023.
.....
miejsowość, data

.....
podpis Współautora

* W przypadku prac dwu- lub wieloautorskich wymagane są oświadczenia kandydata do stopnia doktora oraz współautorów, wskazujące na ich merytoryczny wkład w powstanie każdej pracy (np. twórca hipotezy badawczej, pomysłodawca badań, wykonanie specyficznych badań – np. przeprowadzenie konkretnych doświadczeń, opracowanie i zebranie ankiet itp., wykonanie analizy wyników, przygotowanie manuskryptu artykułu i inne). Określenie wkładu danego autora, w tym kandydata do stopnia doktora, powinno być na tyle precyzyjne, aby umożliwić dokładną ocenę jego udziału i roli w powstaniu każdej pracy.

Oświadczenie Współautora

dr inż. Waldemar Studziński

(tytuł zawodowy, imiona i nazwisko współautora)

Politechnika Bydgoska im. Jana i Jędrzeja Śniadeckich

(miejsce pracy/afiliacja)

OŚWIADCZENIE

Oświadczam, iż mój wkład autorski w niżej wymienionym artykule naukowym był następujący*:

1. Wilczewski Sławomir, Skórczewska Katarzyna, Tomaszewska Jolanta, Lewandowski Krzysztof, **Studziński Waldemar**, Osiał Magdalena, Jencyk Piotr, Grzywacz Hubert, Domańska Agata., Curcuma longa L. rhizome extract as a poly(vinyl chloride)/graphene nanocomposite green modifier, *Molecules* (MDPI), 2022, 27, 8081, DOI: 10.3390/molecules27228081. pkt. MNiSW 140, Impact Factor 4,600

Wykonane zadania w ramach artykułu:

- a) Przeprowadzenie analizy chromatograficznej ekstraktu z *Curcuma longa* L.

Jednocześnie wyrażam zgodę na przedłożenie wyżej wymienionej pracy przez **mgr inż. Sławomira Wilczewskiego** jako część rozprawy doktorskiej opartej na zbiorze opublikowanych i powiązanych tematycznie artykułów naukowych.

4.09.23r.

miejsowość, data

Waldemar Studziński

podpis Współautora

* W przypadku prac dwu- lub wieloautorskich wymagane są oświadczenia kandydata do stopnia doktora oraz współautorów, wskazujące na ich merytoryczny wkład w powstanie każdej pracy (np. twórca hipotezy badawczej, pomysłodawca badań, wykonanie specyficznych badań – np. przeprowadzenie konkretnych doświadczeń, opracowanie i zebranie ankiet itp., wykonanie analizy wyników, przygotowanie manuskryptu artykułu i inne). Określenie wkładu danego autora, w tym kandydata do stopnia doktora, powinno być na tyle precyzyjne, aby umożliwić dokładną ocenę jego udziału i roli w powstaniu każdej pracy.

Oświadczenie Współautora

mgr inż. Piotr Jencyk

(tytuł zawodowy, imiona i nazwisko współautora)

Instytut Podstawowych Problemów Techniki

Polskiej Akademii Nauk

(miejsce pracy/afiliacja)

OŚWIADCZENIE

Oświadczam, iż mój wkład autorski w niżej wymienionych artykułach naukowych był następujący*:

1. Wilczewski Sławomir, Skórczewska Katarzyna, Tomaszewska Jolanta, Lewandowski Krzysztof, Studziński Waldemar, Osial Magdalena, **Jencyk Piotr**, Grzywacz Hubert, Domańska Agata., Curcuma longa L. rhizome extract as a poly(vinyl chloride)/graphene nanocomposite green modifier, *Molecules* (MDPI), 2022, 27, 8081, DOI: 10.3390/molecules27228081. pkt. MNiSW 140, Impact Factor 4,600

Wykonane zadania w ramach artykułu:

- a) Przeprowadzenie obserwacji materiałów kompozytowych metodami SEM, AFM
- b) Konsultacja wyników wyżej wymienionych badań na etapie redagowania artykułu naukowego

2. Wilczewski Sławomir, Skórczewska Katarzyna, Tomaszewska Jolanta, Osial Magdalena, Dąbrowska Agnieszka, Nikoforow Kostiantyn, **Jencyk Piotr**, Grzywacz Hubert., Graphene modification by curcuminoids as an effective method to improve the dispersion and stability of PVC/graphene nanocomposites, *Molecules* (MDPI), 2023, 28, 3383, DOI: 10.3390/molecules28083383 Pkt. MNiSW 140, Impact Factor 4,600

Wykonane zadania w ramach artykułu:

- a) Przeprowadzenie obserwacji materiałów kompozytowych metodami SEM, AFM
- b) Konsultacja wyników wyżej wymienionych badań na etapie redagowania artykułu naukowego

Jednocześnie wyrażam zgodę na przedłożenie wyżej wymienionej pracy przez **mgr inż. Sławomira Wilczewskiego** jako część rozprawy doktorskiej opartej na zbiorze opublikowanych i powiązanych tematycznie artykułów naukowych.

01.08.2022 Warszawa

.....
miejsowość, data

Piotr Jencyk
.....
podpis Współautora

* W przypadku prac dwu- lub wieloautorskich wymagane są oświadczenia kandydata do stopnia doktora oraz współautorów, wskazujące na ich merytoryczny wkład w powstanie każdej pracy (np. twórca hipotezy badawczej, pomysłodawca badań, wykonanie specyficznych badań – np. przeprowadzenie konkretnych doświadczeń, opracowanie i zebranie ankiet itp., wykonanie analizy wyników, przygotowanie manuskryptu artykułu i inne). Określenie wkładu danego autora, w tym kandydata do stopnia doktora, powinno być na tyle precyzyjne, aby umożliwić dokładną ocenę jego udziału i roli w powstaniu każdej pracy.

Oświadczenie Współautora

mgr inż. Hubert Grzywacz

(tytuł zawodowy, imiona i nazwisko współautora)

Instytut Podstawowych Problemów Techniki

Polskiej Akademii Nauk

miejsce pracy/afiliacja)

OŚWIADCZENIE

Oświadczam, iż mój wkład autorski w niżej wymienionych artykułach naukowych był następujący*:

1. Wilczewski Sławomir, Skórczewska Katarzyna, Tomaszewska Jolanta, Lewandowski Krzysztof, Studziński Waldemar, Osial Magdalena, Jencyk Piotr, **Grzywacz Hubert**, Domańska Agata., Curcuma longa L. rhizome extract as a poly(vinyl chloride)/graphene nanocomposite green modifier, *Molecules* (MDPI), 2022, 27, 8081, DOI: 10.3390/molecules27228081. pkt. MNiSW 140, Impact Factor 4,600

Wykonane zadania w ramach artykułu:

- a) Przeprowadzenie badań wytrzymałości na rozciąganie
- b) Udział w redagowaniu artykułu naukowego

2. Wilczewski Sławomir, Skórczewska Katarzyna, Tomaszewska Jolanta, Osial Magdalena, Dąbrowska Agnieszka, Nikoforow Kostiantyn, Jencyk Piotr, **Grzywacz Hubert.**, Graphene modification by curcuminoids as an effective method to improve the dispersion and stability of PVC/graphene nanocomposites, *Molecules* (MDPI), 2023, 28, 3383, DOI: 10.3390/molecules28083383 Pkt. MNiSW 140, Impact Factor 4,600

Wykonane zadania w ramach artykułu:

- a) Przeprowadzenie badań wytrzymałości na rozciąganie
- b) Udział w redagowaniu artykułu naukowego

Jednocześnie wyrażam zgodę na przedłożenie wyżej wymienionej pracy przez **mgr inż. Sławomira Wilczewskiego** jako część rozprawy doktorskiej opartej na zbiorze opublikowanych i powiązanych tematycznie artykułów naukowych.

Warszawa, 07.08.2023

miejsce, data

Hubert Grzywacz

podpis Współautora

* W przypadku prac dwu- lub wieloautorskich wymagane są oświadczenia kandydata do stopnia doktora oraz współautorów, wskazujące na ich merytoryczny wkład w powstanie każdej pracy (np. twórca hipotezy badawczej, pomysłodawca badań, wykonanie specyficznych badań – np. przeprowadzenie konkretnych doświadczeń, opracowanie i zebranie ankiet itp., wykonanie analizy wyników, przygotowanie manuskryptu artykułu i inne). Określenie wkładu danego autora, w tym kandydata do stopnia doktora, powinno być na tyle precyzyjne, aby umożliwić dokładną ocenę jego udziału i roli w powstaniu każdej pracy.

Oświadczenie Współautora

Dr inż. Agata Domańska

(tytuł zawodowy, imiona i nazwisko współautora)

Sieć Badawcza Łukasiewicz

Instytut Inżynierii Materiałów Polimerowych i Barwników

miejsce pracy/afiliacja)

OŚWIADCZENIE

Oświadczam, iż mój wkład autorski w niżej wymienionym artykule naukowym był następujący*:

1. Wilczewski Sławomir, Skórczewska Katarzyna, Tomaszewska Jolanta, Lewandowski Krzysztof, Studziński Waldemar, Osiał Magdalena, Jencyk Piotr, Grzywacz Hubert, **Domańska Agata**, Curcuma longa L. rhizome extract as a poly(vinyl chloride)/graphene nanocomposite green modifier, *Molecules* (MDPI), 2022, 27, 8081, DOI: 10.3390/molecules27228081. pkt. MNiSW 140, Impact Factor 4,600

Wykonane zadania w ramach artykułu:

- a) Przeprowadzenie analizy materiałów kompozytowych metodą termogravimetryczną
- b) Konsultacja wyników badań otrzymanych wyżej wymienioną metodą pomiarową

Jednocześnie wyrażam zgodę na przedłożenie wyżej wymienionej pracy przez **mgr inż. Sławomira Wilczewskiego** jako część rozprawy doktorskiej opartej na zbiorze opublikowanych i powiązanych tematycznie artykułów naukowych.

Piastów, dn. 07.08.2023

.....
miejsce, data

A. Domańska

.....
podpis Współautora

* W przypadku prac dwu- lub wieloautorskich wymagane są oświadczenia kandydata do stopnia doktora oraz współautorów, wskazujące na ich merytoryczny wkład w powstanie każdej pracy (np. twórca hipotezy badawczej, pomysłodawca badań, wykonanie specyficznych badań – np. przeprowadzenie konkretnych doświadczeń, opracowanie i zebranie ankiet itp., wykonanie analizy wyników, przygotowanie manuskryptu artykułu i inne). Określenie wkładu danego autora, w tym kandydata do stopnia doktora, powinno być na tyle precyzyjne, aby umożliwić dokładną ocenę jego udziału i roli w powstaniu każdej pracy.

Oświadczenie Współautora

dr Agnieszka Dąbrowska

(tytuł zawodowy, imiona i nazwisko współautora)

Wydział Chemii, Centrum Nauk Biologiczno-Chemicznych

Uniwersytet Warszawski

(miejsce pracy/afiliacja)

OŚWIADCZENIE

Oświadczam, iż mój wkład autorski w niżej wymienionym artykule naukowym był następujący*:

1. Wilczewski Sławomir, Skórczewska Katarzyna, Tomaszewska Jolanta, Osiał Magdalena, **Dąbrowska Agnieszka**, Nikoforow Kostiantyn, Jencyk Piotr, Grzywacz Hubert., Graphene modification by curcuminoids as an effective method to improve the dispersion and stability of PVC/graphene nanocomposites, *Molecules* (MDPI), 2023, 28, 3383, DOI: 10.3390/molecules28083383 Pkt. MNiSW 140, Impact Factor 4,600

Wykonane zadania w ramach artykułu:

- a) Przeprowadzenie analizy metodą spektroskopii Ramana
- b) Interpretacja wyników badań otrzymanych metodą spektroskopii Ramana

Jednocześnie wyrażam zgodę na przedłożenie wyżej wymienionej pracy przez **mgr inż. Sławomira Wilczewskiego** jako część rozprawy doktorskiej opartej na zbiorze opublikowanych i powiązanych tematycznie artykułów naukowych.

Warszawa, 11-08-2023

.....
miejsce, data

A. Dąbrowska

.....
podpis Współautora

* W przypadku prac dwu- lub wieloautorskich wymagane są oświadczenia kandydata do stopnia doktora oraz współautorów, wskazujące na ich merytoryczny wkład w powstanie każdej pracy (np. twórca hipotezy badawczej, pomysłodawca badań, wykonanie specyficznych badań – np. przeprowadzenie konkretnych doświadczeń, opracowanie i zebranie ankiet itp., wykonanie analizy wyników, przygotowanie manuskryptu artykułu i inne). Określenie wkładu danego autora, w tym kandydata do stopnia doktora, powinno być na tyle precyzyjne, aby umożliwić dokładną ocenę jego udziału i roli w powstaniu każdej pracy.

Oświadczenie Współautora

dr Kostiantyn Nikiforow

(tytuł zawodowy, imiona i nazwisko współautora)

Laboratorium Analizy Powierzchni

Instytut Chemii Fizycznej

Polskiej Akademii Nauk

miejsce pracy/afiliacja)

OŚWIADCZENIE

Oświadczam, iż mój wkład autorski w niżej wymienionym artykule naukowym był następujący*:

1. Wilczewski Sławomir, Skórczewska Katarzyna, Tomaszewska Jolanta, Osial Magdalena, Dąbrowska Agnieszka, **Nikiforow Kostiantyn**, Jencyk Piotr, Grzywacz Hubert., Graphene modification by curcuminoids as an effective method to improve the dispersion and stability of PVC/graphene nanocomposites, *Molecules* (MDPI), 2023, 28, 3383, DOI: 10.3390/molecules28083383 Pkt. MNiSW 140, Impact Factor 4,600

Wykonane zadania w ramach artykułu:

- a) Przeprowadzenie analizy metodą spektroskopii fotoelektronów w zakresie promieniowania X (XPS)
- b) Interpretacja wyników badań XPS

Jednocześnie wyrażam zgodę na przedłożenie wyżej wymienionej pracy przez **mgr inż. Sławomira Wilczewskiego** jako część rozprawy doktorskiej opartej na zbiorze opublikowanych i powiązanych tematycznie artykułów naukowych.

08.08.2023

.....
miejscość, data



.....
podpis Współautora

* W przypadku prac dwu- lub wieloautorskich wymagane są oświadczenia kandydata do stopnia doktora oraz współautorów, wskazujące na ich merytoryczny wkład w powstanie każdej pracy (np. twórca hipotezy badawczej, pomysłodawca badań, wykonanie specyficznych badań – np. przeprowadzenie konkretnych doświadczeń, opracowanie i zebranie ankiet itp., wykonanie analizy wyników, przygotowanie manuskryptu artykułu i inne). Określenie wkładu danego autora, w tym kandydata do stopnia doktora, powinno być na tyle precyzyjne, aby umożliwić dokładną ocenę jego udziału i roli w powstaniu każdej pracy.